

Portland State University

PDXScholar

Dissertations and Theses

Dissertations and Theses

1992

Theoretical Studies of Atmospheric Water Complexes

Xiong Pan

Portland State University

Follow this and additional works at: https://pdxscholar.library.pdx.edu/open_access_etds

Let us know how access to this document benefits you.

Recommended Citation

Pan, Xiong, "Theoretical Studies of Atmospheric Water Complexes" (1992). *Dissertations and Theses*. Paper 1163.

<https://doi.org/10.15760/etd.1162>

This Dissertation is brought to you for free and open access. It has been accepted for inclusion in Dissertations and Theses by an authorized administrator of PDXScholar. Please contact us if we can make this document more accessible: pdxscholar@pdx.edu.

THEORETICAL STUDIES OF ATMOSPHERIC WATER COMPLEXES

by

XIONG PAN

A dissertation submitted in partial fulfillment of the
requirements for the degree of

DOCTOR OF PHILOSOPHY
in
ENVIRONMENTAL SCIENCES AND RESOURCES:
CHEMISTRY

Portland State University
1992

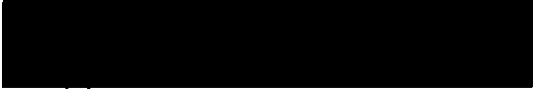
TO THE OFFICE OF GRADUATE STUDIES:

The members of the Committee approve the dissertation of Xiong Pan
presented July 20, 1992.


Robert J. O'Brien, Chair


Thomas M. Hard



Carole R. Gatz


Jack S. Semura


Richard R. Petersen


Lee W. Casperson

APPROVED:


John G. Rueter, Director, Environmental Sciences and Resources Ph.D. Program


Roy W. Koch, Vice Provost for Graduate Studies and Research

AN ABSTRACT OF THE DISSERTATION OF Xiong Pan for the Doctor of
Philosophy in Environmental Sciences and Resources: Chemistry presented July
20, 1992.

Title: Theoretical Studies of Atmospheric Water Complexes.

APPROVED BY THE MEMBERS OF THE DISSERTATION COMMITTEE:




Robert J. O'Brien, Chair


Thomas M. Hard


Carole R. Gatz


Jack S. Semura


Richard R. Petersen


Lee W. Casperson

Intermolecular complexes between H_2O and atmospheric species HO , HO_2 ,
 H_2O_2 , O_3 , NO and NO_2 have been studied by ab initio molecular orbital methods.

The studies have been performed to the MP2 theory level by using 4-31G, 6-31G, D95, 6-31G**, D95**, 6-311G**, 6-311+G**, 6-311++G**, 6-311+G(2d,1p) and 6-311+G(2d,2p) basis sets. The geometries were fully optimized. The vibrational frequencies were calculated. The Basis Set Superposition Error (BSSE) were estimated. Finally, the binding energies of the complexes were predicted with other thermochemical properties. The binding energies of $\text{H}_2\text{O}\cdot\text{HO}$, $\text{H}_2\text{O}\cdot\text{HO}_2$, $\text{H}_2\text{O}\cdot\text{H}_2\text{O}_2$, $\text{H}_2\text{O}\cdot\text{O}_3$, $\text{H}_2\text{O}\cdot\text{NO}$ and $\text{H}_2\text{O}\cdot\text{NO}_2$ are estimated to be 5.7 ± 0.6 , 8.9 ± 1.0 , 7.3 ± 1.3 , 1.8 ± 0.2 , 1.17 (no BSSE correction) and 2.98 (no BSSE correction) Kcal/Mol, respectively. The K_{eq} for dimerization to yield $\text{H}_2\text{O}\cdot\text{HO}$, $\text{H}_2\text{O}\cdot\text{HF}$, $\text{H}_2\text{O}\cdot\text{HO}_2$, $\text{H}_2\text{O}\cdot\text{H}_2\text{O}$ and $\text{H}_2\text{O}\cdot\text{H}_2\text{O}_2$ are estimated to be 0.11, 2.8, 3.3, 0.067 and 0.11 atm^{-1} , respectively. The $\text{H}_2\text{O}\cdot\text{HO}$, $\text{H}_2\text{O}\cdot\text{HF}$, $\text{H}_2\text{O}\cdot\text{HO}_2$, $\text{H}_2\text{O}\cdot\text{H}_2\text{O}$ and $\text{H}_2\text{O}\cdot\text{H}_2\text{O}_2$ are quite strongly bonded complexes, while $\text{H}_2\text{O}\cdot\text{O}_3$, $\text{H}_2\text{O}\cdot\text{NO}$ and $\text{H}_2\text{O}\cdot\text{NO}_2$ are only weakly bonded complexes. The K_{eq} changes with temperature are discussed, and their importance in atmospheric chemistry are addressed.

ACKNOWLEDGEMENTS

I would like to thank Dr. Robert J. O'Brien for his kindness and generous support of my theoretical studies. His initial guidance, constructive criticism led me to finish the project. I also thank Dr. Tom Hard, Dr. Carole Gatz, Dr. Jack Semura, Dr. Richard Petersen and Dr. Lee Casperson for their valuable comment and discussion. I am grateful for the help and encouragement of Dr. Cornelius Chan, Dr. Linda George Dr. David Myton, Dr. Wen Pan and Wen Li. I really appreciate the support I have received through the Chemistry Department and the ESR Program.

Finally, I would like to express my gratitude to my wife, Li Chen, for her patient support.

TABLE OF CONTENTS

ACKNOWLEDGMENTS	iii
LIST OF TABLES	vii
LIST OF FIGURES	xi

CHAPTER

I	INTRODUCTION	1
	Ab Initio Method	5
	Calculation of Thermochemical Properties	8
	Internal Rotation and Calculation of Rotational Barrier	8
II	H ₂ O•HO AND H ₂ O•HF SYSTEM	10
	Monomer Properties of H ₂ O, HO and HF.	11
	Geometries of H ₂ O•HO and H ₂ O•HF	15
	Vibrational Frequencies of H ₂ O•HO and H ₂ O•HF .	19
	Energies of H ₂ O•HO and H ₂ O•HF	22
III	H ₂ O•HO ₂ AND H ₂ O•H ₂ O SYSTEM	28
	Monomer Properties of H ₂ O and HO ₂	28
	Geometries of H ₂ O•HO ₂ and H ₂ O•H ₂ O	32

	Vibrational Frequencies of $\text{H}_2\text{O} \cdot \text{H}_2\text{O}$	
	and $\text{H}_2\text{O} \cdot \text{HO}_2$	40
	Energies of $\text{H}_2\text{O} \cdot \text{H}_2\text{O}$ and $\text{H}_2\text{O} \cdot \text{H}_2\text{O}$	41
IV	$\text{H}_2\text{O} \cdot \text{H}_2\text{O}_2$ SYSTEM	48
	Monomer Properties of H_2O and H_2O_2	48
	Geometries of $\text{H}_2\text{O} \cdot \text{H}_2\text{O}_2$	51
	Vibrational Frequencies of $\text{H}_2\text{O} \cdot \text{H}_2\text{O}_2$	54
	Energies of $\text{H}_2\text{O} \cdot \text{H}_2\text{O}_2$	56
V	$\text{H}_2\text{O} \cdot \text{O}_3$ SYSTEM	60
	Geometries of H_2O , O_3 and $\text{H}_2\text{O} \cdot \text{O}_3$	61
	Vibrational Frequencies of H_2O , O_3 and $\text{H}_2\text{O} \cdot \text{O}_3$	65
	Energies of H_2O , O_3 and $\text{H}_2\text{O} \cdot \text{O}_3$	68
VI	$\text{H}_2\text{O} \cdot \text{NO}$ and $\text{H}_2\text{O} \cdot \text{NO}_2$ SYSTEM	72
	Geometries of H_2O , NO , NO_2 , $\text{H}_2\text{O} \cdot \text{NO}$ and	
	$\text{H}_2\text{O} \cdot \text{NO}_2$	74
	Energies of H_2O , NO , NO_2 , $\text{H}_2\text{O} \cdot \text{NO}$ and $\text{H}_2\text{O} \cdot \text{NO}_2$	78
VII	THERMOCHEMICAL PROPERTIES AND	
	CONCLUSIONS	81
	Temperature Dependence of Thermochemical	
	Properties	83
	Effects of Basis Sets on Energy and Structure.	85
	Rotational Barrier of Complexes	92

REFERENCES	96
------------------	----

APPENDICES

A	CALCULATION OF THERMOCHEMICAL PROPERTIES OF COMPLEXES	101
B	COMPUTER PROGRAM FOR CALCULATION OF THERMOCHEMICAL PROPERTIES OF COMPLEXES	107
C	CALCULATION OF THE ENTROPY CONTRIBUTION OF INTERNAL ROTATION IN COMPLEXES	114

LIST OF TABLES

TABLE

I	Optimized geometries of H ₂ O, HO and HF	11
II	Calculated frequencies with experimental measured and harmonic (in parentheses) frequencies (in cm ⁻¹) of H ₂ O, HO and HF.	12
III	Total energies (au) and $\langle S^2 \rangle$ values of H ₂ O, HO and HF	13
IV	Optimized geometrical structures of H ₂ O•HO and H ₂ O•HF	17
V	Calculated harmonic frequencies of H ₂ O•HO and H ₂ O•HF (cm ⁻¹)	20
VI	Calibrated harmonic frequencies of H ₂ O•HO and H ₂ O•HF (cm ⁻¹) by basis set 6-31G**	21
VII	Total energies and binding energies of H ₂ O•HO and H ₂ O•HF	22
VIII	Total energies and binding energies of H ₂ O•HO and H ₂ O•HF using the geometries optimized by basis set 6-31G**	23

IX	Binding energy differences of $\text{H}_2\text{O}\cdot\text{HO}$ and $\text{H}_2\text{O}\cdot\text{HF}$ between fully optimized geometries and one-point calculation	25
X	BSSE estimates of $\text{H}_2\text{O}\cdot\text{HO}$ and $\text{H}_2\text{O}\cdot\text{HF}$	26
XI	Optimized geometries of H_2O and HO_2	29
XII	Calculated frequencies with experimental measured and harmonic (in parentheses) frequencies (in cm^{-1}) of H_2O and HO_2	30
XIII	Total energies (au) and $\langle S^2 \rangle$ values of H_2O and HO_2	31
XIV	Optimized structures and calculated harmonic frequencies of $\text{H}_2\text{O}\cdot\text{HO}_2$	33
XV	Optimized structures and calculated harmonic frequencies of $\text{H}_2\text{O}\cdot\text{H}_2\text{O}$	35
XVI	Fully optimized structures and vibrational frequencies of $\text{H}_2\text{O}\cdot\text{HO}_2$	39
XVII	Calibrated harmonic frequencies (in cm^{-1}) by 6-31G**	40
XVIII	Total energies and binding energies of $\text{H}_2\text{O}\cdot\text{HO}_2$ and $\text{H}_2\text{O}\cdot\text{H}_2\text{O}$	42
XIX	Total energies and binding energies of H_2O , HO_2 , $\text{H}_2\text{O}\cdot\text{HO}_2$ and $\text{H}_2\text{O}\cdot\text{H}_2\text{O}$ using the geometries optimized by basis set 6-31G**	43
XX	BSSE estimates and binding energies of $\text{H}_2\text{O}\cdot\text{HO}_2$ and $\text{H}_2\text{O}\cdot\text{H}_2\text{O}$	45

XXI	Optimized geometries of H_2O and H_2O_2	49
XXII	Calculated frequencies with experimental measured and harmonic (in parentheses) frequencies of H_2O and H_2O_2 (in cm^{-1})	50
XXIII	Total energies (au) of H_2O and H_2O_2	51
XXIV	Optimized structures of $\text{H}_2\text{O} \cdot \text{H}_2\text{O}_2$	53
XXV	Calculated harmonic frequencies of $\text{H}_2\text{O} \cdot \text{H}_2\text{O}_2$ (cm^{-1})	54
XXVI	Calibrated harmonic frequencies of $\text{H}_2\text{O} \cdot \text{H}_2\text{O}_2$ (cm^{-1}) by 6-31G**	55
XXVII	Energies of $\text{H}_2\text{O} \cdot \text{H}_2\text{O}_2$ calculated by fully optimized geometries	56
XXVIII	Total energies and binding energies of $\text{H}_2\text{O} \cdot \text{H}_2\text{O}_2$ system using the geometries optimized by basis set 6-31G**	57
XXIX	ESSE estimates and binding energies of $\text{H}_2\text{O} \cdot \text{H}_2\text{O}_2$	58
XXX	Optimized structures of H_2O , O_3 and $\text{H}_2\text{O} \cdot \text{O}_3$	64
XXXI	Calculated frequencies with experimental measured and harmonic (in parentheses) frequencies of H_2O , O_3 and $\text{H}_2\text{O} \cdot \text{O}_3$ (cm^{-1})	66
XXXII	Total energies and binding energies of $\text{H}_2\text{O} \cdot \text{O}_3$ system	69
XXXIII	BSSE estimates and binding energies of $\text{H}_2\text{O} \cdot \text{O}_3$	70
XXXIV	Optimized geometries of H_2O , NO and NO_2	74
XXXV	Optimized structures of $\text{H}_2\text{O} \cdot \text{NO}$	75

XXXVI	Optimized structures of $\text{H}_2\text{O}\cdot\text{NO}_2$	77
XXXVII	Total energies of H_2O , NO and $\text{H}_2\text{O}\cdot\text{NO}$ (au) and binding energies of $\text{H}_2\text{O}\cdot\text{NO}$ (kcal/mol)	78
XXXVIII	Total energies of NO_2 and $\text{H}_2\text{O}\cdot\text{NO}_2$ (au) and binding energies of $\text{H}_2\text{O}\cdot\text{NO}_2$ (kcal/mol)	79
XXXIX	Final thermochemical properties of for water system	82
XXXX	Temperature Dependence of thermochemical properties	84
XXXXI	The effects of internal rotation to thermochemical properties	95

LIST OF FIGURES

FIGURE

1. Major chemical reactions affecting odd hydrogen
 (OH, H, HO₂, H₂O₂) and odd nitrogen (NO,
 NO₂, N₂O, HNO₂, HNO₃) in the troposphere 2
2. $\langle S^2 \rangle$ values of HO and H₂O•HO calculated
 by different basis sets 14
3. Two orientations in the H₂O•HX (X=O,F) 17
4. Alpha and beta angles of H₂O•HO and H₂O•HF
 optimized by different basis sets 18
5. BSSE calculated for H₂O•HO and H₂O•HF systems . 27
6. $\langle S^2 \rangle$ values of HO₂ and H₂O•HO₂ calculated
 from different basis sets 31
7. Symmetries of H₂O•HOX complex (X=H,O) 32
8. Optimized structure of H₂O•HO₂ 32
9. Starting structures for H₂O•HO₂ 34
10. Alpha and beta angles of H₂O•H₂O (C_s)
 optimized by different basis sets 37
11. BSSE calculated for H₂O•HO₂ and H₂O•H₂O systems 46

12.	Orientations considered for $\text{H}_2\text{O} \cdot \text{H}_2\text{O}_2$ system	52
13.	Optimized structure of $\text{H}_2\text{O} \cdot \text{H}_2\text{O}_2$	52
14.	BSSE calculated for $\text{H}_2\text{O} \cdot \text{H}_2\text{O}_2$ system	59
15.	Possible structures of $\text{H}_2\text{O} \cdot \text{O}_3$	62
16.	Optimized structure of $\text{H}_2\text{O} \cdot \text{O}_3$	62
17.	Relative energies of $\text{H}_2\text{O} \cdot \text{O}_3$ with different beta angles	71
18.	Structure of $\text{H}_2\text{O} \cdot \text{NO}$	73
19.	Possible structures of $\text{H}_2\text{O} \cdot \text{NO}_2$	73
20.	Optimized structure of $\text{H}_2\text{O} \cdot \text{NO}_2$	76
21.	Relative total energies (SCF) of HO, HF, H_2O , HO_2 and H_2O_2 vs. basis sets	86
22.	Relative total energies (MP2) of HO, HF, H_2O , HO_2 and H_2O_2 vs. basis sets	87
23.	Binding energies (SCF, no BSSE correction) of $\text{H}_2\text{O} \cdot \text{HO}$, $\text{H}_2\text{O} \cdot \text{HF}$, $\text{H}_2\text{O} \cdot \text{H}_2\text{O}$, $\text{H}_2\text{O} \cdot \text{HO}_2$ and $\text{H}_2\text{O} \cdot \text{H}_2\text{O}_2$ vs. basis sets	88
24.	Binding energies (MP2, no BSSE correction) of $\text{H}_2\text{O} \cdot \text{HO}$, $\text{H}_2\text{O} \cdot \text{HF}$, $\text{H}_2\text{O} \cdot \text{H}_2\text{O}$, $\text{H}_2\text{O} \cdot \text{HO}_2$ and $\text{H}_2\text{O} \cdot \text{H}_2\text{O}_2$ vs. basis sets	89
25.	Binding energies (SCF, after BSSE correction) of $\text{H}_2\text{O} \cdot \text{HO}$, $\text{H}_2\text{O} \cdot \text{HF}$, $\text{H}_2\text{O} \cdot \text{H}_2\text{O}$, $\text{H}_2\text{O} \cdot \text{HO}_2$ and $\text{H}_2\text{O} \cdot \text{H}_2\text{O}_2$ vs. basis sets	90
26.	Binding energies (MP2, after BSSE correction)	

of $\text{H}_2\text{O} \cdot \text{HO}$, $\text{H}_2\text{O} \cdot \text{HF}$, $\text{H}_2\text{O} \cdot \text{H}_2\text{O}$, $\text{H}_2\text{O} \cdot \text{HO}_2$ and $\text{H}_2\text{O} \cdot \text{H}_2\text{O}_2$ vs. basis sets	91
27. Rotational barriers of $\text{H}_2\text{O} \cdot \text{HO}$, $\text{H}_2\text{O} \cdot \text{HF}$, $\text{H}_2\text{O} \cdot \text{H}_2\text{O}$, $\text{H}_2\text{O} \cdot \text{HO}_2$ and $\text{H}_2\text{O} \cdot \text{H}_2\text{O}_2$	93

CHAPTER I

INTRODUCTION

The atmosphere is a large chemical reaction system. There would be hundreds of reactions taking place. But the reactions known are just part of them. There are still a large number of reactions which are unknown, especially those reactions involving the species with small concentration. The atmospheric chemists are interested to find those reactions. We are interested in investigating some reactions related to the complexes which are formed from very important atmospheric species like H_2O , HO , HO_2 , H_2O_2 , O_3 , NO and NO_2 .

The species H_2O , HO , HO_2 , H_2O_2 , O_3 , NO and NO_2 play important roles in atmospheric chemistry; they are all involved in reactions among or with "odd hydrogen" and "odd nitrogen" as shown in Figure 1. All of them have important reactions, while H_2O is often the third most abundant atmospheric constituent, at least in the midlatitude lower atmosphere. On the other hand, H_2O has a strong ability to form hydrogen-bonded complexes. The water dimer is a very good example, which has been studied quite extensively by experimental and theoretical methods [2-14].

Because the interaction energies of hydrogen-bonded systems are generally small, experimental investigations have been limited, and the ab initio method has

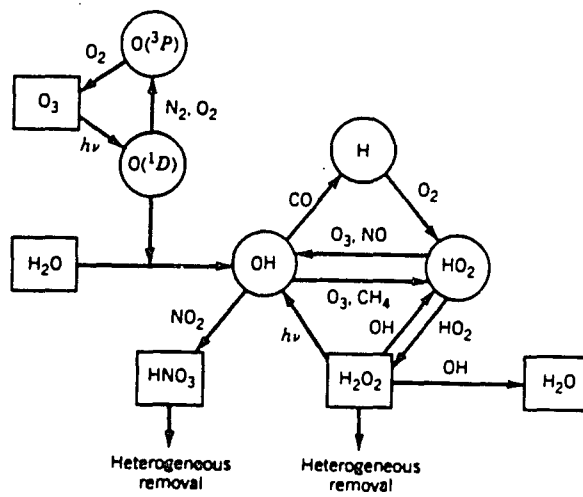


Figure 1. Major chemical reactions affecting odd hydrogen (OH , H , HO_2 , H_2O_2) and odd nitrogen (NO , NO_2 , N_2O , HNO_2 , HNO_3) in the troposphere. (from Logan *et al.*, 1981[1])

often been successfully applied to those systems [15,16]. In recent years, numerous theoretical calculations have explored the nature of gas phase hydrogen bonding, particularly with regard to the water dimer [2 -11], for which experimental data is available [12 - 14]. Along with $\text{H}_2\text{O} \cdot \text{H}_2\text{O}$, $\text{H}_2\text{O} \cdot \text{HF}$ has served as a test compound for the theoretical study of hydrogen bonding, and theoretical results have been in good agreement with experimental data [17 - 31]. These two systems could be treated as $\text{H}_2\text{O} \cdot \text{HX}$ in which X is F or OH.

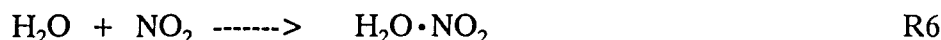
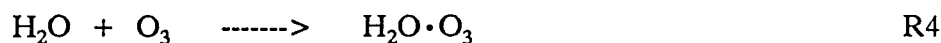
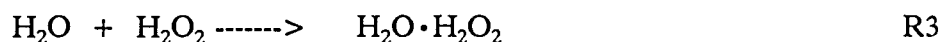
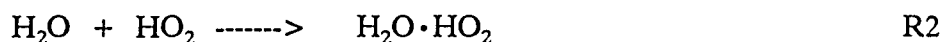
We propose to theoretically investigate those possible complexes formed from HO, HO_2 , H_2O_2 , O_3 , NO and NO_2 with H_2O . The purpose of these studies is to see how strong the complexes are and what chemical properties they have. If significant gas phase complexation exists between H_2O and those species, there may be significant consequences for the chemical reactivity of the troposphere. In this way, it is helpful to understand more about the atmosphere and how HO, HO_2 , H_2O_2 , O_3 , NO and NO_2 are trapped and get balanced in the atmosphere, especially in the "odd hydrogen" family. On the other hand, the calculations will provide useful information about binding energies, vibration frequencies, geometries and other thermochemical properties of weakly bound complexes.

Previously, Hamilton [32] and Rao [33] studied the complex $\text{H}_2\text{O} \cdot \text{HO}_2$, while Del Bene calculated the complex $\text{H}_2\text{O} \cdot \text{H}_2\text{O}_2$ [34]. Both complexes were found to be strongly bonded. However, none of these groups performed electronic correlation nor estimated the basis set superposition error (BSSE) which has been considered important in the supermolecular calculation method [16,35]. Also, the geometries of these complexes were only partially optimized (Rao *et al.* did not

give details of the complexes' geometries). We believed the information about $\text{H}_2\text{O} \cdot \text{HO}_2$ and $\text{H}_2\text{O} \cdot \text{H}_2\text{O}_2$ is quite limited, so we will study those systems in detail.

The HO species is especially interesting to us, because of the key role HO plays in atmospheric chemistry and because of our experimental studies of its atmospheric concentrations [36 -38].

The following systems will be studied by the ab initio method. The energetics, vibrational frequencies and complex structures will be predicted, which will assist experimental chemists to identify the complexes.



It is well-known that calculated ab initio interaction energies for hydrogen-bonded complexes are sensitive to the quality of the basis set employed and the theoretical method used [4,39]. To test this sensitivity we used basis sets which range from quite simple to some of the extensive basis sets in general use. In so doing we extended the calculations to $\text{H}_2\text{O} \cdot \text{H}_2\text{O}$ and $\text{H}_2\text{O} \cdot \text{HF}$ systems.

So, our studies have several meanings. First, the strongest complex among the systems we considered will be searched for. Second, the structures and

vibrational frequencies are predicted. Third, the basis sets effect is tested. Last, the ab initio method is demonstrated to be useful for atmospheric chemistry.

AB INITIO METHOD

The calculations are carried out on two computers using the GAUSSIAN 86 program [40]: an IBM 4381, and an Apollo DN 10000 workstation to which we partially adapted the Gaussian 86 program. The Gaussian program applies the variation method for the approximate solution of the Schrodinger equation:

$$\mathfrak{H} \psi = E \psi$$

Then the interaction energy ΔE of the complexes is given as the difference between the energies of the complex (E_t) and its monomers (E_i):

$$\Delta E = \Sigma E_t - \Sigma E_i$$

Unfortunately the values of ΣE_t and ΣE_i differ very little compared to ΣE_t or ΣE_i themselves. So the energies of the complex and its monomers should be evaluated in a consistent way. This requires size consistency and basis set consistency [41]. Fortunately, the MP2 method we used is size-extensive and size-consistent [42]. But the Basis Set Superposition Error (BSSE) which is caused by basis set inconsistency must be calculated. When the same basis sets are used to describe the complex and its monomers to evaluate the interaction energy, in fact a larger basis set is used in complex calculation. This is because the basis set of complex is formed by superposition of the basis sets of its monomers. Larger

basis set of the complex inevitably yield a larger total energy and, consequently, larger interaction energy. The increase in the total energy of the complex as a result of the unequal basis sets of the complex and its monomers is called the Basis Set Superposition Error (BSSE). This error has nothing in common with the physical effects of interaction but is an artificial mathematical effect. Boys and Bernardi [43] introduced the "function counterpoise" method for eliminating the BSSE. The counterpoise method is used to estimate the BSSE of all the systems we studied. The BSSE for the complex consists of the BSSE for each fragment. The BSSE for each fragment is calculated as the difference of two energies: first, the energy of a fragment with the geometry it has in the complex structure and, second, the energy of this distorted fragment together with the "ghost" basis functions of the other (distorted) fragment as it is in the complex structure but without its nuclei and electrons.

Spin restricted Hartree-Fock (RHF) theory is used for the closed-shell species and the unrestricted form (UHF) is employed for the open-shell species. Because the UHF wavefunctions are not the eigenfunctions of the S^2 operator, the results for radicals are contaminated by higher spin states [44]. Various methods are normally used to alleviate this problem. Among these are the use of spin projection [44] and restricted open-shell Hartree-Fock theory [45]. Fortunately, the S^2 expectation values in our results are very close to those of pure doublets for all the radicals we considered, which means that the effects due to spin contamination are small. Furthermore, in reactions R1, R2, R5 and R6, doublets occur on both sides of the reaction, so some cancellation of spin contamination

would be expected in the calculation of binding energies.

The standard basis sets 4-31G [46], 6-31G [7,47], 6-31G** [48], D95, and D95** [49] of Gaussian 86 are used to fully optimize the geometries. Furthermore, the 6-311G**, 6-311+G**, and 6-311++G** basis sets are used to optimize the $\text{H}_2\text{O}\cdots\text{HO}$ system. The 6-311G** is a triple-split basis set [50] augmented by d orbital on heavy atoms and p orbital on hydrogen atoms. The 6-311+G** is a 6-311G** set augmented by diffuse functions on heavy atoms, whereas 6-311++G** augments all atoms [51]. After the geometries are optimized, electron correlation is performed to the MP2 level [52] using frozen cores. The basis sets 6-311+G(2d,2p) and 6-311+G(2d,1p) are used for single point SCF and MP2 energy calculation. The 6-311+G(2d,1p) set is 6-311G augmented by diffuse functions on heavy atoms: 2 sets of d functions on heavy atoms and 1 set of p functions on hydrogen atoms, whereas 6-311+G(2d,2p) employs 2 sets of p functions on hydrogen atoms too. The exponents of 2 sets of d functions are a factor of 2 larger and smaller than the standard values [4,40]. The same is true for the 2 sets of p function exponents.

For each species, the harmonic vibrational frequencies are calculated analytically [53] at the SCF level using the geometries optimized by 4-31G, 6-31G, D95, 6-31G** and D95**, For the small complexes, frequencies are calculated up to 6-311G**, 6-311+G** and 6-311++G**. It is well-known that the frequencies are overestimated in SCF level and so the results were scaled by a 0.9 factor to correct for this systematic error [39]. But, in order to afford a more complete correction of this systematic error, frequencies are scaled for each mode in the

monomers for the calculations of complexes. The first purpose of the vibrational frequency calculation is to verify that the calculation has found a true energy minimum, which is not always the case. Then, after the minima are located, the vibrational frequencies are used to calculate thermodynamic properties of each species as a function of temperature.

There are no experimental structure data available for the systems we studied. So we compare our $\text{H}_2\text{O} \cdot \text{HO}$ with $\text{H}_2\text{O} \cdot \text{HF}$ and $\text{H}_2\text{O} \cdot \text{HO}_2$ with $\text{H}_2\text{O} \cdot \text{H}_2\text{O}$.

CALCULATION OF THERMOCHEMICAL PROPERTIES

In order to calculate ΔG and ΔH for the complexes, the calculated binding energies ΔE are corrected for differences in vibrational energy (E_{vib}), rotational energy (E_{rot}), and translational energy (E_{trans}) of reactions and products.

$$\Delta H(T) = \Delta E + \Delta E_{\text{vib}}(T) + \Delta E_{\text{rot}}(T) + \Delta E_{\text{trans}}(T) + \Delta(PV)$$

Here $RT/2$ is assigned to each degree of translational and rotational freedom (the rotational temperatures of monomers and complexes are very low compared to 298 K) and $\Delta(PV) = -RT$ for complexation. The GAUSSIAN program evaluated the vibrational partition function, using the calculated frequencies.

INTERNAL ROTATION AND CALCULATION OF ROTATIONAL BARRIER

For the complex between fragments, there is an important internal degree of freedom for the complex, which is the internal rotation about the complexing

bond. At temperatures such that $KT \gg V_o$ (V_o is the rotational barrier), the internal rotation is essentially free and can be treated by methods similar to the rigid rotor. At temperatures such that $KT \ll V_o$, the complex is trapped at the lowest energy form, and the motion is that of a simple torsional vibration, which can be treated by methods similar to that used for the simple harmonic oscillator. At the ordinary temperatures, the motion is intermediate between that of free rotation and torsional vibration which is quite difficult to deal with.

For the complex systems we studied, the rotational barrier about the complexing bond is evaluated as following: first, the fragment is frozen and the rotation angle is assigned to some particular values and, second, the other geometry parameters were optimized to give the lowest energy.

CHAPTER II

$\text{H}_2\text{O}\cdot\text{HO}$ AND $\text{H}_2\text{O}\cdot\text{HF}$ SYSTEM

The hydroxyl radical, HO, plays an important role in the chemistry of both the lower and upper atmosphere. The HO radical is an important initiator of atmospheric hydrocarbon oxidation. Both the generation and destruction of ozone in the troposphere are largely accounted for by chemistry involving the HO_x and NO_x cycles (Figure 1).

The $\text{H}_2\text{O}\cdot\text{HO}$ has not drawn much attention partially because the concentration of HO is low, and the life time of HO is short. But the $\text{H}_2\text{O}\cdot\text{HF}$ has been studied rather thoroughly by experimental and theoretical methods. The $\text{H}_2\text{O}\cdot\text{HO}$ should be analogous to $\text{H}_2\text{O}\cdot\text{HF}$ except that HO is a reactive radical. So, the same theory level calculations were performed for both $\text{H}_2\text{O}\cdot\text{HO}$ and $\text{H}_2\text{O}\cdot\text{HF}$ since the experimental data of $\text{H}_2\text{O}\cdot\text{HO}$ is not available.

The literature contains geometry optimization studies of H_2O , HO, HF and $\text{H}_2\text{O}\cdot\text{HF}$ using different basis sets and different levels of theory. But in order to compare the energy difference, the geometries of all monomers are optimized by using the same level of calculations as the complexes.

MONOMER PROPERTIES OF H₂O, HO AND HF

The results of geometry optimization of monomers H₂O, HO and HF at the SCF level are shown in Table I along with experimental data for purposes of comparison. Generally, polarized basis sets give more accurate bond angle descriptions and dipole moment values. For H₂O, it averages 7.1% larger in the angle calculated with unpolarized basis sets while only 1.5% larger by polarized basis sets comparing to experimental data. In the calculation of dipole moment, it is 35% larger by unpolarized basis sets while only 17% larger by polarized basis sets for H₂O, 29% larger by unpolarized basis sets while only 13% larger by polarized basis sets for HO, and 27% larger by unpolarized basis sets while only

TABLE I
OPTIMIZED GEOMETRIES OF H₂O, HO AND HF [a]

Parameter	Basis set								Exp.
	4-31G	6-31G	D95	6-31G**	D95**	[b]	[c]	[d]	
H ₂ O									
O-H _{1,2}	0.950	0.950	0.951	0.943	0.944	0.941	0.941	0.941	0.958 e
H1OH2	111.2	111.6	112.5	106.0	106.6	105.5	106.2	106.2	104.5
μ(D)	2.486	2.501	2.530	2.148	2.180	2.138	2.197	2.196	1.85 f
HO									
H-O	0.968	0.967	0.971	0.955	0.957	0.951	0.952	0.952	0.970 g
μ(D)	2.130	2.146	2.190	1.868	1.898	1.849	1.896	1.895	1.67 h
HF									
H-F	0.922	0.921	0.920	0.901	0.903	0.896	0.897	0.897	0.917 i
μ(D)	2.288	2.301	2.383	1.944	2.019	1.980	2.026	2.026	1.83 j

a. Geometrical parameters are given in Å and degrees.

b. 6-311G**. c. 6-311+G**. d. 6-311++G**. e. ref.54. f. ref.55.

g. ref.56. h. ref.57. i. ref.58. j. ref.59.

9.2% larger by polarized basis sets for HF, respectively. The unpolarized basis sets do give more accurate bond length descriptions. For bond length, it averages 0.83% smaller by unpolarized basis sets while 1.7% smaller by polarized basis sets for H₂O, 0.13% smaller by unpolarized basis sets while 1.7% larger by polarized basis sets for HO, and 0.43% larger by unpolarized basis sets while only 2.0% smaller by polarized basis sets for HF, respectively.

Because of the importance of electrostatic effects in the SCF treatment of molecular interactions [60], more accurate dipole moments (μ) should give more accurate energy description. So, the dipole moments were presented with optimized geometries.

In Table II, the harmonic frequencies are reported for all monomers, and again compared with experiment. The data were scaled by 0.9 to remove

TABLE II
CALCULATED FREQUENCIES WITH EXPERIMENTAL
MEASURED AND HARMONIC (IN PARENTHESES)
FREQUENCIES (IN CM⁻¹) OF H₂O, HO AND HF

	4-31G	6-31G	D95	6-31G**	D95**	[a]	[b]	[c]	Exp.[d]
H ₂ O									
s-stretch	3563	3590	3625	3732	3748	3728	3728	3728	3657 (3832)
bend	1568	1563	1540	1593	1576	1576	1554	1554	1595 (1649)
a-stretch	3699	3731	3783	3838	3858	3814	3820	3820	3756 (3942)
HO									
stretch	3413	3444	3470	3647	3658	3646	3642	3643	3735
HF									
stretch	3706	3722	3805	4043	4057	4061	4043	4044	3960 (4138)

a. 6-311G**. b. 6-311+G**. c. 6-311++G**.

d. The frequencies of H₂O are from ref.61 and ref.39, HO are from ref.56, HF are from ref.58.

TABLE III
TOTAL ENERGIES (AU) AND $\langle S^2 \rangle$ VALUES
OF H₂O, HO AND HF [a]

	E(SCF)	$\langle S^2 \rangle$	E(MP2)	$\langle S^2 \rangle$
H ₂ O				
4-31G	-75.90864		-76.03598	
6-31G	-75.98536		-76.11205	
D95	-76.01100		-76.13501	
6-31G**	-76.02362		-76.21906	
D95**	-76.04695		-76.24209	
6-311G**	-76.04701		-76.26327	
6-311+G**	-76.05331		-76.27396	
6-311++G**	-76.05342		-76.27416	
HO				
4-31G	-75.28716	0.7536	-75.37614	0.7514
6-31G	-75.36318	0.7537	-75.45128	0.7515
D95	-75.38631	0.7543	-75.47043	0.7518
6-31G**	-75.38833	0.7550	-75.53181	0.7505
D95**	-75.41047	0.7554	-75.55214	0.7508
6-311G**	-75.41074	0.7546	-75.57268	0.7505
6-311+G**	-75.41470	0.7555	-75.57946	0.7511
6-311++G**	-75.41483	0.7555	-75.57965	0.7511
HF				
4-31G	-99.88729		-100.01585	
6-31G	-99.98343		-100.11131	
D95	-100.02198		-100.14350	
6-31G**	-100.01169		-100.19412	
D95**	-100.04793		-100.23031	
6-311G**	-100.04690		-100.26687	
6-311+G**	-100.05326		-100.27835	
6-311++G**	-100.05331		-100.27845	

a. geometries optimized by specified basis set, UHF and UMP2 were used for open-shell species.

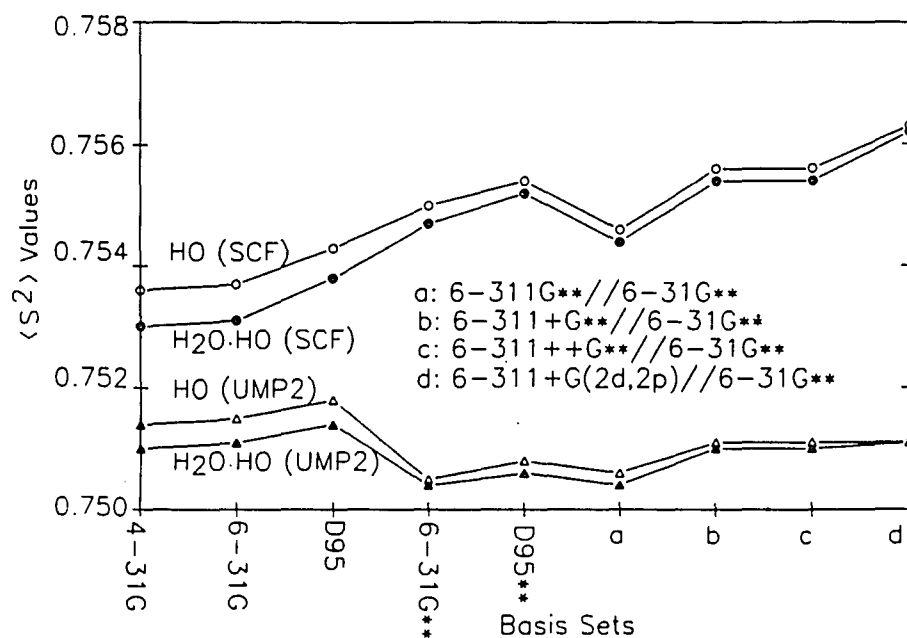


Figure 2. $\langle S^2 \rangle$ values of HO and H₂O·HO calculated by different basis sets.

systematic error [39]. After the scaling, the data are very comparable with experimental data, especially for the polarized basis sets. But, the scaled data are still slightly different from the experimental data. So, for the calculation of complexes, the scale factor will be designed for each high frequency mode for the 6-31G** basis set to get our best estimates of frequencies.

The total energies at the SCF and MP2 level are reported in Table III with their $\langle S^2 \rangle$ value, if they are open-shell species. At the SCF level for open-shell species, the $\langle S^2 \rangle$ value is quite close to that of a pure doublet wavefunction (0.75). The largest $\langle S^2 \rangle$ is 0.7555 for HO of the 6-311++G** basis set. The MP2 calculations reduce the $\langle S^2 \rangle$ further. At the MP2 level, the largest is 0.7518 for HO of the D95 basis set. All these $\langle S^2 \rangle$ values indicate that the effects of spin contamination are very low. Variation in $\langle S^2 \rangle$ with different theory levels is shown for HO and its water complex in Figure 2. At the highest level of theory, $\langle S^2 \rangle$ for monomer and complex have virtually converged at the SCF level and have completely converged near 0.751 at the UMP2 level. At the SCF level, $\langle S^2 \rangle$ increases slowly with basis set quality, while the UMP2 calculations yield values relatively constant with the basis sets.

GEOMETRIES OF $\text{H}_2\text{O} \cdot \text{HO}$ AND $\text{H}_2\text{O} \cdot \text{HF}$

The $\text{H}_2\text{O} \cdot \text{HO}$ is analogous to the $\text{H}_2\text{O} \cdot \text{HF}$ system which has been widely studied [17 - 31]. The nuclear spin statistical weight effects in the microwave spectrum of $\text{H}_2\text{O} \cdot \text{HF}$ show that the complex contains a pair of equivalent protons [17]. Previous workers have obtained either C_{2v} or C_s symmetry, depending upon

the basis set. Typically, unpolarized basis sets yielded C_{2v} symmetry, whereas polarized basis sets gave C_s symmetry. C_s symmetry is consistent with the experimental data [19].

In our calculation, we also obtain C_{2v} and C_s symmetry for $H_2O \cdot HO$ with different basis sets. Figure 3.1 shows the structures of $H_2O \cdot HO$ and $H_2O \cdot HF$ with C_{2v} and C_s symmetry. The geometry is C_{2v} when $\alpha = 180.0^\circ$, $\beta = 0.0^\circ$. Each has H_2O as proton acceptor. Basis sets of 4-31G, 6-31G, D95 and D95** optimize the geometry to C_{2v} ($\alpha = 180.0^\circ$, $\beta = 0.0^\circ$) while 6-31G** optimizes the geometry to C_s ($\alpha = 147.4^\circ$, $\beta = 2.9^\circ$). Surprisingly, D95** and 6-31G**, which are almost the same quality, give two different equilibrium structures. Then we used 6-311G**, 6-311+G** and 6-311++G** to optimize the geometry. The results were that 6-311G** gave C_s symmetry and 6-311+G** and 6-311++G** gave C_{2v} symmetry. All of those optimized geometries of $H_2O \cdot HO$ are shown in Table IV. Then we used all the same basis sets to optimize the $H_2O \cdot HF$ complex which may be checked against experimental data. The results are shown in Table IV with $H_2O \cdot HO$. The 4-31G, 6-31G, and D95 gave C_{2v} symmetry, whereas 6-31G**, 6-311G**, D95**, 6-311+G**, and 6-311++G** gave C_s symmetry with the α angle increasing gradually. But 6-31G** give the best α angle compared to experimental data. The results of 6-311+G** and 6-311++G** were almost the same.

Comparing to the experimental data of $H_2O \cdot HF$, although the situation is not entirely clear, we conclude that 6-31G** gives the best geometry for $H_2O \cdot HF$ and D95**, 6-311G**, 6-311+G**, and 6-311++G** overestimate the α angle.

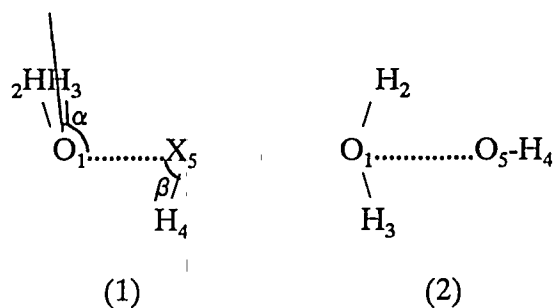


Figure 3. Two orientations in the $\text{H}_2\text{O} \cdot \text{HX}$ ($\text{X}=\text{O}, \text{F}$).

TABLE IV
OPTIMIZED GEOMETRICAL STRUCTURES
OF $\text{H}_2\text{O} \cdot \text{HF}$ AND $\text{H}_2\text{O} \cdot \text{HO}$ [a]

Parameter	Basis set								Exp.[e]
	4-31G	6-31G	D95	6-31G**	D95**	[b]	[c]	[d]	
H₂O•HF									
symmetry	C _{2v}	C _{2v}	C _{2v}	C _s	C _s	C _s	C _s	C _s	
O1-H2,3	0.950	0.949	0.951	0.944	0.945	0.942	0.942	0.942	
O1-F5	2.605	2.617	2.593	2.718	2.701	2.700	2.722	2.720	2.664
H4-F5	0.939	0.937	0.938	0.911	0.914	0.907	0.908	0.908	
H2O1H3	112.9	113.0	113.3	107.0	107.6	106.9	107.5	107.5	
α	180.0	180.0	180.0	136.1	150.4	145.4	162.7	162.4	134
β	0.0	0.0	0.0	4.1	1.9	2.6	0.9	0.9	
μ(D)	5.586	5.578	5.658	4.376	4.666	4.523	4.681	4.681	4.05
H₂O•HO									
symmetry	C _{2v}	C _{2v}	C _{2v}	C _s	C _{2v}	C _s	C _{2v}	C _{2v}	
O1-H2,3	0.951	0.949	0.952	0.944	0.945	0.941	0.942	0.942	
O1-O5	2.804	2.818	2.823	2.938	2.945	2.925	2.951	2.952	
H4-O5	0.974	0.973	0.977	0.959	0.961	0.956	0.956	0.956	
H2O1H3	112.3	112.4	112.9	106.9	107.4	106.7	107.1	107.1	
α	180.0	180.0	180.0	147.4	180.0	165.7	180.0	180.0	
β	0.0	0.0	0.0	2.9	0.0	1.1	0.0	0.0	
μ(D)	5.335	5.332	5.345	4.383	4.593	4.488	4.504	4.501	

a. Geometric parameters are given in Å and degrees.

b. 6-311G**. c. 6-311+G**. d. 6-311++G**. e. from ref.19.

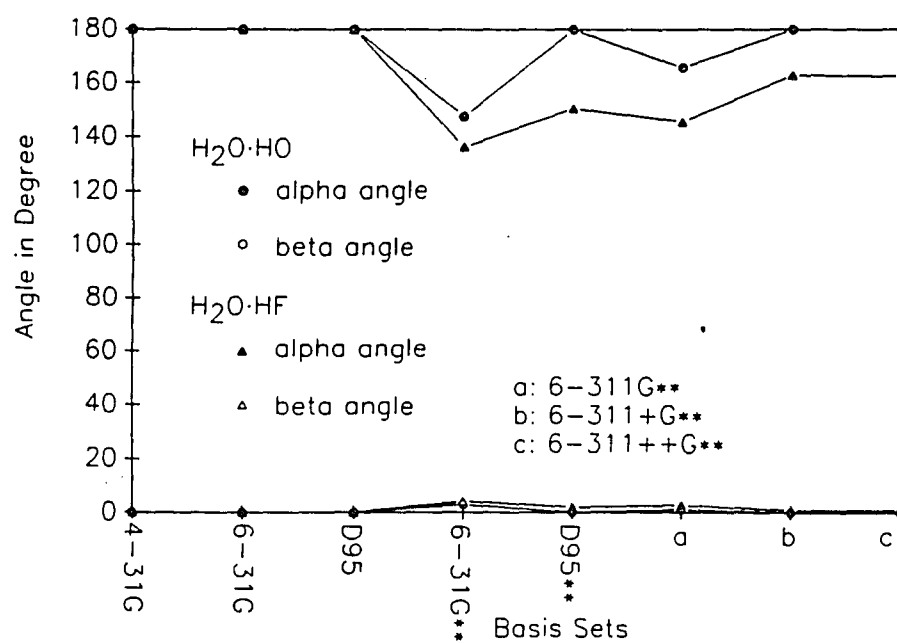


Figure 4. Alpha and beta angles of $\text{H}_2\text{O}\cdot\text{HO}$ and $\text{H}_2\text{O}\cdot\text{HF}$ optimized by different basis sets.

The dependence of the α and β angles of $\text{H}_2\text{O}\cdot\text{HF}$ and $\text{H}_2\text{O}\cdot\text{HO}$ upon basis sets is shown in Figure 4. We found great similarities between those two figures. Thus, Cs geometry optimized by 6-31G** was concluded to be the best geometry for $\text{H}_2\text{O}\cdot\text{HO}$ complex.

The symmetry in Figure 3.2 was also partially optimized to a stationary point. But, after the symmetry was released and smaller convergence criteria were used, the geometry went to the orientation shown in Figure 3.1.

The results of the dipole moment of $\text{H}_2\text{O}\cdot\text{HO}$ and $\text{H}_2\text{O}\cdot\text{HF}$ are also presented in Table IV, and show considerable similarity. For both complexes, 6-31G** gave the smallest dipole moment and smallest α angle. For $\text{H}_2\text{O}\cdot\text{HF}$, the dipole moment and α angle from 6-31G** are close to the experimental data [19]. So, from the point of view of dipole moment, the basis set 6-31G** gives the best geometry description for $\text{H}_2\text{O}\cdot\text{HF}$, and, by analogy, for $\text{H}_2\text{O}\cdot\text{HO}$ also. For other parameters, the unpolarized basis sets gave values close to one another while polarized basis sets form another group. Particularly, the intermolecular distance of unpolarized basis sets are shorter than those of polarized basis sets, while the experimental data seem in between. The larger dipole moments and smaller intermolecular distances of unpolarized basis sets indicate they would overestimate the complex binding energies, as confirmed below.

VIBRATIONAL FREQUENCIES OF $\text{H}_2\text{O}\cdot\text{HO}$ AND $\text{H}_2\text{O}\cdot\text{HF}$

The harmonic frequencies of $\text{H}_2\text{O}\cdot\text{HO}$ scaled by 0.9 [39] are presented in Table V. There is an interesting difference between polarized and unpolarized

TABLE V
CALCULATED HARMONIC FREQUENCIES OF
H₂O•HO AND H₂O•HF (CM⁻¹) [a]

H ₂ O•HO									
	[b]					(H ₂ O)	(H ₂ O)	(H ₂ O)	(HO)
4-31G	166	199	208	509	672	1577(+9)	3311(-102)	3576(+13)	3708(+9)
6-31G	164	202	204	490	655	1576(+13)	3342(-102)	3602(+12)	3737(+6)
D95	176	197	223	499	666	1566(+26)	3359(-111)	3634(+9)	3779(-4)
[c]	125	148	169	395	548	1587(-6)	3584(-63)	3732(0)	3837(-1)
[d]	66	141	160	376	540	1580(+4)	3595(-63)	3745(-3)	3853(-5)
[e]	76	136	169	381	551	1575(-1)	3587(-59)	3727(-1)	3817(+3)
[f]	82	150	158	370	547	1570(+16)	3584(-58)	3724(-4)	3815(-5)
[g]	88	148	158	365	545	1571(+17)	3583(-60)	3724(-4)	3815(-5)
H ₂ O•HF									
	[b]					(H ₂ O)	(H ₂ O)	(H ₂ O)	(HF)
4-31G	203	205	257	681	834	1582(+14)	3586(+23)	3716(+17)	3403(-303)
6-31G	200	213	249	664	816	1581(+18)	3611(+21)	3745(+14)	3419(-303)
D95	230	247	264	719	862	1575(+35)	3642(+17)	3783(0)	3441(-364)
[c]	173	188	213	570	690	1588(-5)	3728(-4)	3833(-5)	3835(-208)
[d]	148	202	204	593	718	1580(+4)	3741(-7)	3820(-38)	3849(-208)
[e]	160	201	207	589	714	1577(+1)	3723(-5)	3812(-2)	3840(-221)
[f]	90	188	199	568	698	1573(+19)	3722(-6)	3815(-5)	3820(-223)
[g]	92	189	201	573	702	1573(+19)	3723(-5)	3815(-5)	3818(-226)
exp.[18]									3608

a. The values in parentheses are frequency-shifts compared to the same mode of the monomer (calculated values).

b. The fragment in the complex mainly involved in the vibrational mode.

c. 6-31G**. d. D95**. e. 6-311G**. f. 6-311+G**. g. 6-311++G**.

basis sets. The high frequency modes, which are mainly monomer frequency modes, are larger for polarized basis sets than those for unpolarized basis sets. But for lower frequency modes which are monomer interactions, these results are reversed. The same situation was found in H₂O•HF which is presented in Table V with H₂O•HO. The stretch mode of O-H in the H₂O•HO complex was

red-shifted quite a lot (58 - 111 cm^{-1}), more so with unpolarized basis sets than with polarized basis sets. This indicates the unpolarized basis sets give too strong interaction, which will be confirmed by the energy calculation later.

Although the 0.9 scaling factor [39] comes close to correcting for systematic error in the calculated frequencies, the new scaling factors are designated for each mode of monomers by the ratio of the experimental data to the calculated frequency for each mode. Then the average of those scaling factors is used for those low frequency modes in the complexes. The results are shown in Table VI (only for 6-31G**). The proper scaling factor is 0.8965 for $\text{H}_2\text{O} \cdot \text{HO}$ and 0.8864 for $\text{H}_2\text{O} \cdot \text{HF}$.

TABLE VI
CALIBRATED HARMONIC FREQUENCIES OF
 $\text{H}_2\text{O} \cdot \text{HO}$ AND $\text{H}_2\text{O} \cdot \text{HF}$ (CM^{-1}) BY BASIS SET 6-31G** [a]

$\text{H}_2\text{O} \cdot \text{HO}$									
SYM.	A'	A''	A'	A'	A''	A'	A'	A''	A'
S.F.	———		0.8965		———		0.9013	0.8819	0.8809
FREQ.	125	148	168	394	546	1590(-5)	3657(0)	3756(0)	3670(-65)
INT.	229	4	18	271	214	102	30	98	237
$\text{H}_2\text{O} \cdot \text{HF}$									
SYM.	A'	A''	A'	A'	A''	A'	A'	A''	A'
S.F.	———		0.8864		———		0.9013	0.8819	0.8809
FREQ.	170	185	209	561	679	1590(-5)	3653(-4)	3752(-4)	3756(-204)
INT.	146	0	106	279	213	107	69	112	609

- a. The values in parentheses are frequency-shifts compared to the same mode of the monomer (experimental values).
 SYM. is the symmetry of the vibrational mode.
 INT. is the IR intensities in KM/MOLE.
 S.F. is the scaling factor.

ENERGIES OF $\text{H}_2\text{O}\cdot\text{HO}$ AND $\text{H}_2\text{O}\cdot\text{HF}$

Table VII gives the total energies of $\text{H}_2\text{O}\cdot\text{HO}$ and $\text{H}_2\text{O}\cdot\text{HF}$ at SCF and UMP2 levels. Again the $\langle S^2 \rangle$ values of $\text{H}_2\text{O}\cdot\text{HO}$ are very close to that of a pure doublet state. In the SCF level, the largest $\langle S^2 \rangle$ value is 0.7554 derived by 6-311+G** and 6-311++G**, while the smallest is 0.7530 derived by 4-31G. The UMP2 calculation reduces the $\langle S^2 \rangle$ value close to 0.75 (pure doublet state). The

TABLE VII
TOTAL ENERGIES AND BINDING ENERGIES OF
 $\text{H}_2\text{O}\cdot\text{HO}$ AND $\text{H}_2\text{O}\cdot\text{HF}$ [a]

basis set	E	$\langle S^2 \rangle$	ΔE	E	$\langle S^2 \rangle$	ΔE
$\text{H}_2\text{O}\cdot\text{HO}$						
4-31G	-151.21142	0.7530	-9.802	-151.42837	0.7510	-10.197
6-31G	-151.36342	0.7531	-9.337	-151.57872	0.7511	-9.657
D95	-151.41167	0.7538	-9.011	-151.62081	0.7514	-9.645
6-31G**	-151.42226	0.7547	-6.470	-151.76277	0.7504	-7.467
D95**	-151.46700	0.7552	-6.012	-151.80519	0.7506	-6.878
6-311G**	-151.46820	0.7544	-6.557	-151.84787	0.7504	-7.480
6-311+G**	-151.47733	0.7554	-5.848	-151.86386	0.7510	-6.551
6-311++G**	-151.47752	0.7554	-5.817	-151.86425	0.7510	-6.511
$\text{H}_2\text{O}\cdot\text{HF}$						
4-31G	-175.81837		-14.081	-176.07464		-14.313
6-31G	-175.99034		-13.523	-176.24517		-13.686
D95	-176.05467		-13.611	-176.30143		-14.383
6-31G**	-176.04975		-9.061	-176.42974		-10.392
D95**	-176.10906		-8.898	-176.48875		-10.260
6-311G**	-176.10894		-9.431	-176.54737		-10.812
6-311+G**	-176.12000		-8.427	-176.56726		-9.381
6-311++G**	-176.12024		-8.478	-176.56768		-9.457

a. The geometries were optimized by the specified basis set; E'S are in a.u., and ΔE in kcal/mol. $\text{H}_2\text{O}\cdot\text{HO}$ is calculated by UHF and UMP2. $\text{H}_2\text{O}\cdot\text{HF}$ is calculated by RHF and MP2.

largest is 0.7514 by UMP2/D95 and smallest is 0.7504 derived by UMP2/6-31G** and UMP2/6-311G**. The $\langle S^2 \rangle$ values of HO and H₂O•HO changing with basis sets are also displayed in Figure 2. Interestingly, in general the $\langle S^2 \rangle$ values in SCF level become larger with more extensive basis sets, but in UMP2 level, they become smaller with more extensive basis sets. The $\langle S^2 \rangle$ value differences between HO and H₂O•HO become smaller with more extensive basis sets.

The binding energies for unpolarized basis sets were much higher than those for polarized basis sets for both SCF and UMP2 levels. So lower quality of the basis sets indeed overestimate the binding energy.

TABLE VIII
TOTAL ENERGIES AND BINDING ENERGIES OF
H₂O•HO AND H₂O•HF USING THE GEOMETRIES
OPTIMIZED BY BASIS SET 6-31G** [a]

	E(H ₂ O)	E(HO)	$\langle S^2 \rangle$	E(H ₂ O•HO)	$\langle S^2 \rangle$	ΔE
SCF						
6-311G**	-76.04699	-75.41072	0.7546	-151.46814	0.7544	-6.545
6-311+G**	-76.05330	-75.41469	0.7556	-151.47711	0.7554	-5.723
6-311++G**	-76.05342	-75.41482	0.7556	-151.47731	0.7554	-5.692
[b]	-76.05671	-75.41697	0.7563	-151.48151	0.7562	-4.913
MP2						
6-311G**	-76.26333	-75.57277	0.7506	-151.84819	0.7504	-7.587
6-311+G**	-76.27410	-75.57954	0.7511	-151.86414	0.7510	-6.589
6-311++G**	-76.27430	-75.57973	0.7511	-151.86455	0.7510	-6.601
[b]	-76.29564	-75.59706	0.7511	-151.90217	0.7511	-5.943

TABLE VIII
TOTAL ENERGIES AND BINDING ENERGIES OF
 $\text{H}_2\text{O} \cdot \text{HO}$ AND $\text{H}_2\text{O} \cdot \text{HF}$ USING THE GEOMETRIES
OPTIMIZED BY BASIS SET 6-31G** [a]
(continued)

	E(HF)	E($\text{H}_2\text{O} \cdot \text{HF}$)	ΔE
SCF			
6-311G**	-100.04688	-176.10886	-9.406
6-311+G**	-100.05325	-176.11977	-8.296
6-311++G**	-100.05329	-176.12001	-8.346
[b]	-100.05555	-176.12421	-7.499
MP2			
6-311G**	-100.26703	-176.54765	-10.850
6-311+G**	-100.27849	-176.56770	-9.482
6-311++G**	-100.27859	-176.56810	-9.544
[b]	-100.30264	-176.61236	-8.835

a. E'S are in a.u. and ΔE are in kcal/mol. $\text{H}_2\text{O} \cdot \text{HO}$ is calculated by UHF and UMP2. $\text{H}_2\text{O} \cdot \text{HF}$ is calculated by RHF and MP2.

b: 6-311+G(2d,2p).

After Cs symmetry for $\text{H}_2\text{O} \cdot \text{HO}$ was obtained with 6-31G**, the 6-311G**, 6-311+G**, 6-311++G** and 6-311+G(2d,2p) basis sets were used to calculate total energies at both SCF and UMP2 levels with the geometries optimized by 6-31G**. The results for these one point calculations are shown in Table VIII. For $\text{H}_2\text{O} \cdot \text{HO}$ in the SCF level, the binding energies are in the range of -4.913 to -6.545 Kcal/mol, while in UMP2 level, the binding energies are in the range of -5.9 to -6.5 kcal/mol. Comparing the UMP2 results of 6-311G**, 6-311+G**, and 6-311++G** in Tables VII and VIII, the results are shown in Table IX. We find only small geometry effects on the total energies of the complexes, so our

TABLE IX
 BINDING ENERGY DIFFERENCES OF $\text{H}_2\text{O}\cdot\text{HO}$
 AND $\text{H}_2\text{O}\cdot\text{HF}$ BETWEEN FULLY OPTIMIZED
 GEOMETRIES AND ONE-POINT CALCULATION [a]

	$\text{H}_2\text{O}\cdot\text{HO}$		$\text{H}_2\text{O}\cdot\text{HF}$	
	$\Delta(\Delta E_{\text{SCF}})$	$\Delta(\Delta E_{\text{UMP2}})$	$\Delta(\Delta E_{\text{SCF}})$	$\Delta(\Delta E_{\text{MP2}})$
6-311G**	-0.012	0.107	-0.025	0.038
6-311+G**	-0.125	0.038	-0.131	0.101
6-311++G**	-0.125	0.090	-0.132	0.087

a: unit is kcal/mol; one-point calculation based on geometries of 6-31G**.

single-point calculations with higher basis sets are acceptable.

The BSSE was estimated at both SCF and MP2 levels for the geometries specified and the results are shown in Table X. They are also displayed in Figure 5. The BSSE of 6-311G**, 6-311+G**, 6-311++G** and 6-311+G(2d,2p) gradually decreased at both SCF and MP2 levels, but did not become negligible. The BSSE calculated upon the geometries of D95** (C_{2v}) and 6-311++G** (C_{2v}), were not negligible either. So if we take C_s symmetry of 6-31G** as the best geometry representation of the complex, and take the BSSE as uncertainty of the binding energy, the binding energy is in the range of -5.9 to -5.1 kcal/mol for the $\text{H}_2\text{O}\cdot\text{HO}$ complex and -8.8 to -7.7 kcal/mol for the $\text{H}_2\text{O}\cdot\text{HF}$ complex which is larger than -7.2 ± 1.7 kcal/mol, determined by infrared intensity [18] but quite smaller than -10.3 ± 0.2 kcal/mol determined by absolute intensities of rotational transitions [20].

TABLE X
BSSE ESTIMATES OF $\text{H}_2\text{O}\cdot\text{HO}$ AND $\text{H}_2\text{O}\cdot\text{HF}$ [a]

		E(BSSE)	$\Delta E'$
$\text{H}_2\text{O}\cdot\text{HO}$			
D95**//D95**		0.228	-6.012 to -5.784
6-311++G**	[b]	0.532	-5.817 to -5.285
6-31G**	[c]	0.759	-6.470 to -5.711
6-311G**	[c]	1.189	-6.545 to -5.356
6-311+G**	[c]	0.654	-5.723 to -5.069
6-311++G**	[c]	0.617	-5.692 to -5.075
6-311+G(2d,2p)	[c]	0.371	-4.913 to -4.542
UMP2/D95**//D95**		0.926	-6.878 to -5.952
UMP2/6-311++G**	[b]	1.143	-6.551 to -5.408
UMP2/6-31G**	[c]	1.457	-7.467 to -6.010
UMP2/6-311G**	[c]	2.061	-7.587 to -5.526
UMP2/6-311+G**	[c]	1.399	-6.589 to -5.190
UMP2/6-311++G**	[c]	1.386	-6.601 to -5.215
UMP2/6-311+G(2d,2p)	[c]	0.852	-5.943 to -5.091
$\text{H}_2\text{O}\cdot\text{HO}$			
6-31G**	[c]	1.074	-9.061 to -7.987
6-311G**	[c]	1.740	-9.406 to -7.666
6-311+G**	[c]	0.837	-8.296 to -7.459
6-311++G**	[c]	0.875	-8.346 to -7.471
6-311+G(2d,2p)	[c]	0.461	-7.499 to -7.038
MP2/6-31G**	[c]	1.993	-10.392 to -8.399
MP2/6-311G**	[c]	3.061	-10.850 to -7.789
MP2/6-311+G**	[c]	1.890	-9.482 to -7.592
MP2/6-311++G**	[c]	1.952	-9.544 to -7.592
MP2/6-311+G(2d,2p)	[c]	1.184	-8.835 to -7.651
exp.[18]			-7.2 \pm 1.7
exp.[20]			-10.3 \pm 0.2

- a. All energies in kcal/mol; $\Delta E'$ is the range of binding energy: the binding energies between corrected and uncorrected by BSSE.
b. 6-311++G** based on geometries optimized by 6-311++G**.
c. based on geometries optimized by 6-31G**.

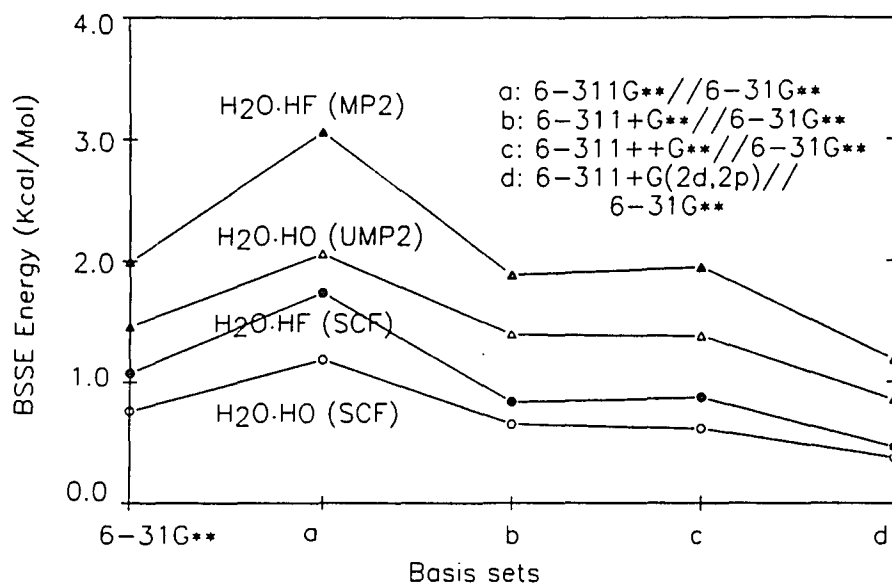


Figure 5. BSSE calculated for H₂O·HO and H₂O·HF systems.

CHAPTER III

$\text{H}_2\text{O} \cdot \text{HO}_2$ AND $\text{H}_2\text{O} \cdot \text{H}_2\text{O}$ SYSTEM

The hydroperoxyl radical, HO_2 , plays important roles in atmospheric chemistry just like the HO radical. As mentioned before, with HO, HO_2 is involved in the generation and destruction of ozone in the atmosphere.

Another type of reaction, the atmospherically important self-reaction of HO_2 in the gas phase is increased by up to a factor of 2.5 at 298K in the presence of H_2O [62]. The formation of the complex $\text{H}_2\text{O} \cdot \text{HO}_2$ has been proposed as the key step for this rate increase [63]. This complex $\text{H}_2\text{O} \cdot \text{HO}_2$ has been studied by Hamilton [32], but because of technology and theory limitations at that time, the calculation remained at the SCF level and the geometry was only partially optimized.

MONOMER PROPERTIES OF H_2O AND HO_2

The results of geometry optimization of monomers HO_2 and H_2O at the SCF level are shown in Table XI along with experimental data for purposes of comparison. Again, polarized basis sets give more accurate angle descriptions and dipole moment values, but are somewhat short in calculated bond lengths, while unpolarized basis sets give more accurate bond length descriptions. For example,

the dipole moment of 2.095, derived by 6-31G** is very close to experimental data of 2.09. The bond angle of 105.8°, derived by 6-31G**, is only 1.7% larger than experimental data. But the bond length derived from 6-31G** averages 2.4% shorter than experimental data.

TABLE XI
OPTIMIZED GEOMETRIES OF H₂O AND HO₂ [a]

Parameter	Basis set					Exp.
	4-31G	6-31G	D95	6-31G**	D95**	
H2O						
O-H1,2	0.950	0.950	0.951	0.943	0.944	0.958 b
H1OH2	111.2	111.6	112.5	106.0	106.6	104.5
μ (D)	2.486	2.501	2.530	2.148	2.180	1.85 c
HO ₂						
H-O1	0.959	0.957	0.959	0.950	0.951	0.977 d
O1-O2	1.396	1.382	1.374	1.309	1.309	1.335
HO1O2	106.2	106.9	107.7	105.8	106.0	104.1
μ (D)	2.326	2.345	2.367	2.095	2.104	2.09 e

a. Geometrical parameters are given in Å and degrees.

b. ref.54. c. ref.55. d. ref.64. e. ref.65.

In Table XII, the harmonic frequencies are reported for all monomers, and again compared with experiment. The data were scaled by 0.9 to remove systematic error [39]. After scaling, the data derived from polarized basis sets are very comparable with experimental data. Furthermore, the scaling factor will be designed for each mode for the 6-31G** basis set to get our best estimates of frequencies below.

TABLE XII
CALCULATED FREQUENCIES WITH EXPERIMENTAL
MEASURED AND HARMONIC (IN PARENTHESES)
FREQUENCIES (IN CM⁻¹) OF H₂O AND HO₂

	4-31G	6-31G	D95	6-31G**	D95**	Exp.[a]
H ₂ O						
s-stretch	3563	3590	3625	3732	3748	3657 (3832)
bend	1568	1563	1540	1593	1576	1595 (1649)
a-stretch	3699	3731	3783	3838	3858	3756 (3942)
HO ₂						
ho stretch	3519	3546	3588	3670	3688	3436
oo stretch	1357	1368	1369	1441	1433	1392
bend	747	807	910	1128	1145	1098

a. The frequencies of H₂O are from ref.61 and ref.39, HO₂ are from ref.66.

The total energies in SCF and MP2 level are reported in Table XIII with their $\langle S^2 \rangle$ value, if they are open-shell species. In the SCF level for open-shell species, the $\langle S^2 \rangle$ value is quite close to that of a pure doublet wavefunction (0.75). The largest $\langle S^2 \rangle$ is 0.7716 for HO₂ of 4-31G basis set. For polarized basis sets, the $\langle S^2 \rangle$ values are even smaller, with the 0.7609 as the largest for HO₂ of D95**, and the MP2 calculations reduce the $\langle S^2 \rangle$ further. At the MP2 level, the largest is 0.7628 for HO₂ of 4-31G. Again the largest for polarized basis sets is 0.7519 for HO₂ by D95**. All those $\langle S^2 \rangle$ values indicate that the effects due to spin contamination are very low.

Furthermore, the $\langle S^2 \rangle$ values derived from different basis sets vs basis sets for HO₂ and HO₂ are shown in figure 6. With the higher and higher quality of basis sets, the $\langle S^2 \rangle$ become closer and closer to 0.75. The $\langle S^2 \rangle$ values seem to

TABLE XIII
TOTAL ENERGIES (AU) AND $\langle S^2 \rangle$ VALUES
OF H_2O AND HO_2 [a]

	E(SCF)	$\langle S^2 \rangle$	E(MP2)	$\langle S^2 \rangle$
H_2O				
4-31G	-75.90864		-76.03598	
6-31G	-75.98536		-76.11205	
D95	-76.01100		-76.13501	
6-31G**	-76.02362		-76.21906	
D95**	-76.04695		-76.24209	
HO_2				
4-31G	-149.96325	0.7716	-150.18659	0.7628
6-31G	-150.11378	0.7671	-150.33538	0.7592
D95	-150.16090	0.7660	-150.37273	0.7580
6-31G**	-150.17664	0.7594	-150.50748	0.7513
D95**	-150.21933	0.7609	-150.54478	0.7519

a. geometries optimized by specified basis set, UHF and UMP2 were used for open-shell species.

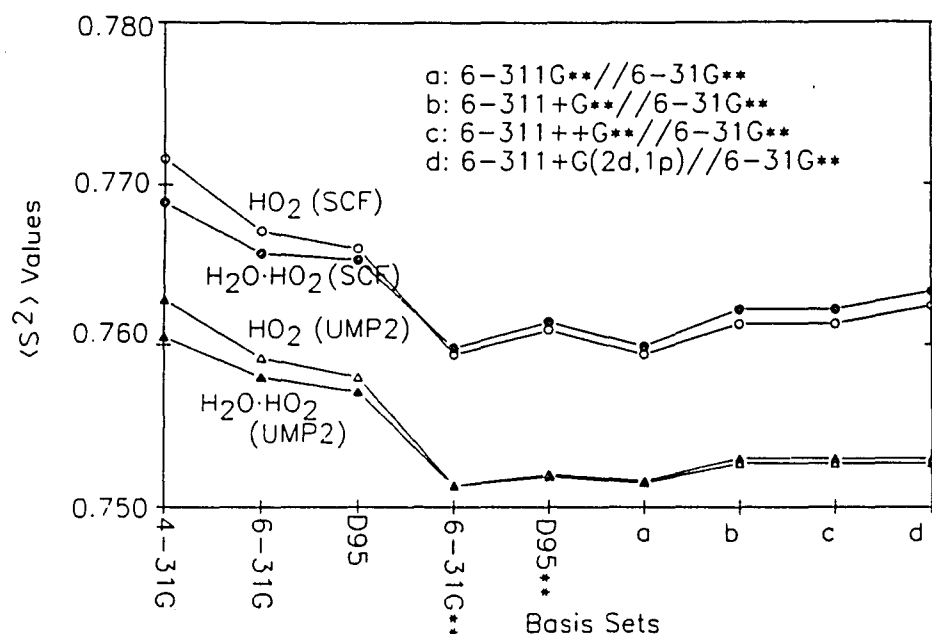


Figure 6. $\langle S^2 \rangle$ values of HO_2 and $\text{HO}_2 \cdot \text{HO}_2$ calculated from different basis sets.

converge to 0.752.

GEOMETRIES OF $\text{H}_2\text{O} \cdot \text{HO}_2$ AND $\text{H}_2\text{O} \cdot \text{H}_2\text{O}$

This system is somewhat analogous to the water dimer, although HO_2 could serve as a hydrogen acceptor as in the complex $\text{HO}_2 \cdot \text{HO}$ studied by Jackels and Phillips [67]. The water dimer is an ideal hydrogen-bonded model system and has been the subject of experimental and theoretical studies for decades [2-14]. The water dimer has been shown to have C_s symmetry, shown in Figure 7.1, and its dissociation energy was experimentally determined to be $5.4(\pm 0.7)$ kcal/mol [13].

Previous work [32] on $\text{H}_2\text{O} \cdot \text{HO}_2$ performed a point-by-point partial geometry optimization and derived an almost planar structure (the H_2O plane was 4° out of the HO_2 plane). In our studies, first we tried to determine the complex symmetry. Both planar and C_s symmetries were placed on the system and each was partially

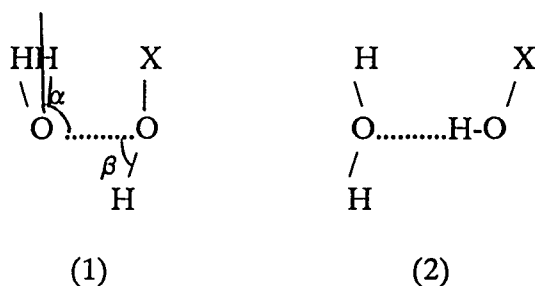


Figure 7. Symmetries of $\text{H}_2\text{O} \cdot \text{HOX}$ complex ($\text{X}=\text{H}, \text{O}$).
 (1): C_s symmetry. (2): Planar symmetry

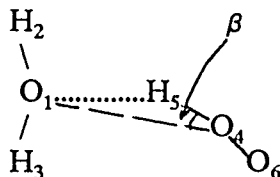


Figure 8. Optimized structure of $\text{H}_2\text{O} \cdot \text{HO}_2$.

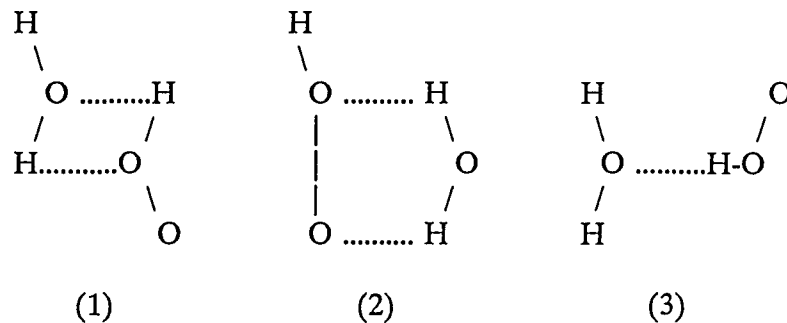


Figure 9. Starting structures for $\text{H}_2\text{O}\cdot\text{HO}_2$.

TABLE XIV
OPTIMIZED STRUCTURES AND CALCULATED HARMONIC
FREQUENCIES OF $\text{H}_2\text{O}\cdot\text{HO}_2$ [a]

Parameter	4-31G	6-31G	D95	6-31G**	D95**
Planar					
O1-H2	0.950	0.949	0.952	0.943	0.945
O1-H3	0.950	0.949	0.951	0.943	0.944
O1-O4	2.679	2.693	2.704	2.827	2.840
O4-H5	0.971	0.970	0.971	0.956	0.957
O4-O6	1.390	1.378	1.370	1.307	1.307
H2O1H3	112.7	112.8	113.0	107.5	107.7
H2O1O4	117.7	117.8	120.1	115.0	115.1
O1O4H5	4.9	5.1	3.3	7.8	7.8
H5O4O6	105.2	105.9	107.0	105.3	105.5
$\mu(\text{D})$	5.675	5.669	5.681	4.768	4.756
C_s					
O1-H2,3	0.950	0.949	0.951	0.944	0.945
O1-O4	2.681	2.694	2.700	2.829	2.848
O4-H5	0.971	0.970	0.971	0.957	0.957
O4-O6	1.390	1.378	1.370	1.307	1.307
H2O1H3	112.6	112.7	112.9	106.6	107.2
α	175.5	176.1	178.8	127.4	145.6
β	1.4	1.5	0.7	8.1	3.7
H5O4O6	105.8	106.5	107.6	105.2	105.7
$\mu(\text{D})$	5.719	5.716	5.713	4.050	4.502

TABLE XIV
OPTIMIZED STRUCTURES AND CALCULATED HARMONIC
FREQUENCIES OF $\text{H}_2\text{O} \cdot \text{HO}_2$ [a]
(continued)

4-31G		6-31G		D95		6-31G**		D95**	
Planar	C_s	Planar	C_s	Planar	C_s	Planar	C_s	Planar	C_s
50	i ^[b]	49	i	33	17	i	i	i	i
77	98	75	97	86	110	41	68	51	74
225	231	235	229	237	236	89	207	101	188
253	238	246	237	275	245	199	212	188	205
363	285	363	291	366	326	287	280	289	227
669	788	651	768	680	775	465	625	483	606
787	791	833	836	932	934	1137	1137	1154	1154
1533	1483	1533	1486	1536	1495	1538	1520	1528	1507
1580	1583	1579	1582	1573	1575	1584	1592	1578	1583
3285	3284	3320	3319	3361	3359	3577	3556	3590	3578
3581	3581	3607	3607	3637	3637	3737	3727	3745	3742
3712	3711	3741	3740	3778	3778	3843	3828	3853	3847

a. Geometric parameters are given in Å and degrees. Frequencies are in cm^{-1} .

b. Frequency is negative.

optimized to stationary points shown in Figure 7. After calculating vibrational frequencies, the geometries optimized by 4-31G, 6-31G and D95 basis sets for planar symmetry were energy minima. The C_s symmetry was not an energy minimum except for the D95 basis set. The planar and C_s symmetries optimized by basis sets 6-31G** and D95** have imaginary vibrational frequencies, which means they are not the energy minima. The results are shown in Table XIV. In order to clarify the performance of the basis sets we used, the same basis sets were used to optimize the $\text{H}_2\text{O} \cdot \text{H}_2\text{O}$ dimer with both planar and C_s symmetry, although very high quality basis sets have already been used to calculate the

$\text{H}_2\text{O}\cdot\text{H}_2\text{O}$ dimer [3,4,5]. The vibrational frequencies were calculated for the optimized structure. The results are shown in Table XV. The C_s symmetry is shown to be the energy minimum for all basis sets. The O--O distances of D95** and 6-31G** are very close to the experimental value of 2.98 Å [12], which means the 6-31G** and D95** give a acceptable description of the dimer geometries. If we examine the alpha angle, shown in Figure 10, we find that 6-31G** gives the smallest value, the unpolarized basis sets give larger values and the D95** value is

TABLE XV
OPTIMIZED STRUCTURES AND CALCULATED HARMONIC
FREQUENCIES OF $\text{H}_2\text{O}\cdot\text{H}_2\text{O}$ [a]

parameter	4-31G	6-31G	D95	6-31G**	D95**	[b]	exp[12]
Planar							
O1-H2	0.950	0.949	0.951	0.943	0.944		
O1-H3	0.950	0.950	0.952	0.943	0.945		
O1-O4	2.836	2.847	2.843	3.003	3.009		
O4-H5	0.958	0.957	0.959	0.947	0.948		
O4-H6	0.949	0.948	0.950	0.942	0.943		
H2O1H3	112.1	112.3	112.8	106.9	107.2		
H2O1O4	138.1	138.3	136.6	140.3	139.9		
O1O4H5	3.4	3.9	4.3	3.0	3.7		
H5O2H6	111.5	111.8	113.0	105.8	106.5		
$\mu(\text{D})$	4.545	4.514	4.515	3.962	3.955		
C_s							
O1-H2,3	0.950	0.950	0.951	0.944	0.945		
O1-O4	2.832	2.843	2.837	2.980	2.986	2.911	2.98
O4-H5	0.958	0.957	0.959	0.948	0.949	0.964	
O4-H6	0.949	0.948	0.950	0.942	0.943		
H2O1H3	112.0	112.2	112.8	106.3	106.9		
α	148.4	151.5	158.4	117.6	134.0	123.2	140 ± 10
β	0.0	0.3	0.4	10.6	14.5	4.5	<10
H5O4H6	111.3	111.6	111.7	105.9	106.5		
$\mu(\text{D})$	4.003	4.290	4.438	2.644	3.213		

TABLE XV
OPTIMIZED STRUCTURES AND CALCULATED HARMONIC
FREQUENCIES OF $\text{H}_2\text{O}\cdot\text{H}_2\text{O}$ [a]
(continued)

4-31G		6-31G		D95		6-31G**		D95**	
Planar	C _s	Planar	C _s	Planar	C _s	Planar	C _s	Planar	C _s
i ^[c]	118	i	113	i	122	i	106	i	121
139	151	139	152	150	174	i	124	37	131
144	158	147	159	186	183	113	128	117	131
186	189	183	185	187	194	144	159	142	153
432	374	427	366	439	381	331	339	333	315
573	685	563	672	594	696	408	551	432	553
1574	1576	1572	1574	1562	1563	1587	1591	1579	1580
1621	1610	1613	1602	1589	1583	1623	1618	1606	1602
3485	3483	3513	3511	3540	3539	3700	3689	3711	3703
3574	3572	3600	3599	3633	3634	3736	3728	3746	3743
3667	3666	3700	3698	3750	3748	3817	3814	3837	3834
3706	3704	3736	3735	3779	3779	3841	3830	3854	3849

- a. Geometric parameters are given in Å and degrees. Frequencies are in cm^{-1} .
b. from ref.5, optimized by MP2/6-311++G(2d,2p).
c. Frequency is negative.

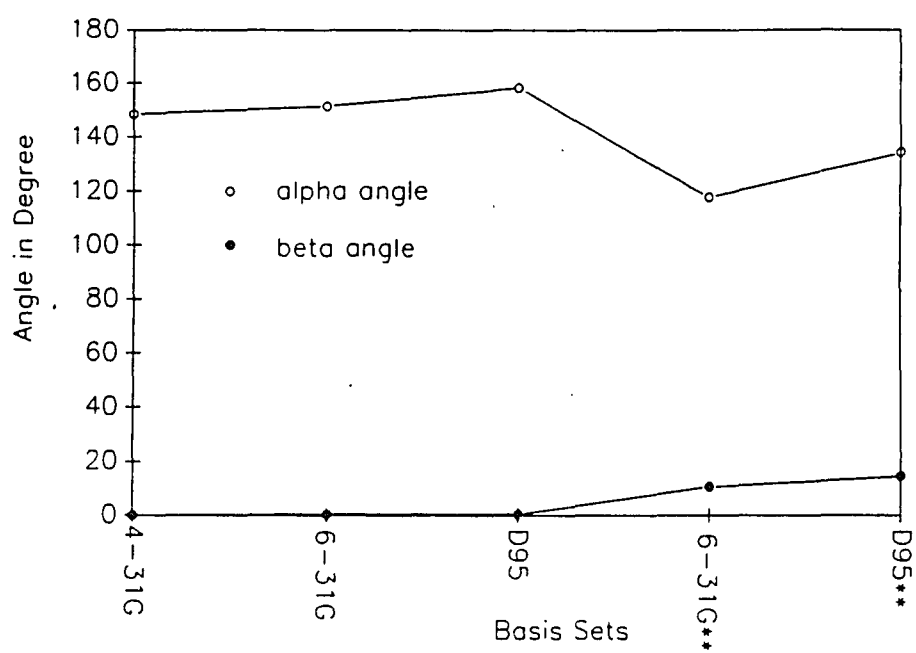


Figure 10. Alpha and Beta angles of $\text{HO}_2 \cdot \text{H}_2\text{O}$ (C_s) optimized by different basis sets.

intermediate. This behavior of basis sets we used is similar to that of $\text{H}_2\text{O}\cdot\text{HO}$ and $\text{H}_2\text{O}\cdot\text{HF}$.

Fully optimized geometries of $\text{H}_2\text{O}\cdot\text{HO}_2$ with 6-31G** and D95** is shown in Table XVI and displayed in Figure 8, which have no symmetry at all. Now, the polarized basis sets and unpolarized basis sets give quite different results for $\text{H}_2\text{O}\cdot\text{HO}_2$. Unpolarized basis sets give the planar symmetries while polarized basis sets give no symmetry. The O--O distance is shorter in the geometries optimized with unpolarized basis sets (2.679-2.704 Å) than those optimized by polarized basis sets (2.812-2.841 Å). The shorter O--O bond distance relative to those of $\text{H}_2\text{O}\cdot\text{HO}$ (2.938 Å) and $\text{H}_2\text{O}\cdot\text{H}_2\text{O}$ (2.980-2.986 Å), reflect the stronger interaction in the $\text{H}_2\text{O}\cdot\text{HO}_2$ complex. Hamilton's [32] geometry for $\text{H}_2\text{O}\cdot\text{HO}_2$ is similar to our optimized results with unpolarized basis sets, except the H_2O plane is about 4° out of the HO_2 plane.

In the last chapter of studying complexes $\text{H}_2\text{O}\cdot\text{HO}$ and $\text{H}_2\text{O}\cdot\text{HF}$, we found basis set 6-31G** gave more accurate geometrical description and dipole moment descriptions for $\text{H}_2\text{O}\cdot\text{HF}$. In this chapter we also found that basis set 6-31G** gives more accurate geometry dipole moment description of $\text{H}_2\text{O}\cdot\text{H}_2\text{O}$. So we believe that, by analogy, the geometry of $\text{H}_2\text{O}\cdot\text{HO}_2$ derived by basis set 6-31G** is a more accurate geometrical description.

Different orientations of the $\text{H}_2\text{O}\cdot\text{HO}_2$ complex, shown in Figure 9, were used to start the geometry optimization. Only the orientation (3) was found to be an energy minimum.

TABLE XVI
FULLY OPTIMIZED STRUCTURES AND VIBRATIONAL
FREQUENCIES OF $\text{H}_2\text{O} \cdot \text{HO}_2$ [a]

	6-31**	D95**
Geometry		
O1-H2	0.944	0.945
O1-H3	0.945	0.945
O1--O4	2.812	2.841
O4-H5	0.957	0.957
O4-O6	1.307	1.307
H2O1H3	106.9	107.3
H2O1O4	120.9	125.3
O1O4H5	12.9	7.2
H5O4O6	104.9	105.4
H3O1H2H5	121.0	140.6
H2O1H5O4	107.3	121.3
O1H5O4O6	9.2	5.0
$\mu(\text{D})$	3.995	4.496
Frequency		
	47	47
	89	60
	205	177
	219	192
	320	290
	556	540
	1136(+8)	1154(+9)
	1539(+98)	1526(+93)
	1588(-5)	1580(+4)
	3558(-112)	3580(-108)
	3727(-5)	3741(-7)
	3830(-8)	3847(-11)

- a. Geometric parameters are given in Å and degrees. Frequencies are given in cm^{-1} .
- b. The values in parentheses are frequency-shifts compared to the same mode of monomer (calculated values).

VIBRATIONAL FREQUENCIES OF $\text{H}_2\text{O}\cdot\text{H}_2\text{O}$ AND $\text{H}_2\text{O}\cdot\text{HO}_2$

If we examine the harmonic frequencies of the 6-31G** and D95** calculations (Table XVII), the HO stretch of HO_2 in the $\text{H}_2\text{O}\cdot\text{HO}_2$ dimer is considerably red-shifted, and the O--O stretch is shifted to the blue. This means the O-H bond is weakened in complex formation and the O-O bond (in the HO_2 fragment) is strengthened. So, the complex $\text{H}_2\text{O}\cdot\text{HO}_2$ is helping to dissociate the atom H from atom O in HO_2 . The modes of H_2O do not change much, which means the H_2O fragment would not change much compared to the H_2O monomer.

TABLE XVII

CALIBRATED HARMONIC FREQUENCIES (CM^{-1}) BY 6-31G** [a]

$\text{H}_2\text{O}\cdot\text{HO}_2$				$\text{H}_2\text{O}\cdot\text{H}_2\text{O}$			
[b]	S.F.	Freq.	IR_INT.	[b]	S.F.	Freq.	IR_INT.
	0.8753	45	26		0.8880	105	93
	0.8753	86	57		0.8880	122	252
	0.8753	199	26		0.8880	126	119
	0.8753	213	191		0.8880	157	124
	0.8753	311	90		0.8880	335	89
	0.8753	541	237		0.8880	543	203
HO_2	0.8764	1106(+8)	44	Acceptor	0.9013	1594(-1)	112
HO_2	0.8690	1486(+94)	74	Donor	0.9013	1620(+25)	99
H_2O	0.9013	1590(-5)	105	Donor	0.8819	3615(-42)	181
HO_2	0.8425	3331(-105)	437	Acceptor	0.8819	3653(-4)	27
H_2O	0.8819	3652(-5)	34	Donor	0.8809	3733(-23)	105
H_2O	0.8809	3749(-7)	106	Acceptor	0.8809	3749(-7)	89

- The values in parentheses are frequency-shifts compared to the same mode of the monomer (experimental values).
- The fragment in the complex mainly involved in the vibrational mode. IR_INT. is the IR intensity in KM/MOLE. S.F. is the scaling factor.

In order to give the most reasonable prediction of harmonic frequencies of complexes $\text{H}_2\text{O}\cdot\text{HO}_2$ and $\text{H}_2\text{O}\cdot\text{H}_2\text{O}$, the new scaling factors are calculated for each mode of monomers as the ratio of the experimental data and the calculated frequency of the same mode. Then the average of those scaling factors is used for the low frequency modes in the complex. The results are presented in Table XVII (only for 6-31G** basis set). The calculated scaling factor is 0.8753 for $\text{H}_2\text{O}\cdot\text{HO}_2$ and 0.8880 for $\text{H}_2\text{O}\cdot\text{H}_2\text{O}$.

Comparing the frequency-shift between the complexes $\text{H}_2\text{O}\cdot\text{HO}_2$ and $\text{H}_2\text{O}\cdot\text{H}_2\text{O}$, which are shown in Table XVII, the OH stretch mode of donor fragment shifts quite differently, with the $\text{H}_2\text{O}\cdot\text{HO}_2$ shift 105 cm^{-1} and $\text{H}_2\text{O}\cdot\text{H}_2\text{O}$ shift 42 cm^{-1} , which means the $\text{H}_2\text{O}\cdot\text{HO}_2$ has a stronger interaction energy than $\text{H}_2\text{O}\cdot\text{H}_2\text{O}$.

ENERGIES OF $\text{H}_2\text{O}\cdot\text{H}_2\text{O}$ AND $\text{H}_2\text{O}\cdot\text{HO}_2$

Total energies of $\text{H}_2\text{O}\cdot\text{HO}_2$ and $\text{H}_2\text{O}\cdot\text{H}_2\text{O}$ at the SCF and MP2 levels are shown in Table XVIII with their symmetries and $\langle S^2 \rangle$ values. The $\langle S^2 \rangle$ values are very close to its pure doublet value 0.75. In the SCF level, the $\langle S^2 \rangle$ value is in the range of 0.7598 to 0.7689, with the 4-31G highest and 6-31G** lowest. The UMP2 calculations reduce the $\langle S^2 \rangle$ value to better results. The $\langle S^2 \rangle$ value in UMP2 level is in the range of 0.7505 to 0.7513, also with 4-31G highest and 6-31G** lowest. The $\langle S^2 \rangle$ value changes with basis sets are shown in Figure 6 with monomer HO_2 . From Figure 6, basis set 6-31G** not only gives the lowest $\langle S^2 \rangle$ values in both SCF and UMP2 level, but also gives the least different

TABLE XVIII
TOTAL ENERGIES AND BINDING ENERGIES OF
 $\text{H}_2\text{O} \cdot \text{HO}_2$ AND $\text{H}_2\text{O} \cdot \text{H}_2\text{O}$ [a]

	Symmetry	E	$\langle S^2 \rangle$	ΔE
$\text{H}_2\text{O} \cdot \text{HO}_2$				
4-31G//4-31G	C_{2v}	-225.89251	0.7689	-12.939
6-31G//6-31G	C_{2v}	-226.11887	0.7657	-12.381
D-95//D95	C_{2v}	-226.19071	0.7653	-11.803
6-31G**//6-31G**	C_1	-226.21363	0.7598	-8.390
D-95**//D95**	C_1	-226.27829	0.7614	-7.536
UMP2/4-31G//4-31G	C_{2v}	-226.24541	0.7605	-14.332
UMP2/6-31G//6-31G	C_{2v}	-226.46922	0.7580	-13.673
UMP2/D-95//D95	C_{2v}	-226.52904	0.7571	-13.366
UMP2/6-31G**//6-31G**	C_1	-226.74413	0.7513	-11.076
UMP2/D-95**//D95**	C_1	-226.80238	0.7520	-9.733
$\text{H}_2\text{O} \cdot \text{H}_2\text{O}$				
4-31G//4-31G	C_s	-151.83038		-8.220
6-31G//6-31G	C_s	-151.98322		-7.844
D-95//D95	C_s	-152.03419		-7.646
6-31G**//6-31G**	C_s	-152.05606		-5.535
D-95**//D95**	C_s	-152.10188		-5.008
MP2/4-31G//4-31G	C_s	-152.08613		-8.892
MP2/6-31G//6-31G	C_s	-152.23748		-8.396
MP2/D-95//D95	C_s	-152.28364		-8.547
MP2/6-31G**//6-31G**	C_s	-152.44950		-7.141
MP2/D-95**//D95**	C_s	-152.49397		-6.143

a. The geometries were optimized by the specific basis sets; E's are in a.u., ΔE in kcal/mole. $\text{H}_2\text{O} \cdot \text{HO}_2$ is calculated by UHF and UMP2. $\text{H}_2\text{O} \cdot \text{H}_2\text{O}$ is calculated by RHF and MP2.

$\langle S^2 \rangle$ value between HO_2 and $\text{H}_2\text{O} \cdot \text{HO}_2$.

Again the binding energies calculated by unpolarized basis sets are much larger than those derived by polarized basis sets. Also, the binding energy of $\text{H}_2\text{O} \cdot \text{HO}_2$ is about 1.5 times larger than that of $\text{H}_2\text{O} \cdot \text{H}_2\text{O}$.

The geometries of $\text{H}_2\text{O} \cdot \text{H}_2\text{O}$ and $\text{H}_2\text{O} \cdot \text{HO}_2$ optimized by 6-31G** are used to do the 6-311G**, 6-311+G**, 6-311++G** and 6-311+G(2d,1p) calculations at the SCF and MP2 levels. The results for these one point calculations are shown in Table XIX. The $\langle S^2 \rangle$ values are also shown in Figure 6. They are close but a little higher than those derived by 6-31G**. The binding energies are

TABLE XIX
TOTAL ENERGIES AND BINDING ENERGIES OF
 H_2O , HO_2 , $\text{H}_2\text{O} \cdot \text{HO}_2$ AND $\text{H}_2\text{O} \cdot \text{H}_2\text{O}$ USING THE GEOMETRIES
OPTIMIZED BY BASIS SET 6-31G** [a]

Basis set	$E(\text{HO}_2)$	$\langle S^2 \rangle$	$E(\text{H}_2\text{O} \cdot \text{HO}_2)$	$\langle S^2 \rangle$	ΔE
6-311G**	-150.21874	0.7594	-226.27928	0.7599	-8.503
6-311+G**	-150.22315	0.7613	-226.28776	0.7622	-7.097
6-311++G**	-150.22328	0.7613	-226.28800	0.7622	-7.091
6-311+G(2d,1p)	-150.22799	0.7624	-226.29268	0.7633	-6.570
MP2/6-311G**	-150.58522	0.7515	-226.86643	0.7516	-11.22
MP2/6-311+G**	-150.59333	0.7527	-226.88262	0.7530	-9.532
MP2/6-311++G**	-150.59352	0.7527	-226.88307	0.7530	-9.570
MP2/6-311+G(2d,1p)	-150.62734	0.7527	-226.93125	0.7530	-9.268

	$E(\text{H}_2\text{O})$	$E(\text{H}_2\text{O} \cdot \text{H}_2\text{O})$	ΔE
6-311G**	-76.04699	-152.10284	-5.560
6-311+G**	-76.05330	-152.11397	-4.625
6-311++G**	-76.05342	-152.11416	-4.593
6-311+G(2d,1p)	-76.05422	-152.11537	-4.384
MP2/6-311G**	-76.26333	-152.53774	-6.953
MP2/6-311+G**	-76.27410	-152.55741	-5.779
MP2/6-311++G**	-76.27430	-152.55784	-5.798
MP2/6-311+G(2d,1p)	-76.28914	-152.58730	-5.706

a. E's are in a.u. and ΔE 's are in kcal/mole. HO_2 and $\text{H}_2\text{O} \cdot \text{HO}_2$ are calculated by UHF and UMP2. H_2O and $\text{H}_2\text{O} \cdot \text{H}_2\text{O}$ are calculated by RHF and MP2.

also shown in Table XIX.

In the SCF level, the binding energies of $\text{H}_2\text{O} \cdot \text{H}_2\text{O}$ are in the range of -4.384 to -5.535 kcal/mol. Those are in the range of or smaller than experimental data of -5.4 ± 0.7 kcal/mol. But they are much lower than those derived from unpolarized basis sets (-7.646 to -8.220 kcal/mol). But in the MP2 level, the binding energies of $\text{H}_2\text{O} \cdot \text{H}_2\text{O}$ are in the range of -5.706 to -7.141 kcal/mol, which are in the range of or higher than experimental data. Also they are much lower than those derived from unpolarized basis sets (-8.547 to -8.892 kcal/mol). It seems the electron correlation gives too much correction to the binding energy. Comparing to those results of $\text{H}_2\text{O} \cdot \text{H}_2\text{O}$, the binding energies of $\text{H}_2\text{O} \cdot \text{HO}_2$ in the SCF level are in the range of -6.570 to -8.390 kcal/mol, while in the MP2 level, the binding energies of $\text{H}_2\text{O} \cdot \text{H}_2\text{O}$ are in the range of -9.268 to -11.076 kcal/mol. They are all lower than those derived from unpolarized basis sets.

The BSSE energies are calculated for the $\text{H}_2\text{O} \cdot \text{HO}_2$ and $\text{H}_2\text{O} \cdot \text{H}_2\text{O}$ systems. The results are shown in Table XX and Figure 11. Except those calculated by 6-311G**, the BSSE energies become smaller when more extensive basis sets are used. This is consistent with the BSSE concept: when basis sets become infinite, the BSSE energies should become zero. The BSSE energies derived from MP2 level are about twice larger than those derived from SCF level in both complexes.

After BSSE correction, apparently the binding energies of $\text{H}_2\text{O} \cdot \text{H}_2\text{O}$ derived in SCF level are too low. But in the MP2 level, the binding energies is in the range of -4.649 to -5.301 kcal/mol, which are in the lower bound of experimental

TABLE XX
BSSE ESTIMATES AND BINDING ENERGIES OF
 $\text{H}_2\text{O} \cdot \text{HO}_2$ AND $\text{H}_2\text{O} \cdot \text{HO}_2$ [a]

		E(BSSE)	$\Delta E'$
$\text{H}_2\text{O} \cdot \text{HO}_2$			
D95**//D95**		0.438	-7.536 to -7.098
6-31G**	[b]	1.255	-8.390 to -7.135
6-311G**	[b]	1.870	-8.503 to -6.633
6-311+G**	[b]	0.872	-7.097 to -6.225
6-311++G**	[b]	0.868	-7.091 to -6.223
6-311+G(2d,1p)	[b]	0.684	-6.570 to -5.886
UMP2/D95**//D95**		1.359	-9.733 to -8.374
UMP2/6-31G**	[b]	2.327	-11.076 to -8.749
UMP2/6-311G**	[b]	3.206	-11.220 to -8.014
UMP2/6-311+G**	[b]	1.928	-9.532 to -7.604
UMP2/6-311++G**	[b]	1.968	-9.570 to -7.602
UMP2/6-311+G(2d,1p)	[b]	1.406	-9.268 to -7.862
$\text{H}_2\text{O} \cdot \text{HO}_2$ [a]			
6-31G**	[b]	0.984	-5.535 to -4.551
6-311G**	[b]	1.466	-5.560 to -4.094
6-311+G**	[b]	0.575	-4.625 to -4.050
6-311++G**	[b]	0.549	-4.593 to -4.044
6-311+G(2d,1p)	[b]	0.505	-4.384 to -3.879
MP2/6-31G**	[b]	1.840	-7.141 to -5.301
MP2/6-311G**	[b]	2.610	-6.953 to -4.343
MP2/6-311+G**	[b]	1.302	-5.779 to -4.477
MP2/6-311++G**	[b]	1.329	-5.798 to -4.469
MP2/6-311+G(2d,1p)	[b]	1.057	-5.706 to -4.649
exp.[13]			-5.4 \pm 0.7
[c]			-4.7 \pm 0.35
[d]			-4.6 to -5.3

a. All energies in kcal/mol; $\Delta E'$'s are the range of binding energy.

b. based on geometries optimized by 6-31G**.

c. from ref.3 calculated by perturbation method.

d. from ref.5 calculated by

MP4/6-311++G(3df,3dp)//MP2/6-311++G(2d,2p).

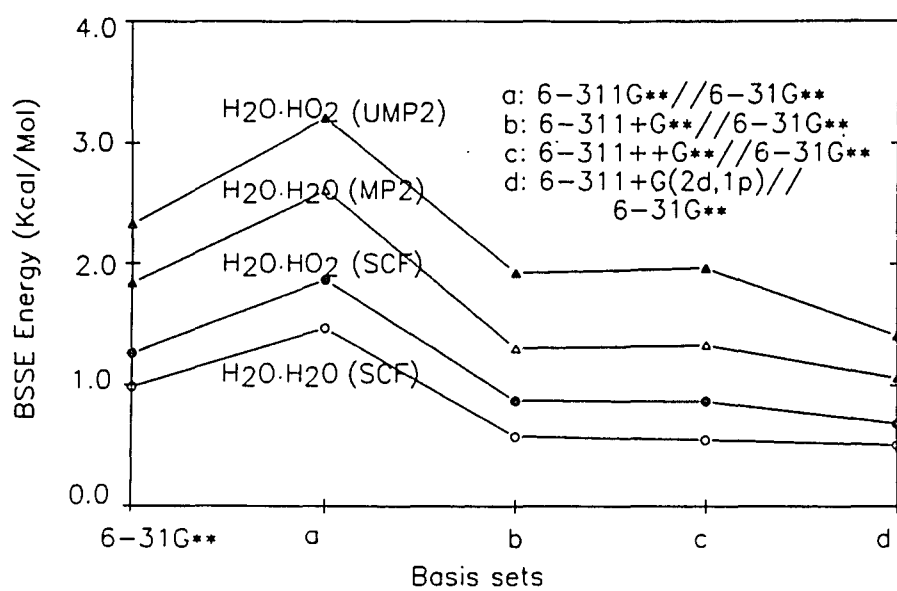


Figure 11. BSSE calculated for HO₂·HO₂ and HO₂·H₂O systems.

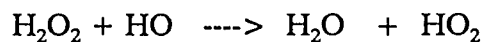
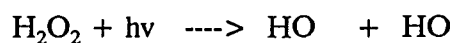
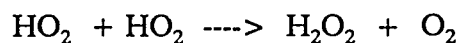
data of -5.4 ± 0.7 kcal/mol. So it might suggest that the BSSE energies are overestimated. For the case of $\text{H}_2\text{O} \cdot \text{HO}_2$, after BSSE correction, the binding energies derived in SCF level are in the range of -5.886 to -7.135 kcal/mol, while those derived in the UMP2 level are in the range of -7.862 to -8.749 kcal/mol.

If we took the mp2/6-311+G(2d,1p)//6-31G** calculation as the best results and treat the BSSE energy as partially in effect, then the binding energy is in the range of -9.3 to -7.9 kcal/mol for $\text{H}_2\text{O} \cdot \text{HO}_2$ and -5.7 to -4.7 kcal/mol for $\text{H}_2\text{O} \cdot \text{H}_2\text{O}$. Our results indicate the previous binding energy for $\text{H}_2\text{O} \cdot \text{HO}_2$ is near the upper bound. Our result of $\text{H}_2\text{O} \cdot \text{H}_2\text{O}$ binding energy is consistent with previous work of -4.7 ± 0.35 by perturbation method [3] and -4.6 to -5.3 kcal/mol by MP4/6-311++G(3df,3dp)//MP2/6-311++G(2d,2p) [5] and -5.4 ± 0.7 kcal/mol of experimental data [13].

CHAPTER IV

$\text{H}_2\text{O} \cdot \text{H}_2\text{O}_2$ SYSTEM

As mentioned before, "odd hydrogen" radicals HO and HO_2 are very important species in the atmospheric chemistry. Those two species can be converted to each other by H_2O_2 by the following reactions:



In the natural troposphere, H_2O_2 is produced mainly by HO_2 self-reaction and destroyed by photochemical reactions and washout. H_2O_2 is much more stable than HO and HO_2 , especially at night. So H_2O_2 is the reservoir of the "odd hydrogen" family. Also because H_2O_2 has two hydrogen binding sites to two oxygen, it would be expected to form fairly stable hydrogen binding with water molecules.

MONOMER PROPERTIES OF H_2O AND H_2O_2

Before presenting our results for the complexes, we begin with an examination of the properties of the monomers. The results of geometry

optimization of monomers H_2O and H_2O_2 at the SCF level are shown in Table XXI along with experimental data. The results of H_2O shown in Table XXI is just for easy comparison. Once again, polarized basis sets give more accurate angle descriptions and dipole moment values, but are somewhat short in calculated bond lengths, while unpolarized basis sets give more accurate bond length description. Especially, the basis sets of 4-31G and 6-31G give almost planar structures (179.8 and 179.6). The dihedral angle (144.3) of H_2O_2 derived from D95 is better than those from 4-31G and 6-31G. The 6-31G** gives the best geometry description in the general sense.

In Table XXII, the harmonic frequencies are reported for monomers, and again compared with experiment. The data were scaled by 0.9 to remove

TABLE XXI
OPTIMIZED GEOMETRIES OF H_2O AND H_2O_2 [a]

Parameter	Basis set					Exp.
	4-31G	6-31G	D95	6-31G**	D95**	
H2O						
O-H1,2	0.950	0.950	0.951	0.943	0.944	0.958 b
H1OH2	111.2	111.6	112.5	106.0	106.6	104.5
$\mu(\text{D})$	2.486	2.501	2.530	2.148	2.180	1.85 c
H ₂ O ₂						
H1,4-O2,3	0.955	0.954	0.956	0.946	0.947	0.965 d
O2-O1	1.468	1.462	1.444	1.396	1.391	1.452
H1O2O3	100.8	101.2	102.8	102.3	102.8	100.0
H1O2O3H4	179.8	179.6	144.3	116.3	113.8	119.1
$\mu(\text{D})$	0.006	0.015	1.391	1.925	2.003	1.57 e

a. Geometrical parameters are given in Å and degrees.

b. ref.54. c. ref.55. d. ref.68. e. ref.69.

systematic error [39]. After the scaling, the data are very comparable with experimental data, especially for the polarized basis sets. The torsion mode of H_2O_2 derived from 4-31G, 6-31G and D95 is much smaller than that of experimental data, which reflects the torsion angle problem in the geometry optimization. Since the scaled data are still somewhat different from the experimental data, the scaling factor will be designed for each high frequency mode for the 6-31G** basis set to get our best estimates of frequencies for the complex.

The total energies in SCF and MP2 level were reported in Table XXIII.

TABLE XXII
CALCULATED FREQUENCIES WITH EXPERIMENTAL
MEASURED AND HARMONIC (IN PARENTHESES)
FREQUENCIES OF H_2O AND H_2O_2 (IN CM^{-1})

	4-31G	6-31G	D95	6-31G**	D95**	EXP.[a]
H_2O						
s-stretch	3563	3590	3625	3732	3748	3657 (3832)
bend	1568	1563	1540	1593	1576	1995 (1649)
a-stretch	3699	3731	3783	3838	3858	3756 (3942)
H_2O_2						
oh stretch	3569	3599	3635	3737	3752	3607
oh bend	1484	1489	1466	1454	1444	1394
oo stretch	925	915	960	1035	1051	864
torsion	78	46	179	348	370	317
oh stretch	3579	3609	3639	3738	3753	3608
oh bend	1144	1146	1188	1327	1327	1266

a. The harmonic frequencies of H_2O are from ref.64 and H_2O_2 are from ref.70.

TABLE XXIII
TOTAL ENERGIES (AU) OF H₂O AND H₂O₂ [a]

	E(SCF)	E(MP2)
H ₂ O		
4-31G	-75.90864	-76.03598
6-31G	-75.98536	-76.11205
D95	-76.01100	-76.13501
6-31G**	-76.02362	-76.21906
D95**	-76.04695	-76.24209
H ₂ O ₂		
4-31G	-150.55991	-150.81502
6-31G	-150.71001	-150.96317
D95	-150.75671	-151.00104
6-31G**	-150.77697	-151.14832
D95**	-150.82011	-151.18792

a. geometries optimized by specified basis set.

GEOMETRIES OF H₂O•H₂O₂

Del Bene[34] used the minimum basis set STO-3G to calculate this system with fixed monomer geometry and found two stable complex structures. In one (labeled WP) H₂O is a hydrogen donor, and in the other (labeled PW) H₂O₂ is the hydrogen donor. The dissociation energy is 7.64 kcal/mol for the PW form which is more than twice as strong as that in the WP form. The O--O distance (closer one) is 2.67 Å for the PW form and 2.85 Å for the WP form. From Del Bene's results, H₂O is more likely to be a hydrogen acceptor, as in the complexes H₂O•HO and H₂O•HO₂. We started with several different orientations shown in Figure 12, but found only the PW form as the energy minimum which has no symmetry at all. In this complex, the geometries of 6-31G** and D95** are very

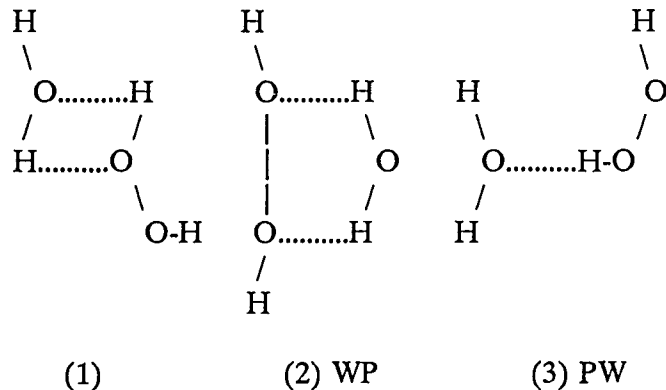


Figure 12. Orientations considered for $\text{H}_2\text{O} \cdot \text{H}_2\text{O}_2$ system.

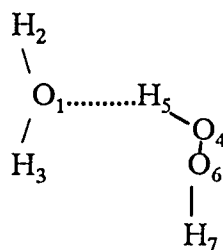


Figure 13. Optimized structure of $\text{H}_2\text{O} \cdot \text{H}_2\text{O}_2$.

close. Specifically, the geometry of 6-31G** is shown in the Figure 13.

The optimized geometries are presented in the Table XXIV. The geometries obtained from the unpolarized basis sets are apparently different from those obtained by polarized basis sets. The dihydral angles of H_2O_2 optimized by 4-31G and 6-31G are almost 180° . This error is still reflected in the geometries of complexes optimized by unpolarized basis sets: the twist angle is 159.3° in the fragment of H_2O_2 by 4-31G, 159.8° by 6-31G and 147.0° by D95, respectively. But the twist angle is 113.3° in both case of 6-31G** and D95**. The O--O distance is in the range of 2.668 Å to 2.691 Å in the geometries optimized by unpolarized

TABLE XXIV
OPTIMIZED STRUCTURES OF $\text{H}_2\text{O} \cdot \text{H}_2\text{O}_2$ [a]

Parameter	4-31G	6-31G	D95	6-31G**	D95**
symmetry	C1	C1	C1	C1	C1
O1-H2	0.949	0.948	0.950	0.943	0.945
O1-H3	0.953	0.952	0.953	0.945	0.947
O1---O4	2.668	2.676	2.691	2.828	2.856
O1---O6	2.811	2.819	2.903	2.916	2.955
H5-O4	0.968	0.967	0.968	0.952	0.953
O4-O6	1.471	1.465	1.448	1.398	1.394
O6-H7	0.954	0.953	0.955	0.945	0.947
H2O1H3	113.1	113.4	113.8	107.1	107.2
H2O1H5	138.8	142.3	142.5	126.5	126.8
O1H5O4	150.3	149.9	152.6	147.3	147.6
H5O4O6	99.2	99.7	101.1	101.4	101.9
O4O6H7	101.5	101.9	103.1	102.4	102.7
H3O1H2H5	131.4	142.0	163.6	101.8	102.8
H2O1H5O4	133.9	144.1	164.7	113.4	114.5
O1H5O4O6	0.6	0.7	4.6	9.8	10.2
H5O4O6H7	159.3	159.8	147.0	113.3	113.3
$\mu(\text{D})$	2.660	2.749	3.228	2.279	2.296

a. Geometric parameters are given in Å and degrees.

basis sets and 2.828 Å to 2.856 Å when optimized by polarized basis sets. The O--HO angle is 150 to 154° in the geometries optimized by unpolarized basis sets and about 147° in those optimized by polarized basis sets. H_2O_2 is no longer in symmetry in the complex shown in Figure 13.3 with the hydrogen-bonded OH bond in H_2O_2 0.006 Å longer than the second OH bond in the 6-31G** case. Also the 6-31G** case gives the lowest dipole moment of 2.279.

VIBRATIONAL FREQUENCIES OF $\text{H}_2\text{O} \cdot \text{H}_2\text{O}_2$

The harmonic frequencies are reported in Table XXV. The data were scaled by 0.90. Similar to $\text{H}_2\text{O} \cdot \text{HO}$ and $\text{H}_2\text{O} \cdot \text{HO}_2$, the modes mainly from the H_2O fragment were little changed. But for the modes mainly contributed from the H_2O_2 fragment, one of O-H stretching mode, which is close to the H_2O fragment geometrically, shifts to red about 90 cm^{-1} in both 6-31G** and D95** cases, while shifts to red about 200 cm^{-1} in all unpolarized basis sets. Another H-O stretching mode oppositely shifts to blue only a little ($3 - 19 \text{ cm}^{-1}$). Also, two bending modes in H_2O_2 shift to blue by 20 to 70 cm^{-1} .

TABLE XXV

CALCULATED HARMONIC FREQUENCIES OF $\text{H}_2\text{O} \cdot \text{H}_2\text{O}_2$ (cm^{-1}) [a]

[b]	4-31G	6-31G	D95	6-31G**	D95**
	92	87	49	100	85
	114	100	122	119	134
	124	114	132	187	173
	242	236	230	217	228
	252	253	262	258	261
	419	401	369	383	367
	654	632	641	579	582
H_2O_2	919 (-6)	909 (-6)	952 (-8)	1027(-8)	1044(-7)
H_2O_2	1211(+67)	1213(+67)	1234(+46)	1353(+26)	1348(+21)
H_2O_2	1542(+58)	1542(+53)	1536(+70)	1506(+52)	1496(+52)
H_2O	1574(+6)	1570(+7)	1559(+19)	1584(-9)	1577(+1)
H_2O_2	3352(-217)	3390(-209)	3436(-199)	3647(-90)	3661(-91)
H_2O	3564(+1)	3593(+3)	3631(+6)	3723(-9)	3733(-15)
H_2O_2	3589(+10)	3618(+19)	3650(+11)	3742(+4)	3756(+3)
H_2O	3705(+6)	3738(+7)	3780(-3)	3830(-8)	3842(-16)

a. The values in parentheses are frequency-shifts compared to the same mode of the monomer (calculated values).

TABLE XXVI
CALIBRATED HARMONIC FREQUENCIES
OF $\text{H}_2\text{O} \cdot \text{H}_2\text{O}_2$ (cm⁻¹) BY 6-31G** [a]

[b]	S.F.	freq.	IR INT.
	0.855	95	38
	0.855	113	162
	0.855	177	13
	0.855	206	148
	0.855	245	88
	0.855	364	78
	0.855	550	291
H_2O_2	0.752	858(-6)	3
H_2O_2	0.8587	1291(+25)	108
H_2O_2	0.8630	1444(+50)	34
H_2O	0.9013	1587(-8)	117
H_2O_2	0.8686	3520(-87)	272
H_2O	0.8819	3648(-9)	37
H_2O_2	0.8687	3612(+4)	56
H_2O	0.8809	3749(-7)	106

- a. The values in parentheses are frequency-shifts compared to the same mode of the monomer (experimental values).
S.F. is the scaling factor.
IR INT is the IR intensity in KM/MOLE.
- b. The fragment in the complex mainly involved in the vibrational mode.

In order to give the most reasonable prediction of harmonic frequencies of complexes $\text{H}_2\text{O} \cdot \text{H}_2\text{O}_2$, a new scaling factor is designated for each mode of monomers by dividing the experimental data by the calculated frequency for the same mode. Then the average of those scaling factors is used for those low frequency modes in the complex. The results are presented in Table XXVI. The average scaling factor is 0.855 for the 6-31G** basis set.

ENERGIES OF $\text{H}_2\text{O} \cdot \text{H}_2\text{O}_2$

The total energies of both SCF and MP2 levels and binding energies of $\text{H}_2\text{O} \cdot \text{H}_2\text{O}_2$ were shown in the Table XXVII. Again the unpolarized basis sets gave 50% more binding energy than the polarized basis sets did. But the polarized basis sets give more electron correlation correction energies, twice more than those by unpolarized basis sets.

TABLE XXVII
ENERGIES OF $\text{H}_2\text{O} \cdot \text{H}_2\text{O}_2$ CALCULATED
BY FULLY OPTIMIZED GEOMETRIES

	$E(\text{H}_2\text{O} \cdot \text{H}_2\text{O}_2)(\text{au})$	$\Delta E(\text{kcal/mol})$
4-31G//4-31G	-226.48658	-11.314
6-31G//6-31G	-226.71246	-10.724
D95//D95	-226.78350	-9.908
6-31G**//6-31G**	-226.81253	-7.492
D95**//D95**	-226.87727	-6.407
MP2/4-31G//4-31G	-226.87056	-12.274
MP2/6-31G//6-31G	-227.09358	-11.521
MP2/D95//D95	-227.15358	-11.000
MP2/6-31G**//6-31G**	-227.38286	-9.714
MP2/D95**//D95**	-227.44342	-8.415

Like the systems $\text{H}_2\text{O} \cdot \text{HO}$ and $\text{H}_2\text{O} \cdot \text{HO}_2$, higher basis set calculations were performed upon the geometries optimized by 6-31G**. The results were shown in Table XXVIII. In the SCF level, calculated by polarized basis sets, the binding energy is in the range of -5.993 to -7.492 kcal/mol, with more extensive basis sets responding to smaller binding energy (absolute value), which are much lower than

those derived by unpolarized basis sets (-9.908 to -11.314 kcal/mol). In the MP2 level, calculated by polarized basis sets, the binding energy is in the range of -7.825 to -9.714 kcal/mol, with more extensive basis sets responding to smaller binding energy (absolute value), which are much lower than those derived by unpolarized basis sets too (-11.000 to -12.274 kcal/mol).

TABLE XXVIII
TOTAL ENERGIES AND BINDING ENERGIES OF $\text{H}_2\text{O} \cdot \text{H}_2\text{O}_2$
SYSTEM USING THE GEOMETRIES OPTIMIZED
BY BASIS SET 6-31G** [a]

	E(H_2O)	E(H_2O_2)	E($\text{H}_2\text{O} \cdot \text{H}_2\text{O}_2$)	ΔE
6-311G**	-76.04699	-150.82028	-226.87907	-7.405
6-311+G**	-76.05330	-150.82548	-226.88837	-6.018
6-311++G**	-76.05342	-150.82566	-226.88863	-5.993
MP2/6-311G**	-76.26333	-151.22948	-227.50810	-9.595
MP2/6-311+G**	-76.27410	-151.24035	-227.52690	-7.812
MP2/6-311++G**	-76.27430	-151.24062	-227.52739	-7.825

a. E's are in a.u. and ΔE 's are in kcal/mole.

The results of BSSE calculation are shown in Table XXIX. Their changes with basis sets are displayed in Figure 14. In general, the BSSE is reduced with more extensive basis sets. The BSSE calculated in the MP2 level is about twice larger than those calculated in the SCF level. Although the binding energies in the MP2 level are much larger than those in SCF level, after BSSE correction, they are closer to each other (SCF level: -5.306 to -5.947 kcal/mol; MP2 level: -5.962 to -6.822 kcal/mol). As mentioned earlier, the BSSE may be overestimated in the calculation (as suggested by the experimental data for $\text{H}_2\text{O} \cdot \text{H}_2\text{O}$). So, if

we take the BSSE as uncertain, the binding energy calculated by MP2/6-311++G**//6-31G** is in the range of -7.8 to -6.0 kcal/mol, which indicates the Del Bene's result (-7.6 kcal/mol [34]) is near the upper bound.

TABLE XXIX
BSSE ESTIMATES AND BINDING ENERGIES OF $\text{H}_2\text{O} \cdot \text{H}_2\text{O}_2$ [a]

		E(BSSE)	$\Delta E'$
D95**//D95**		0.597	-6.407 to -5.810
6-31G**	[b]	1.545	-7.492 to -5.947
6-311G**	[b]	1.853	-7.405 to -5.552
6-311+G**	[b]	0.712	-6.018 to -5.306
6-311++G**	[b]	0.538	-5.993 to -5.455
MP2/D95**//D95**		1.752	-8.415 to -6.663
MP2/6-31G**	[b]	2.892	-9.714 to -6.822
MP2/6-311G**	[b]	3.321	-9.595 to -6.274
MP2/6-311+G**	[b]	1.695	-7.812 to -6.117
MP2/6-311++G**	[b]	1.863	-7.825 to -5.962
[c]			-7.6

a. All energies in kcal/mol; $\Delta E'$ is the range of binding energy.

b. based on geometries optimized by 6-31G**.

c. from ref.34, calculated by STO-3G.

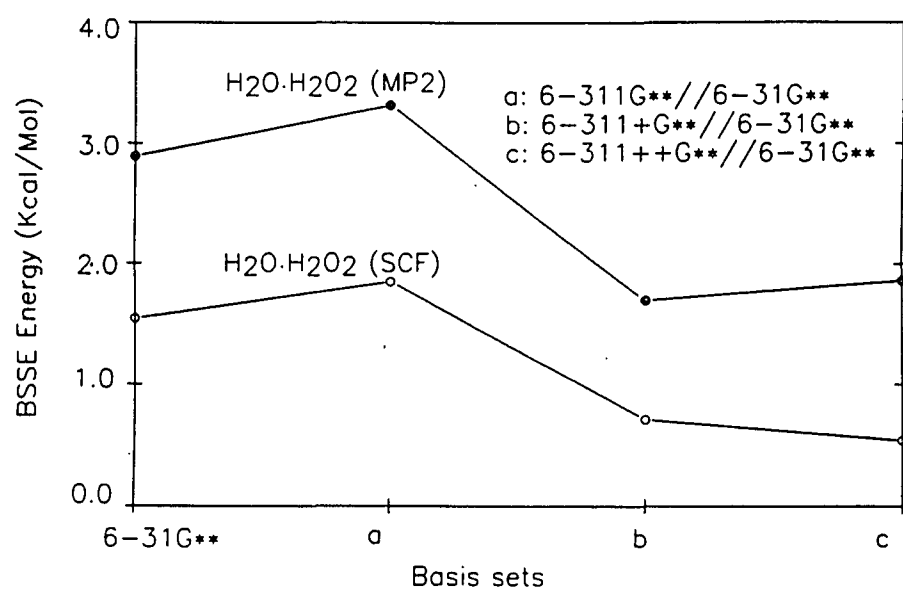
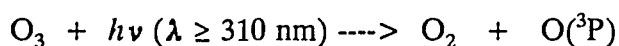
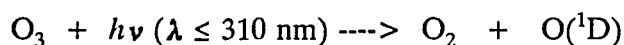


Figure 14. BSSE calculated for H₂O·H₂O₂ system.

CHAPTER V

$\text{H}_2\text{O} \cdot \text{O}_3$ SYSTEM

Ozone plays an important role in tropospheric photochemistry. In the lower atmosphere, ozone is mainly produced by diffusion from the stratosphere and in photochemical smog. It has a concentration of 0 to 0.05 ppm in nonpolluted air and 0 to 0.5 ppm in photochemical smog. Because it shields the earth's surface from damaging ultraviolet radiation from the sun, the change of ozone level in the atmosphere would affect the global environment seriously. Because of depletion of the ozone layer in the stratosphere, ozone attracts more and more scientist's attention. Ozone is photolyzed according to the reactions:



We ask whether there are any species which will form complexes with O_3 and change these reaction mechanisms. On the other hand, ozone is a relatively unstable species which is easily destroyed by various chemical processes. Is it possible an ozone-water complex would increase the stability of ozone?



In the $\text{H}_2\text{O} \cdot \text{O}_3$ system, H_2O could not be a hydrogen-acceptor, but it could be a hydrogen donor to form hydrogen bonds. On the other hand, the middle O atom of the O_3 is positively charged and this middle O atom could be bonded to the O atom in H_2O to form an O--O complex.

GEOMETRIES OF H_2O , O_3 AND $\text{H}_2\text{O} \cdot \text{O}_3$

The structures of $\text{H}_2\text{O} \cdot \text{O}_3$ were tested for several formations of bifurcated complexes, O--O bonded complexes and linear form, shown in Figure 15. Both bifurcated and O--O bonded complexes could be chair (I,III), boat (II,VI) and planar (IV,V). Excepting the linear form VII, all structures have at least planar symmetry. Two planar forms have the higher symmetry of C_{2v} . All these forms were initially used to optimize the structure using the 6-31G** basis set. Three stationary points were found: two planar forms (IV and V) and one boat form VI of O--O bonded complex. In the form VI, the alpha and beta angles are defined in figure 16. Alpha angle is the angle between the bisector of HOH and O...O line. The beta angle is the angle between the bisector of OOO and O...O line.

From the above other system studies, it is obvious that at least the polarized functions should be included in the basis sets, and we demonstrated that the basis set 6-31G** gives a very good geometrical description. So, in the $\text{H}_2\text{O} \cdot \text{O}_3$ studies, only the basis set 6-31G** or more extensive basis sets were used.

The results of the SCF geometry optimization of $\text{H}_2\text{O} \cdot \text{O}_3$ are presented in Table XXX with the monomer structures. The bond lengths of monomers are a little shorter (98.4% by 6-31G** and 98.2% by 6-311G** for H_2O , 94.7% by

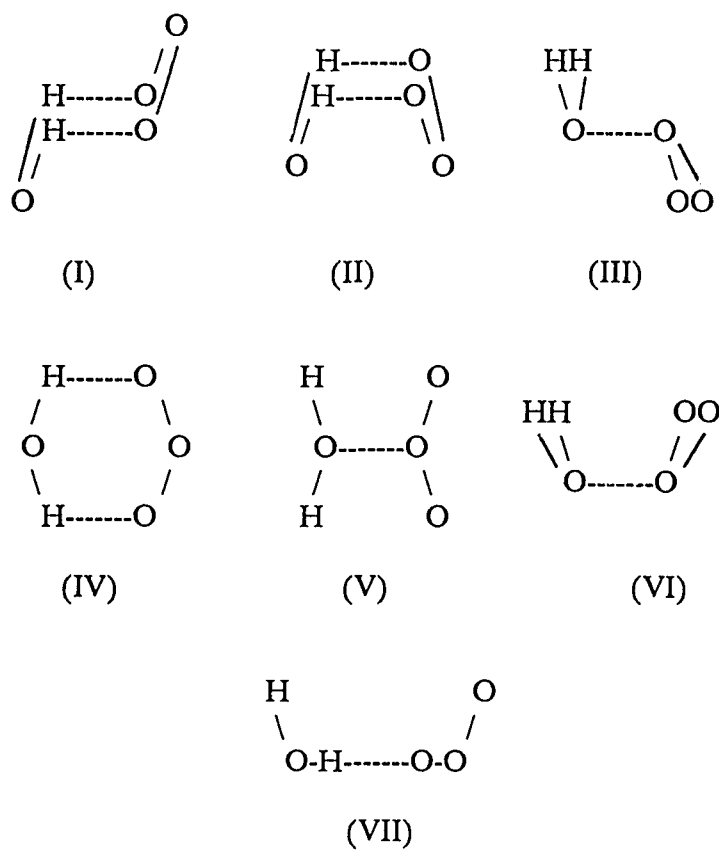


Figure 15. Possible structures of $\text{H}_2\text{O} \cdot \text{O}_3$.

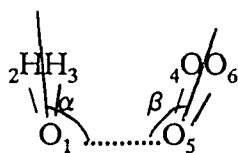


Figure 16. Optimized structure of $\text{H}_2\text{O} \cdot \text{O}_3$.

6-31G** and 93.9% by 6-311G** for O₃) than the experimental data [54,71] and the bond angles are a little larger (101.0% to 102.1%) than experimental data [54,71]. Although geometry optimization by the electron correlation method could give very accurate geometries as shown in calculation of O₃ [73 - 76], we still optimized the geometries in SCF level since the geometry optimization of H₂O•O₃ is limited by the computer system we used. Comparing the complexes with their monomer structures derived with the same basis sets, the bond lengths of monomers in the complex have very little change, which means the interreaction between H₂O and O₃ is very weak. The complex bonding of O--H in planar is 2.666 Å (6-31G**) and 2.657 Å (6-311G**) in form IV. In form VI, the distance between two middle O atoms of two monomers is 2.873 Å by 6-31G** and 2.838 Å by 6-311G**. In form V, the distance between two middle O atoms of two monomers is 3.099 Å by 6-31G** and 3.104 Å by 6-311G**. The alpha and beta angles in the form VI are 130.3° and 90.3° by 6-31G**, 141.3° and 90.9° by 6-311G**, respectively. In fact, form V is related to form VI as α and β both equal 180°. Form IV is related to form VI as α and β both equal 0°. The forms I, II and III can be related to form VI as α and β are equal to some specific numbers. The structures suggest the binding energies might be small. The dipole moments in planar forms are much larger than those of the boat form of the O--O bonded complex, even larger than the dipole moments of two monomers together, which suggests the binding energies of planar forms could be overestimated by the large dipole moment [60].

TABLE XXX
OPTIMIZED STRUCTURES OF H₂O, O₃ AND H₂O•O₃ [a]

Parameter	Basis set		Exp.
	6-31G**	6-311G**	
H ₂ O			
O-H1,2	0.943	0.941	0.958 b
H1OH2	106.0	105.5	104.5
μ(D)	2.148	2.138	1.85 c
O ₃			
O-O2,3	1.204	1.194	1.272 d
O2OO3	119.0	119.2	116.8
μ(D)	0.826	0.866	0.53 e
H ₂ O•O ₃ form IV			
O1-H2,H3	0.943	0.941	
O1-O5	3.835	3.821	
O4-H2 (O6-H3)	2.666	2.657	
O5-O4,O6	1.204	1.194	
H ₂ O1H3	105.1	104.7	
O4O5O6	119.0	119.2	
μ(D)	3.234	3.261	
H ₂ O•O ₃ form V			
O1-H2,H3	0.943	0.941	
O1-O5	3.099	3.104	
O4-H2 (O6-H3)	4.289	4.288	
O5-O4,O6	1.204	1.194	
H ₂ O1H3	106.1	105.6	
O4O5O6	118.7	119.0	
μ(D)	3.137	3.160	

TABLE XXX
OPTIMIZED STRUCTURES OF H₂O, O₃ AND H₂O·O₃ [a]
(continued)

Parameter	Basis set		Exp.
	6-31G**	6-311G**	
H ₂ O•O ₃ form VI			
O1-H2,H3	0.943	0.941	
O1-O5	2.873	2.838	
O5-O4,O6	1.203	1.193	
H ₂ O1H3	106.2	105.8	
O4O5O6	118.9	119.1	
α	130.3	141.3	
β	90.3	90.9	
μ(D)	1.723	1.867	

a. Geometric parameters are given in Å and degrees.
b. ref.54. c. ref.55. d. ref.71. e. ref.72.

VIBRATIONAL FREQUENCIES OF H₂O, O₃ AND H₂O·O₃

The harmonic frequencies were calculated at the SCF level by the 6-31G** and 6-311G** basis sets. For H₂O, the calculated frequencies are close to experimental data [61] (7.3% larger). For O₃, the calculated frequencies are much larger than experimental data [77] (29.6% larger). So, the scaling factor is developed for each mode in the monomers by dividing the experimental data by the calculated frequency for the same mode. Then the average of those scaling factors is used for the low frequency modes in the complex. The results are presented in Table XXXI.

For the two planar forms of IV and V, negative frequencies were found. If we check the force moments, those two planar forms have negative eigenvalues. Only

TABLE XXXI
CALCULATED FREQUENCIES WITH EXPERIMENTAL
MEASURED AND HARMONIC (IN PARANTHESES)
FREQUENCIES OF H₂O, O₃ AND H₂O·O₃ (CM⁻¹)

sym.		6-31G**	6-311G**	EXP. [a]			
H ₂ O							
bend		1770	1751	1595 (1649)			
s-stretch		4147	4142	3657 (3832)			
a-stretch		4264	4237	3756 (3942)			
O ₃							
bend		764	785	716			
s-stretch		1309	1284	1089			
a-stretch		1384	1388	1135			
H ₂ O•O ₃							
[b]	sym.	S.F.	6-31G**	IR_Int.	S.F.	6-311G**	IR int.
form VI							
	A''	0.8324	51	5.9	0.8334	48	1.0
	A'	0.8324	52	97	0.8334	53	160
	A''	0.8324	65	54	0.8334	75	47
	A'	0.8324	96	49	0.8334	91	47
	A''	0.8324	139	12	0.8334	142	17
	A'	0.8324	145	212	0.8334	143	138
O ₃	A'	0.8431	720	13	0.8214	720	17
O ₃	A''	0.7489	1091	772	0.7630	1094	851
O ₃	A'	0.7382	1141	0.7	0.7358	1142	1.2
H ₂ O	A'	0.9013	1595	110	0.9109	1596	88
H ₂ O	A'	0.8819	3657	23	0.8829	3657	25
H ₂ O	A''	0.8809	3755	68	0.8864	3756	69

TABLE XXXI
CALCULATED FREQUENCIES WITH EXPERIMENTAL
MEASURED AND HARMONIC (IN PARANTHESES)
FREQUENCIES OF H_2O , O_3 AND $\text{H}_2\text{O} \cdot \text{O}_3$ (CM^{-1})
(continued)

[b]	sym.	S.F.	6-31G**	IR_Int.	S.F.	6-311G**	IR int.
form IV							
			i				
		0.8324	31				
		0.8324	60				
		0.8324	68				
		0.8324	110				
		0.8324	232				
O_3		0.8431	720				
O_3		0.7489	1085				
O_3		0.7382	1137				
H_2O		0.9013	1603				
H_2O		0.8819	3666				
H_2O		0.8809	3757				
form V							
			i				
		0.8324	35				
		0.8324	64				
		0.8324	67				
		0.8324	119				
		0.8324	217				
O_3		0.8431	702				
O_3		0.7489	1114				
O_3		0.7382	1125				
H_2O		0.9013	1621				
H_2O		0.8819	3674				
H_2O		0.8809	3779				

a. The frequencies of H_2O are from ref.61 and ref. 39. O_3 are from ref.77.

b. The fragment in the complex mainly involved in the vibrational mode

the boat form of complex (form VI) has all positive eigenvalues. Later we will show that the total energies of boat form VI is lower than those of the two planar forms IV and V.

The high frequency modes in the complex which are mainly from monomer frequency modes are very close to their monomers', especially the H₂O fragment.

ENERGIES OF H₂O, O₃ AND H₂O•O₃

Table XXXII presents the total energies for monomers and three forms of complexes at the SCF and MP2 levels. In order to see how low the two planar forms are, their energies are calculated too. Using the 6-31G** basis set, the energies of planar form IV and V are 0.64 and 1.21 kcal/mol higher than that of the true minimum structure, respectively. In the 6-311G** case, the energies of planar form IV and V are 0.85 and 1.49 kcal/mol higher than that of the true minimum structure, respectively.

Because the two planar forms (form IV and V) are only the stationary points, there is no need to do further calculations with more extensive basis sets. For the boat form VI, which is a true energy minimum, the geometries optimized by both 6-31G** and 6-311G** will be used to do one-point calculation by more extensive basis sets of 6-311+G** and 6-311++G**.

The binding energies calculated using 6-31G**, 6-311G**, and 6-311+G** in the MP2 level are in the range of -2.9 to -3.5 kcal/mol. If we compare the MP2 results of 6-311G** and 6-311+G** based on geometries of 6-31G** and 6-311+G** in Table XXXII, we could find the geometry effect to the total

TABLE XXXII
TOTAL ENERGIES AND BINDING ENERGIES OF
 $\text{H}_2\text{O} \cdot \text{O}_3$ SYSTEM [a]

	E(SCF)	ΔE (SCF)	E(MP2)	ΔE (MP2)
H_2O				
6-31G**//6-31G**	-76.02362		-76.21906	
6-311G**//6-31G**	-76.04699		-76.26333	
6-311+G**//6-31G**	-76.05330		-76.27410	
6-311++G**//6-31G**	-76.05342		-76.27430	
6-311G**//6-311G**	-76.04701		-76.26327	
6-311+G**//6-311G**	-76.05329		-76.27400	
O_3				
6-31G**//6-31G**	-224.26144		-224.84907	
6-311G**//6-31G**	-224.32233		-224.96518	
6-311+G**//6-31G**	-224.32927		-224.97882	
6-311G**//6-311G**	-224.32264		-224.96128	
6-311+G**//6-311G**	-224.32960		-224.97495	
$\text{H}_2\text{O} \cdot \text{O}_3$ form VI				
6-31G**//6-31G**	-300.28910	-2.537	-301.07275	-2.898
6-311G**//6-31G**	-300.37383	-2.833	-301.23331	-3.012
6-311+G**//6-31G**	-300.38676	-2.631	-301.25841	-3.446
6-311++G**//6-31G**	-300.38686	-2.617		
6-311G**//6-311G**	-300.37421	-2.859	-301.22938	-3.029
6-311+G**//6-311G**	-300.38717	-2.684	-301.25458	-3.532
$\text{H}_2\text{O} \cdot \text{O}_3$ form IV				
6-31G**//6-31G**	-300.28808	-1.897		
6-311G**//6-311G**	-300.37281	-1.980		
$\text{H}_2\text{O} \cdot \text{O}_3$ form V				
6-31G**//6-31G**	-300.28718	-1.332		
6-311G**//6-311G**	-300.37180	-1.347		

a. E's are in a.u. and ΔE 's are in kcal/mol.

energies of complexes are only 0.017 kcal/mol. So our higher basis sets one point energy calculation would be acceptable.

The BSSE were estimated in both the SCF and MP2 levels for the geometries specified and the results were shown in Table XXXIII. The E(BSSE) of 6-311G** and 6-311+G** were gradually decreased in SCF level, but not in MP2 level. The E(BSSE) in the SCF level is about one third of the binding energy in the same level. For the MP2 level, the E(BSSE) is about half of the binding energy. So the E(BSSE) for the $\text{H}_2\text{O} \cdot \text{O}_3$ is quite large. After the BSSE correction, the binding energies in the SCF and MP2 levels are not much

TABLE XXXIII
ESSE ESTIMATES AND BINDING ENERGIES OF $\text{H}_2\text{O} \cdot \text{O}_3$ [a]

	E(BSSE)	$\Delta E'$
SCF		
6-31G**//6-31G**	1.003	-2.537 to -1.534
6-311G**//6-31G**	1.044	-2.833 to -1.789
6-311+G**//6-31G**	0.848	-2.631 to -1.783
6-311G**//6-311G**	1.022	-2.859 to -1.837
6-311+G**//6-311G**	0.876	-2.684 to -1.808
MP2		
6-31G**//6-31G**	1.500	-2.898 to -1.398
6-311G**//6-31G**	1.540	-3.012 to -1.472
6-311+G**//6-31G**	1.767	-3.446 to -1.679
6-311G**//6-311G**	1.501	-3.029 to -1.528
6-311+G**//6-311G**	1.824	-3.532 to -1.708

a. All energies in Kcal/mol. $\Delta E'$ is the range of binding energy.

different (SCF: -1.534 to -1.808 kcal/mol; MP2: -1.398 to -1.708 kcal/mol). So the binding energy is reduced to -1.8 kcal/mol, which means the $\text{H}_2\text{O} \cdot \text{O}_3$ is indeed a very weak Van der Waals type of complex.

If we let the beta angle in the form VI change from 0° to 180° by using the basis set 6-31G**, the results are shown in Figure 17. We can see that when beta is 0° , the complex becomes form IV and the energy is 0.64 kcal/mol higher; when beta is 180° , the complex becomes form V and the energy is 1.21 kcal/mol higher; when beta is in between 0° to 90° , the complex becomes form II and the energy is higher than form VI. So from this rotation barrier calculation, it also proved that the form VI is energy minimum.

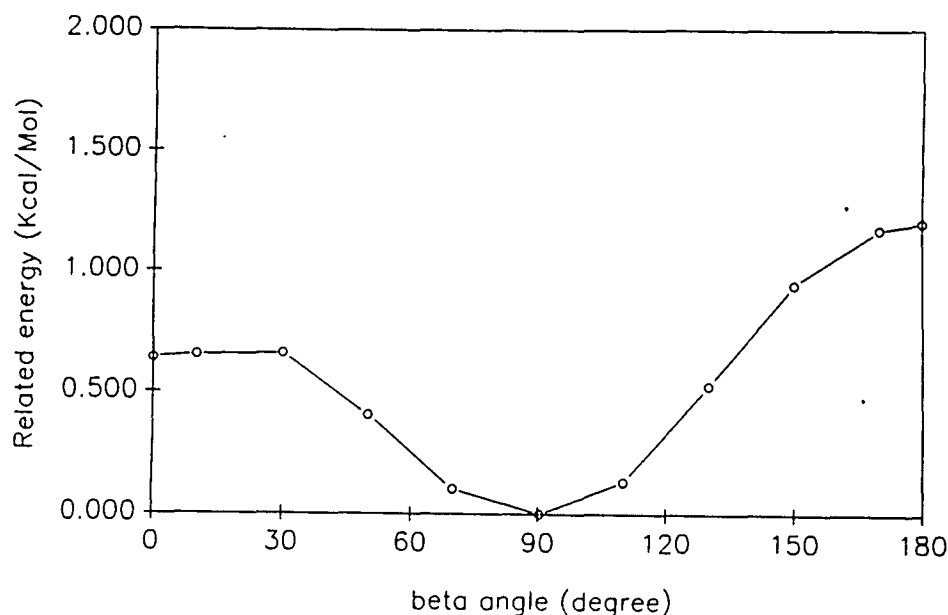


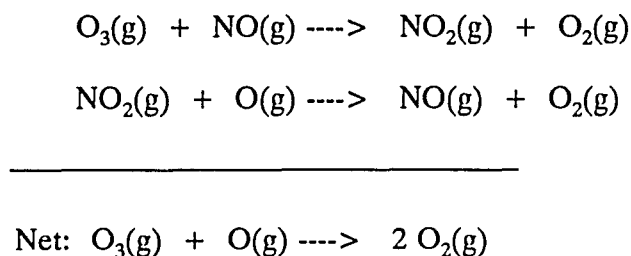
Figure 17. Relative energies of $\text{H}_2\text{O} \cdot \text{O}_3$ with different beta angles.

CHAPTER VI

$\text{H}_2\text{O} \cdot \text{NO}$ AND $\text{H}_2\text{O} \cdot \text{NO}_2$ SYSTEM

Nitric Oxide, NO, is a colorless gas while Nitrogen Dioxide, NO_2 , is a brown gas. They are mainly released to the atmosphere by internal combustion engines, combustion of organic matter and lighting.

Nitric oxide and nitrogen dioxide are important constituents in photochemical smog. NO can serve as a catalyst in the depletion of ozone by the NO_x family. Ozone reacts with NO to form NO_2 and O_2 . Then NO_2 reacts with atomic oxygen to regenerate NO and form O_2 . The NO is then ready again to react with O_3 . This deletion routine is as following:



In the NO and NO_2 molecules, the atom N is positively charged and the atom O is negatively charged. So, for the NO, like the $\text{H}_2\text{O} \cdot \text{HO}$, the structure of the complex, shown in Figure 18, was tested. For NO_2 , like $\text{H}_2\text{O} \cdot \text{O}_3$, possible structures of the complexes, shown in Figure 19, were tested.

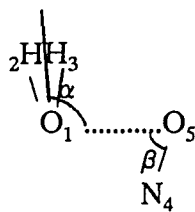


Figure 18. Structure of the $\text{H}_2\text{O}\cdot\text{NO}$.

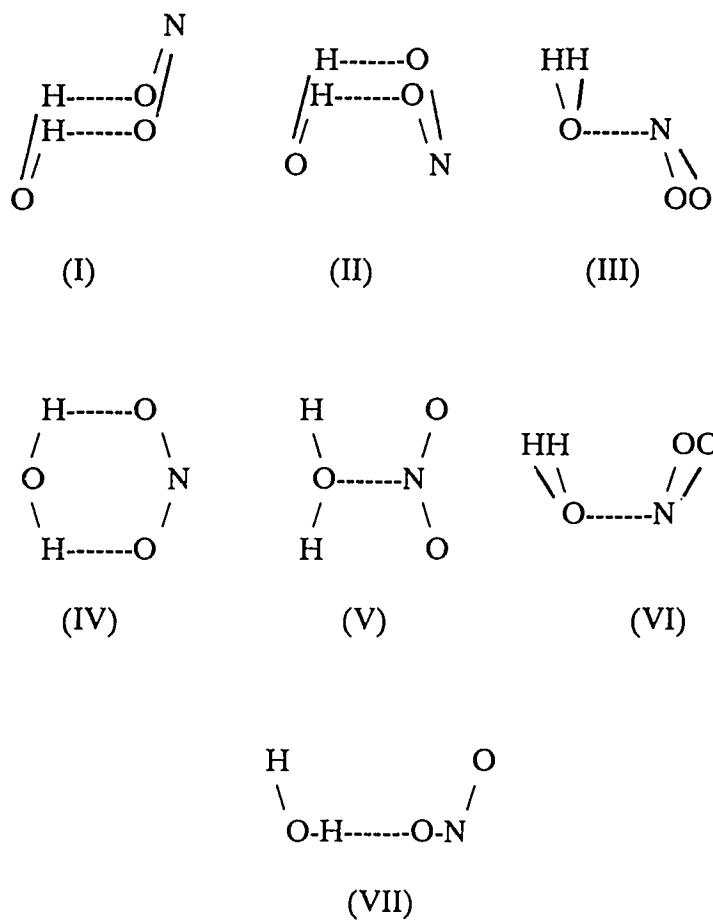


Figure 19. Possible structures of $\text{H}_2\text{O}\cdot\text{NO}_2$.

GEOMETRIES OF H_2O , NO , NO_2 , $\text{H}_2\text{O} \cdot \text{NO}$ AND $\text{H}_2\text{O} \cdot \text{NO}_2$

Like $\text{H}_2\text{O} \cdot \text{O}_3$, only the basis set 6-31G** or more extensive basis sets were used in these studies. The results of geometry optimization of the monomers H_2O , NO and NO_2 at the SCF level are shown in Table XXXIV along with experimental data for purposes of comparison. Again, the bond length derived from the basis sets 6-31G** and 6-311G** are shorter than the experimental bond length. In the NO case, the bond length averages 2.5% shorter, while in the NO_2 case, is 2.9% shorter; the bond angle in NO_2 is 1.6% larger than the experimental data [78,79].

TABLE XXXIV
OPTIMIZED GEOMETRIES OF H_2O , NO AND NO_2 [a]

Parameter	Basis set		Exp.
	6-31G**	6-311G**	
H ₂ O			
O-H1,2	0.950	0.950	0.958 b
H1OH2	111.2	111.6	104.5
μ(D)	2.486	2.501	1.85 c
NO			
N-O	1.127	1.117	1.151 d
μ(D)	0.210	0.203	1.9 e
NO ₂			
N-O1,2	1.165	1.156	1.193 f
O1NO2	136.1	136.3	134.1
μ(D)	0.681	0.662	0.55 e

a. Geometrical parameters are given in Å and degrees.

b. ref.54. c. ref.55. d. ref.78. e. ref.80. f. ref.79.

The structure of $\text{H}_2\text{O}\cdot\text{NO}$ shown in Figure 19 was optimized. The optimized geometry is presented in Table XXXV. Like the geometry of $\text{H}_2\text{O}\cdot\text{HO}$ optimized by the basis set 6-31G**, the α angle is defined as the angle between the bisector of the angle HOH and $\text{O}_{\text{HOH}}\cdots\text{O}_{\text{NO}}$ and the β angle is the angle between ON and $\text{O}_{\text{NO}}\cdots\text{O}_{\text{HOH}}$. The α is 134.7° and β is 58.6° by 6-31G**, while the α is 150.2° and β is 62.9° by 6-311G**.

TABLE XXXV
OPTIMIZED STRUCTURES OF $\text{H}_2\text{O}\cdot\text{NO}$ [a]

Parameter	Basis set	
	6-31G**	6-311G**
O1-H2,H3	0.943	0.941
O1-O5	3.478	3.430
O5-N4	1.127	1.117
H2O1H3	106.0	105.6
α	134.7	150.1
β	58.6	62.9
$\mu(\text{D})$	2.445	2.449

a. Geometric parameters are given in Å and degrees.

In the $\text{H}_2\text{O}\cdot\text{HO}$ and $\text{H}_2\text{O}\cdot\text{HF}$, the $\text{O}\cdots\text{H}\cdots\text{O}$ and $\text{O}\cdots\text{H}\cdots\text{F}$ are almost in a straight line. But in the $\text{H}_2\text{O}\cdot\text{NO}$, the $\text{O}\cdots\text{N}\cdots\text{O}$ is around 60° . The reason for this large beta angle is the electric structure of atom N. The dipole moment of the $\text{H}_2\text{O}\cdot\text{NO}$ is 2.45 D, which is little less than the dipole moment of H_2O alone. This is mainly caused by the triangle structure of $\text{O}\cdots\text{N}\cdots\text{O}$.

For $\text{H}_2\text{O}\cdot\text{NO}_2$, several structures were optimized which are shown in Figure 19. Those structures include bifurcated complexes, N--O bonded complexes and

linear forms. Both bifurcated and N--O bonded complexes could be chair (I,III), boat (II,VI) and planar (IV,V). Except the linear form VII, all other structures have at least a planar symmetry. Two planar forms have the higher symmetry of C_{2v} . All those forms were initially used to optimize the structure using the 6-31G** basis set. Three stationary points were found: two planar forms and one boat form VI of N--O bonded complex. In the form VI, the parameter α and β are shown in Figure 20. The α is the angle between the bisector of the HOH and the O----N line. The β is the angle between the bisector of the ONO and the N----O line.

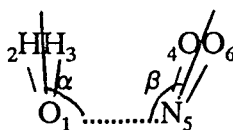


Figure 20. Optimized structure of $H_2O \cdot NO_2$.

The results of the SCF geometry optimization of $H_2O \cdot NO_2$ are presented in Table XXXVI. Comparing the complexes with their monomer structures, the bond lengths of the monomers in the complex have very little change. The complex bonding of O--H in planar is 2.653 Å (6-31G**) and 2.669 Å (6-311G**) in form IV. In form V, the distance between the atom O and atom N of the two monomers is 2.873 Å by 6-31G** and 2.838 Å by 6-311G**. In form VI, the distance between the atom O and atom N of the two monomers is 2.814 Å by 6-31G** and 2.798 Å by 6-311G**. This distance is a little shorter than O---O distance in $H_2O \cdot O_3$.

The α and β angles in the form VI are 139.8° and 107.3° by 6-31G**, 154.4°

TABLE XXXVI
OPTIMIZED STRUCTURES OF $\text{H}_2\text{O} \cdot \text{NO}_2$ [a]

Parameter	Basis set	
	6-31G**	6-311G**
form IV (ring)		
O1-H2,H3	0.943	0.941
O1-N5	3.638	3.652
O4-H2 (O6-H3)	2.653	2.669
N5-O4,O6	1.164	1.156
$\text{H}_2\text{O1H3}$	105.9	105.5
O4N5O6	135.9	136.1
$\mu(\text{D})$	3.054	3.013
form V		
O1-H2,H3	0.943	0.941
O1-N5	3.001	2.990
O4-H2 (O6-H3)	4.019	4.006
N5-O4,O6	1.165	1.156
$\text{H}_2\text{O1H3}$	106.2	105.7
O4N5O6	135.7	135.9
$\mu(\text{D})$	3.102	3.072
form VI (boat)		
O1-H2,H3	0.943	0.941
O1-N5	2.814	2.798
N5-O4,O6	1.164	1.156
$\text{H}_2\text{O1H3}$	106.4	106.0
O4N5O6	135.8	136.1
α	139.8	154.4
β	107.3	106.4
$\mu(\text{D})$	1.950	2.372

a. Geometric parameters are given in Å and degrees.

and 106.4° by 6-311G**, respectively. So both the α and β angles are larger than those in the $\text{H}_2\text{O} \cdot \text{O}_3$ complex. Just like $\text{H}_2\text{O} \cdot \text{O}_3$ system, form V is related to form VI as the α and β angles are both equal to 180° . The form IV is related to

form VI as the α and β angles are both equal to 0° . The form I, II and III can be related to form VI as the α and β angles are equal to some specific numbers.

The structures of $\text{H}_2\text{O}\cdot\text{NO}$ and $\text{H}_2\text{O}\cdot\text{NO}_2$ suggest the binding energies might be small. This will be confirmed in the energy calculation.

ENERGIES OF H_2O , NO , NO_2 , $\text{H}_2\text{O}\cdot\text{NO}$ AND $\text{H}_2\text{O}\cdot\text{NO}_2$

The total energies of the species in the $\text{H}_2\text{O}\cdot\text{NO}$ system in SCF are reported in Table XXXVII with their $\langle S^2 \rangle$ values, if they are open-shell species. In the SCF level, the $\langle S^2 \rangle$ value is quite close to that of a pure doublet wavefunction (0.75). The largest $\langle S^2 \rangle$ is 0.7680 for NO in basis set 6-31G** case. The difference of $\langle S^2 \rangle$ values between NO and $\text{H}_2\text{O}\cdot\text{NO}$ is very small. The binding energies of $\text{H}_2\text{O}\cdot\text{NO}$, showed in Table XXXVII, are -1.19 kcal/mol by basis set 6-31G** and -1.17 kcal/mol by basis set 6-311G**. Comparing to the binding

TABLE XXXVII

TOTAL ENERGIES OF H_2O , NO AND $\text{H}_2\text{O}\cdot\text{NO}$ (AU)
AND BINDING ENERGIES OF $\text{H}_2\text{O}\cdot\text{NO}$ (KCAL/MOL)

	E(SCF)	$\langle S^2 \rangle$	$\Delta E(\text{SCF})$
H_2O			
6-31G**	-76.02362		
6-311G**	-76.04701		
NO			
6-31G**	-129.24788	0.7680	
6-311G**	-129.28305	0.7665	
$\text{H}_2\text{O}\cdot\text{NO}$			
6-31G**	-205.27340	0.7670	-1.19
6-311G**	-205.33192	0.7659	-1.17

energies of $\text{H}_2\text{O}\cdot\text{HO}$ and $\text{H}_2\text{O}\cdot\text{HF}$, those binding energies are very small. So the $\text{H}_2\text{O}\cdot\text{NO}$ is very weak complex.

The Table XXXVIII presents the total energies of species in the $\text{H}_2\text{O}\cdot\text{NO}_2$ system with $\langle S^2 \rangle$ values at the SCF level. Three forms of $\text{H}_2\text{O}\cdot\text{NO}_2$ are presented. By using the basis set 6-31G**, the energies of planar form IV and V are 1.52 and 0.92 kcal/mol higher than that of the form VI, while by using the basis set 6-311G**, the energies of planar form IV and V are 1.68 and 1.08 kcal/mol higher. These results are different from the $\text{H}_2\text{O}\cdot\text{O}_3$ system. In the $\text{H}_2\text{O}\cdot\text{O}_3$ system, the energy of form IV (ring) is lower than that of form V, while in the $\text{H}_2\text{O}\cdot\text{NO}_2$ system, the energy of form IV (ring) is higher than that of form V. It means atom N is more likely to react with atom O in the H_2O .

The binding energies, showed in Table XXXVIII, calculated using 6-31G**

TABLE XXXVIII
TOTAL ENERGIES OF NO_2 AND $\text{H}_2\text{O}\cdot\text{NO}_2$ (AU)
AND BINDING ENERGIES OF $\text{H}_2\text{O}\cdot\text{NO}_2$ (KCAL/MOL)

	E(SCF)	$\langle S^2 \rangle$	$\Delta E(\text{SCF})$
NO_2			
6-31G**	-204.03149	0.7661	
6-311G**	-204.08730	0.7658	
$\text{H}_2\text{O}\cdot\text{NO}_2$ form IV			
6-31G**	-280.05720	0.7658	-1.31
6-311G**	-280.13638	0.7654	-1.30
$\text{H}_2\text{O}\cdot\text{NO}_2$ form V			
6-31G**	-280.05816	0.7659	-1.91
6-311G**	-280.13733	0.7655	-1.90
$\text{H}_2\text{O}\cdot\text{NO}_2$ form VI			
6-31G**	-280.05962	0.7659	-2.83
6-311G**	-280.13906	0.7656	-2.98

and 6-311G** in the SCF level are -1.31 and -1.30 kcal/mol for form IV (ring), -1.91 and -1.90 kcal/mol for form V, -2.83 and -2.98 kcal/mol for form VI (boat), respectively. So the form VI has the lowest energy, and the $\text{H}_2\text{O}\cdot\text{NO}_2$ is a very weak complex, same as in the $\text{H}_2\text{O}\cdot\text{O}_3$ system.

CHAPTER VII

THERMOCHEMICAL PROPERTIES AND CONCLUSIONS

From the interaction energies of complexes $\text{H}_2\text{O} \cdot \text{HO}$, $\text{H}_2\text{O} \cdot \text{HO}_2$, $\text{H}_2\text{O} \cdot \text{H}_2\text{O}_2$, $\text{H}_2\text{O} \cdot \text{O}_3$, $\text{H}_2\text{O} \cdot \text{NO}$ and $\text{H}_2\text{O} \cdot \text{NO}_2$, we could see that the last three complexes are less stable because they lack hydrogen bonding. The calculations of $\text{H}_2\text{O} \cdot \text{NO}$ and $\text{H}_2\text{O} \cdot \text{NO}_2$ are only in SCF level and there is no BSSE correction performed. So we will discuss $\text{H}_2\text{O} \cdot \text{HO}$, $\text{H}_2\text{O} \cdot \text{HO}_2$, $\text{H}_2\text{O} \cdot \text{H}_2\text{O}_2$ vs. $\text{H}_2\text{O} \cdot \text{HF}$ and $\text{H}_2\text{O} \cdot \text{H}_2\text{O}$ in more detail.

In order to calculate $\Delta G(1)$ and $\Delta H(1)$, the calibrated vibrational frequencies of 6-31G**, scaled for each mode, were used to calculate ΔE_{vib} and ΔS . We have also chosen to correct our binding energies by "calibrating" the individual BSSE values using the experimental binding energy of $\text{H}_2\text{O} \cdot \text{H}_2\text{O}$. Comparing our calculated value for the binding energy of the water dimer (-5.706 kcal/mol by MP2/6-311+G(2d,1p)//6-31G** before BSSE correction, and 1.057 kcal/mol of the BSSE calculated by same basis set) with the experimental binding energy of -5.4 kcal/mol [13]. It is seen that only 27% of the BSSE value is required to bring the calculated value into agreement with the

experimental value. (This correction, of course, is within the experimental uncertainty). We believe the correction of the BSSE energies of the other complexes by 27% appears justified since there still is a controversy about the appropriateness of the BSSE correction [81], and some people treat the energy corrected by BSSE as the lower bound of binding energy [5].

TABLE XXXIX
FINAL THERMOCHEMICAL PROPERTIES FOR
WATER COMPLEXES [a]

system	ΔE	$\Delta H^\circ(298)$	$\Delta S^\circ(298)$	$\Delta G^\circ(298)$	$K_{eq}(298)$	[b]
$H_2O \cdot HO$	-5.7	-4.4	-19.3	1.3	0.11	0.2%
$H_2O \cdot HF$	-8.5	-7.0[-6.2]	-21.4	-0.6	2.8	5.6%
$H_2O \cdot HO_2$	-8.9	-7.2(-7.4)	-22.0(-24.3)	-0.7(-0.1)	3.3	6.6%
$H_2O \cdot H_2O$	-5.4	-3.8[-3.7]	-18.2	1.6	0.067	0.1%
$H_2O \cdot H_2O_2$	-7.3	-5.6	-23.1	1.3	0.11	0.2%
$H_2O \cdot O_3$	-1.8					
$H_2O \cdot NO$	-1.2					
$H_2O \cdot NO_2$	-3.0					

a. ΔE , ΔH and ΔG are in kcal/mol; ΔS is in cal/mol-deg; K_{eq} is in atm^{-1} . Values in parentheses for $H_2O \cdot HO_2$ are from ref. 32. Value in bracket are experimental data with $H_2O \cdot HF$ from ref.18 and $H_2O \cdot H_2O$ from ref.13.

b. ratio of complexed to uncomplexed forms ($[H_2O]K_{eq}$) for 2% water at atmospheric pressure.

The thermochemical properties of complexes are summarized in Table XXXIX. ΔE is the binding energy at 298.16 K. Because the binding energies of $H_2O \cdot NO$, $H_2O \cdot NO_2$ and $H_2O \cdot O_3$ are so small, further thermochemical properties are not performed. From Table 35, all the ΔH

are negative. But because of the large effect of entropy change for the dimerization, the ΔG for $\text{H}_2\text{O} \cdot \text{HF}$ and $\text{H}_2\text{O} \cdot \text{HO}_2$ are small negative, others are positive.

If we assume that there is 2% H_2O at 298 K in the atmosphere, then HO_2 is 6.6% in the complex form (HF is not an important tropospheric constituent). Others have only tenth percent in complex form.

TEMPERATURE DEPENDENCE OF THERMOCHEMICAL PROPERTIES

In the atmosphere, the temperature changes with altitude. so does the ΔG . So the percentage of complex will change with altitude too. It is interesting to see the temperature dependence of all thermochemical properties.

Temperatures decrease sharply with altitude in the troposphere, and the low temperatures which characterize the tropopause prevent significant water vapor concentrations in the stratosphere. Thus, although HO_x -water complexes will have greater stability with altitude due to lower temperatures, the stronger temperature dependence of water vapor pressure counteracts this effect and results in highest concentrations of the complex near sea level in warm tropical regions. Thermodynamic properties of the complexes are given as a function of temperature in Table XXXX.

From the Table XXXX, $\Delta E(0 \rightarrow T)$, ΔS , ΔH do not change too much with temperature. However, in spite of the compensating effects of

TABLE XXXX
TEMPERATURE DEPENDENCE
OF THERMOCHEMICAL PROPERTIES [a]

T(K)	$\Delta E(0 \rightarrow T)$	ΔS	ΔH	ΔG	K	altitude (km)	ratio complexed i.e. $K[\text{H}_2\text{O}]$ % [b]
$\text{H}_2\text{O} \cdot \text{HO}$							
298.15	1.93	-19.3	-4.4	1.3	0.11	0	0.22
291	1.91	-19.3	-4.4	1.2	0.13	2	0.10
283	1.88	-19.3	-4.4	1.1	0.14	4	0.04
273	1.85	-19.4	-4.4	0.9	0.19	6	0.02
261	1.81	-19.4	-4.4	0.7	0.26	8	0.02
247	1.77	-19.5	-4.4	0.4	0.43	10	0.009
231	1.73	-19.5	-4.4	0.1	0.80	12	0.004
$\text{H}_2\text{O} \cdot \text{HO}_2$							
298.15	2.26	-22.0	-7.2	-0.7	3.3	0	6.6
291	2.23	-22.0	-7.2	-0.8	4.0	2	3.2
283	2.20	-22.1	-7.3	-1.1	7.1	4	2.1
273	2.16	-22.2	-7.3	-1.3	11	6	1.1
261	2.11	-22.3	-7.3	-1.5	18	8	1.3
247	2.05	-22.4	-7.3	-1.8	39	10	0.8
231	1.99	-22.5	-7.4	-2.2	121	12	0.6
$\text{H}_2\text{O} \cdot \text{H}_2\text{O}_2$							
298.15	2.25	-23.1	-5.6	1.3	0.11	0	0.22
291	2.21	-23.2	-5.7	1.0	0.18	2	0.14
283	2.18	-23.2	-5.7	0.9	0.20	4	0.06
273	2.14	-23.3	-5.7	0.7	0.28	6	0.03
261	2.09	-23.4	-5.7	0.4	0.46	8	0.03
247	2.03	-23.5	-5.8	0.0	1.0	10	0.02
231	1.97	-23.6	-5.8	-0.3	1.9	12	0.01

a. unit: ΔE , ΔH and ΔG are in kcal/mol; ΔS is in cal/mol-deg;
 K_{eq} is in atm^{-1}

b. H_2O distribution (mole percent) vs. altitude from ref. 68:
0km(2%), 2(0.8), 4(0.3), 6(0.1), 8(0.07), 10(0.02), 12(0.005).

temperature on complex stability and water vapor concentration, there is a significant altitudinal variation of relative complex concentration.

EFFECTS OF BASIS SETS ON ENERGY AND STRUCTURE

The quality of basis set is very important in the calculation of energies and geometries. More extensive basis sets will give lower total energies for the same species. Figure 21 displays the total energies of monomers in the SCF level changes with the basis sets. Figure 22 displays the total energies of monomers in the MP2 level changes with the basis sets. We can see that the total energy changes quite a lot with different unpolarized basis sets. But the energy changes with polarized basis sets, especially the basis sets more extensive than 6-311G**, are not that significant. Usually the basis set D95** gives lower energy than basis set 6-31G**. But D95** will overestimate the bond angle in the geometry optimization.

Figure 23 shows the binding energies of complexes without BSSE correction in the SCF level with different basis sets. Figure 24 shows the binding energies of complexes in the MP2 level without BSSE correction with different basis sets. From the figures, we can see the unpolarized basis sets overestimate the binding energies and polarized basis sets, especially those more extensive than 6-311G**, give quite consistent binding energies.

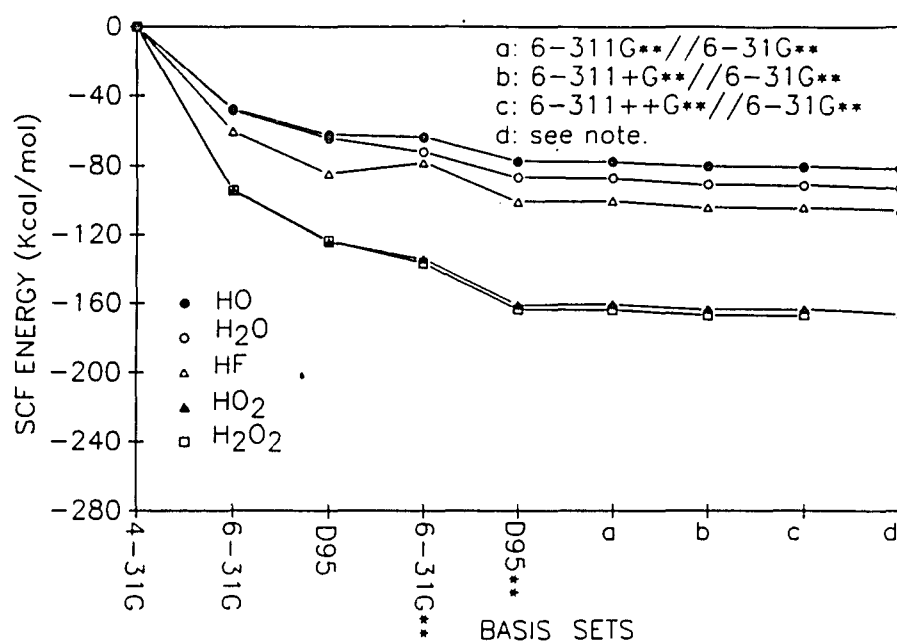


Figure 21. Relative total energies (SCF) of HO, HF, H₂O, HO₂ and H₂O₂ vs. basis sets. (Note: For HO and HF: 6-311+G(2d,2p)//6-31G**. For H₂O and HO₂: 6-311+G(2d,1p)//6-31G**)

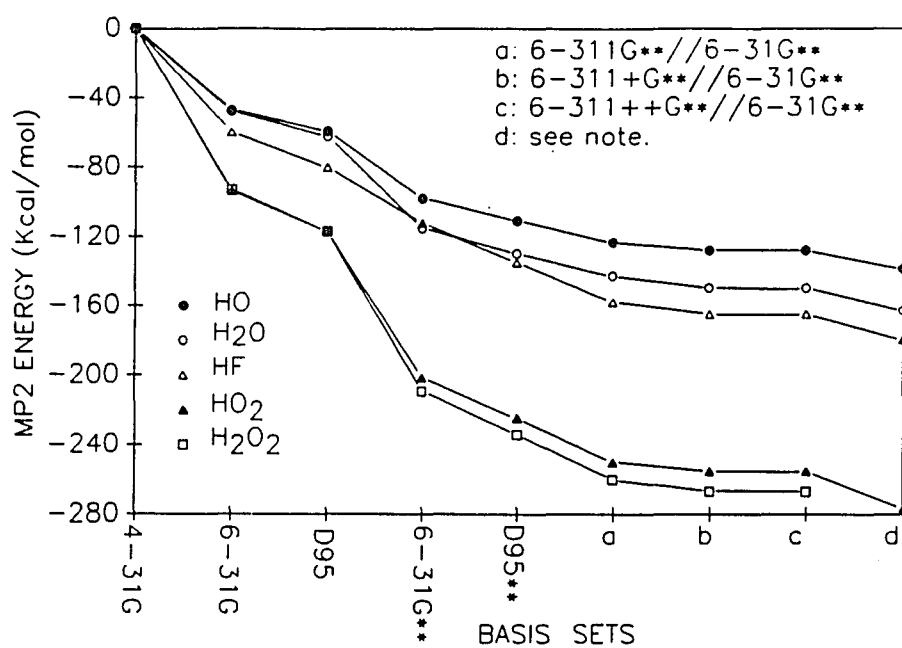


Figure 22. Relative total energies (MP2) of HO, HF, H₂O, HO₂ and H₂O₂ vs. basis sets. (Note: For HO and HF: 6-311+G(2d,2p)//6-31G**. For H₂O and HO₂: 6-311+G(2d,1p)//6-31G**)

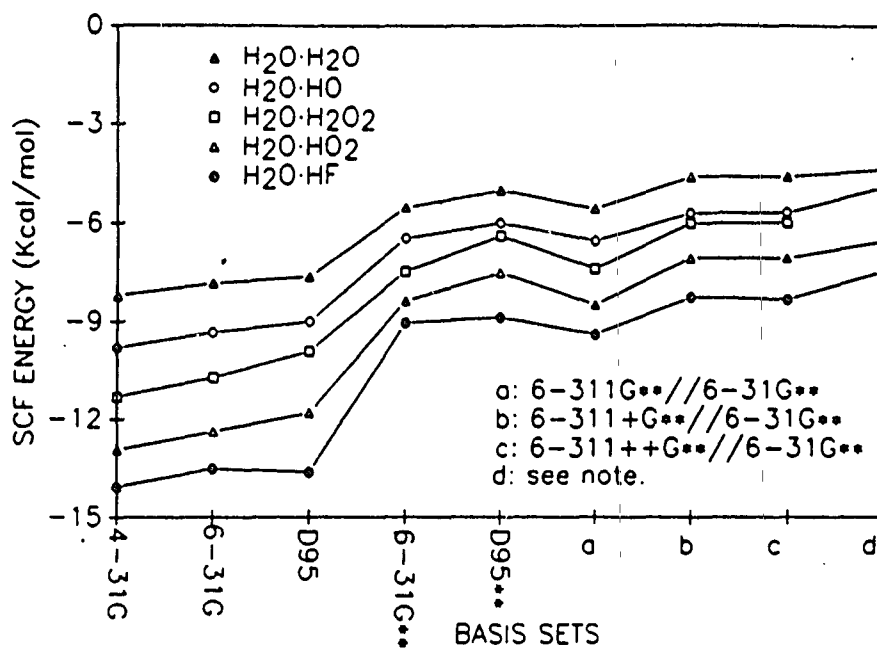


Figure 23. Binding energies (SCF, no BSSE correction) of H₂O·HO, H₂O·HF, H₂O·H₂O, H₂O·HO₂ and H₂O·H₂O₂ vs. basis sets. (Note: For H₂O·HF and H₂O·HO: 6-311+G(2d,2p)//6-31G**. For H₂O·H₂O and H₂O·HO₂: 6-311+G(2d,1p)//6-31G**)

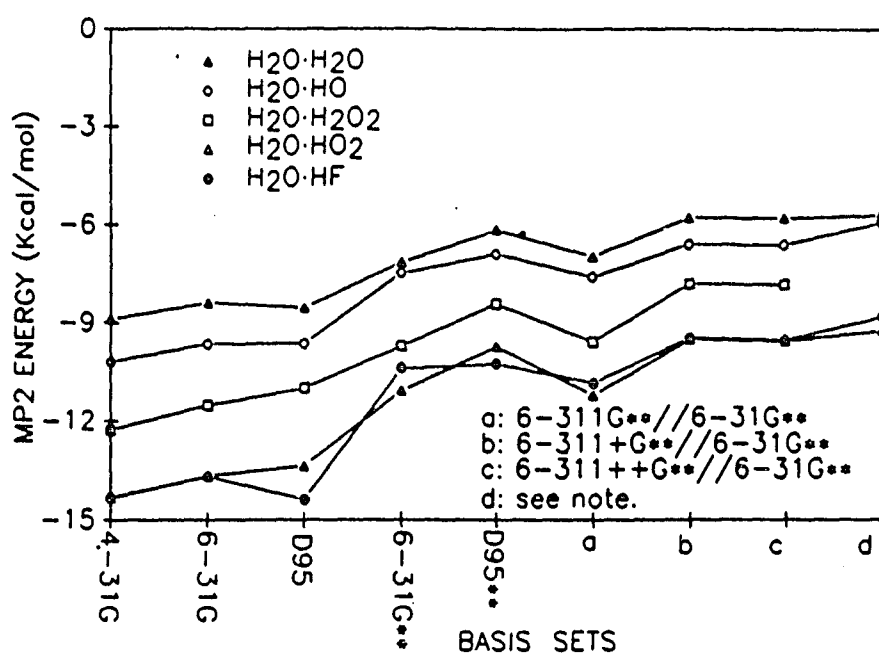


Figure 24. Binding energies (MP2, no BSSE correction) of H₂O·HO, H₂O·HF, H₂O·H₂O, H₂O·HO₂ and H₂O·H₂O₂ vs. basis sets. (Note: For H₂O·HF and H₂O·HO: 6-311+G(2d,2p)//6-31G**. For H₂O·H₂O and H₂O·HO₂: 6-311+G(2d,1p)//6-31G**)

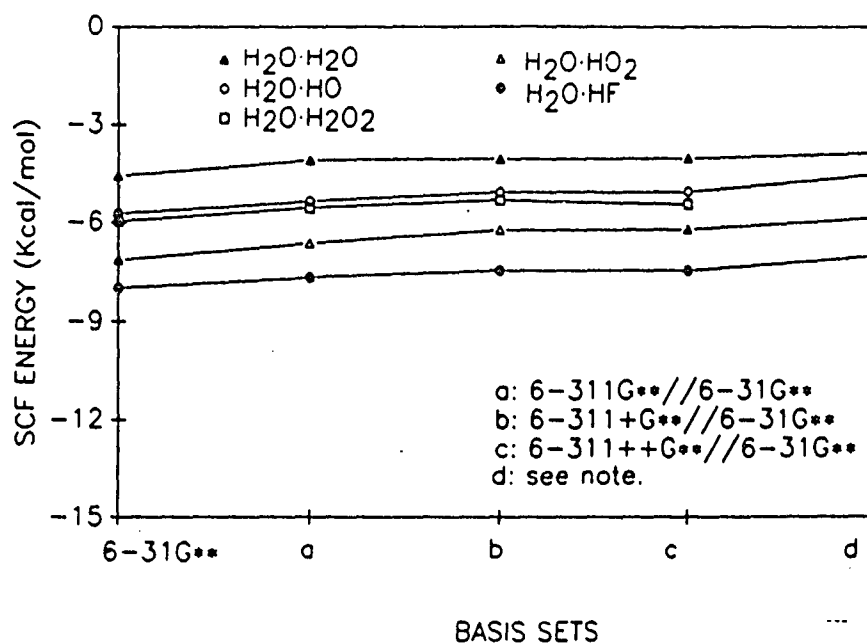


Figure 25. Binding energies (SCF, after BSSE correction) of $\text{H}_2\text{O} \cdot \text{HO}$, $\text{H}_2\text{O} \cdot \text{HF}$, $\text{H}_2\text{O} \cdot \text{H}_2\text{O}$, $\text{H}_2\text{O} \cdot \text{HO}_2$ and $\text{H}_2\text{O} \cdot \text{H}_2\text{O}_2$ vs. basis sets. (Note: For $\text{H}_2\text{O} \cdot \text{HF}$ and $\text{H}_2\text{O} \cdot \text{HO}$: 6-311+G(2d,2p)//6-31G**. For $\text{H}_2\text{O} \cdot \text{H}_2\text{O}$ and $\text{H}_2\text{O} \cdot \text{HO}_2$: 6-311+G(2d,1p)//6-31G**)

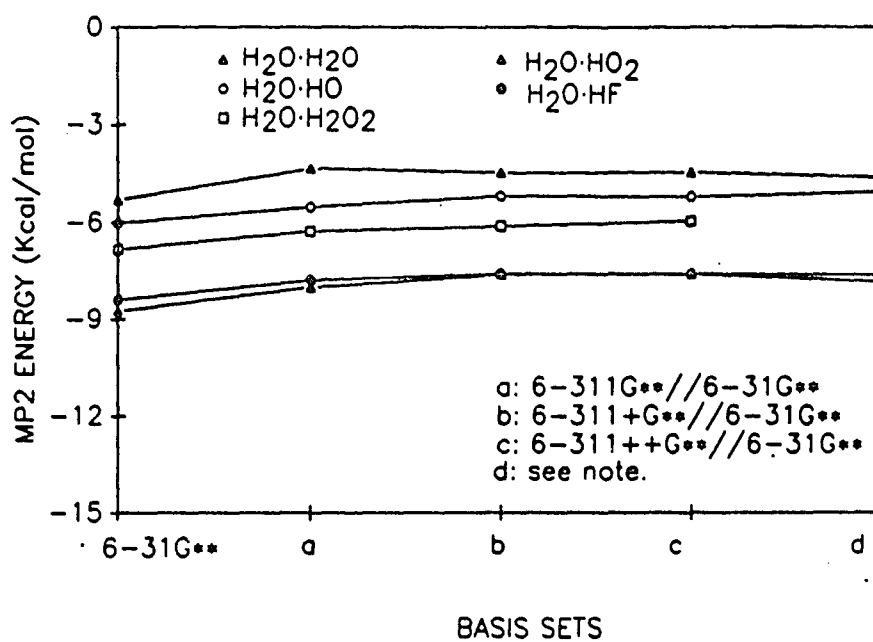


Figure 26. Binding energies (MP2, after BSSE correction) of H₂O·HO, H₂O·HF, H₂O·H₂O, H₂O·HO₂ and H₂O·H₂O₂ vs. basis sets. (Note: For H₂O·HF and H₂O·HO: 6-311+G(2d,2p)//6-31G**. For H₂O·H₂O and H₂O·HO₂: 6-311+G(2d,1p)//6-31G**)

Figure 25 shows the binding energies of complexes in the SCF level after BSSE correction with different basis sets. Figure 26 shows the binding energies of complexes in the MP2 level after BSSE correction with different basis sets. From the figures, we can see binding energies are almost constant with different basis sets. It seems the binding energy differences calculated by different basis sets are caused by BSSE.

When we examine the optimized geometries of H_2O_2 , $\text{H}_2\text{O} \cdot \text{HF}$ and $\text{H}_2\text{O} \cdot \text{H}_2\text{O}$, we found the basis set 6-31G** gave the best geometry description. The more extensive basis sets give lower total energy, but do not always give the best optimized geometries, as we demonstrated in the $\text{H}_2\text{O} \cdot \text{HO}$, $\text{H}_2\text{O} \cdot \text{HF}$ and $\text{H}_2\text{O} \cdot \text{H}_2\text{O}$ calculation. Also we found that in the one-point energy calculations of $\text{H}_2\text{O} \cdot \text{HO}$ and $\text{H}_2\text{O} \cdot \text{HF}$, the energy difference between the fully optimized geometry and the geometry optimized by basis set 6-31G** was not very significant. So if we want to give meaningful results, the geometry should be optimized at least by 6-31G**, the energy should be calculated by 6-311G** or more extensive basis sets based on the geometry optimized by 6-31G**.

ROTATIONAL BARRIER OF COMPLEXES

Figure 27 shows the rotational barrier of the complexes $\text{H}_2\text{O} \cdot \text{HO}$, $\text{H}_2\text{O} \cdot \text{HF}$, $\text{H}_2\text{O} \cdot \text{H}_2\text{O}$, $\text{H}_2\text{O} \cdot \text{HO}_2$ and $\text{H}_2\text{O} \cdot \text{H}_2\text{O}_2$. The $\text{H}_2\text{O} \cdot \text{HO}$ is rotated along the O---O bond. The $\text{H}_2\text{O} \cdot \text{HF}$ is rotated along the O---F bond. The $\text{H}_2\text{O} \cdot \text{H}_2\text{O}$

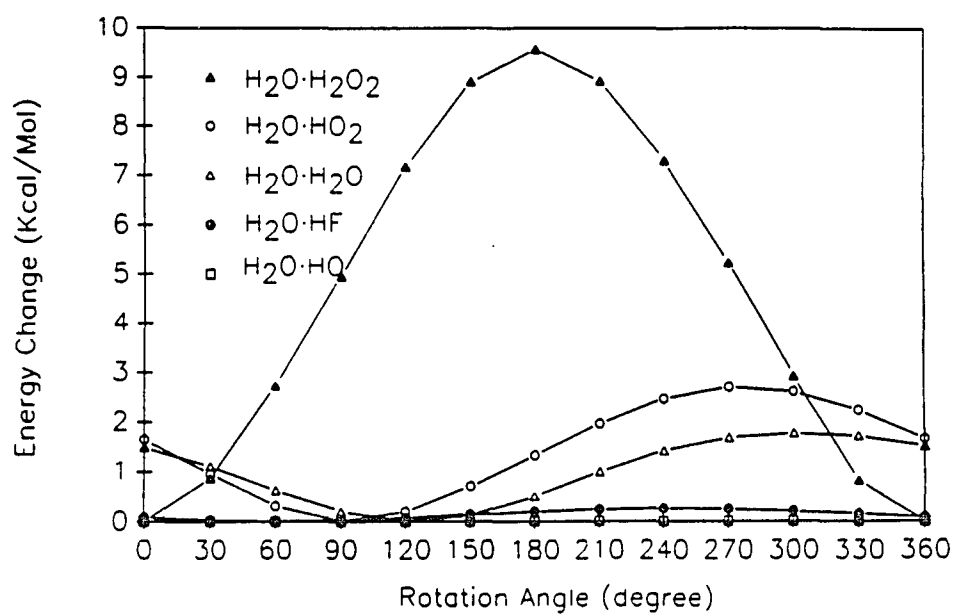


Figure 27. Rotational Barriers of $\text{H}_2\text{O}\cdot\text{HO}$, $\text{H}_2\text{O}\cdot\text{HF}$, $\text{H}_2\text{O}\cdot\text{H}_2\text{O}$, $\text{H}_2\text{O}\cdot\text{HO}_2$ and $\text{H}_2\text{O}\cdot\text{H}_2\text{O}_2$.

is rotated along the O---O bond. The $\text{H}_2\text{O}\cdot\text{HO}_2$ and $\text{H}_2\text{O}\cdot\text{H}_2\text{O}_2$ are rotated along the O---O bond which have shorter distance.

The $\text{H}_2\text{O}\cdot\text{HO}$ and $\text{H}_2\text{O}\cdot\text{HF}$ have the lowest rotational barriers. This is because the beta angle (defined in Figure 3) are almost 0° .

The $\text{H}_2\text{O}\cdot\text{H}_2\text{O}$ and $\text{H}_2\text{O}\cdot\text{HO}_2$ have 2 to 3 kcal/mol rotational barriers. For those complexes, not only the beta angle (defined in Figure 8 and 9) are larger, but also there are one more atom H or O bonded to atom O, which resists the rotation. The $\text{H}_2\text{O}\cdot\text{H}_2\text{O}_2$ has the highest rotational barrier of 9.5 kcal/mol, which is the same size as the binding energy.

Since the rotation barriers of complexes are so small, the contribution of internal rotation to entropies of complexes is estimated. In the cases of $\text{H}_2\text{O}\cdot\text{HO}$ and $\text{H}_2\text{O}\cdot\text{HF}$, the O---H-O and O---H-F are almost in the linear forms and their internal contributions are not significant. Other complexes are estimated from the formula of Pitzer and Gwinn [82] using the reduced moments of inertia along the O---O axis (see Appendix C for detail). The results are shown in Table XXXXI with their effects to the free energies, K_{eq} and the ratio of complexed to uncomplexed forms.

The effects of internal rotation of complexes $\text{H}_2\text{O}\cdot\text{H}_2\text{O}$ and $\text{H}_2\text{O}\cdot\text{H}_2\text{O}_2$ are not significant. But in the case of $\text{H}_2\text{O}\cdot\text{HO}_2$, the complexed form of HO_2 is almost tripled.

TABLE XXXXI
THE EFFECTS OF INTERNAL ROTATION
TO THERMOCHEMICAL PROPERTIES [a]

system	$S^{\text{ir}}(298)$	$\Delta G^{\circ}(298)$	$\Delta G^{\circ}(298, \text{after IR})$	$K_{\text{eq}}(298)$	[b]
$\text{H}_2\text{O} \cdot \text{HO}_2$	2.0	-0.7	-1.3	9.0	18%
$\text{H}_2\text{O} \cdot \text{H}_2\text{O}$	1.85	1.6	1.0	0.18	0.4%
$\text{H}_2\text{O} \cdot \text{H}_2\text{O}_2$	0.9	1.3	1.0	0.18	0.4%

a. ΔG 's are in kcal/mol; S 's are in cal/mol-deg; K_{eq} 's are in atm^{-1} .

b. ratio of complexed to uncomplexed forms ($[\text{H}_2\text{O}]K_{\text{eq}}$) for 2% water at atmospheric pressure.

REFERENCES

1. J.A.Logan, M.J.Prather, S.C.Wofsy, and M.B.McElroy, *J. Geophys. Research*, **86** (1981) 7210.
2. M.M.Szczesniak, R.J.Brenstein, S.M.Cybulski, and S.Scheiner, *J. Phys. Chem.* **94**(1990) 1781.
3. K.Szalewicz, S.J.Cole, W.Kolos, and R.J.Bartlett, *J. Chem. Phys.*, **89**(1988) 3662.
4. J.E.Del Bene, *J. Chem. Phys.*, **86**(1987) 2110.
5. M.J.Frisch, J.E.Del Bene, J.S.Binkley, and H.F.Schaefer, *J. Chem. Phys.*, **84**(1986) 2279.
6. M.M.Szczesniak and S.Scheiner, *J. Chem. Phys.*, **84**(1986) 6328. *Ibid*, **80**(1984) 1535.
7. E.Clementi and P.Habitz, *J. Phys. Chem.*, **87**(1983) 2815.
8. S.Roszak, W.A.Sokalski, P.C.Hariharan, and J.J.Kautman, *Theor. Chim. Acta.*, **70**(1986) 81.
9. R.J.Harrison and R.J.Bartlett, *Int. J. Quant. Chem. Symp.*, **20**(1986) 437.
10. M.J.Frisch, J.A.Pople, and J.E.Del Bene, *J. Phys. Chem.*, **89**(1985) 3684
11. J.E.Del Bene, H.D.Mettee, M.J.Frisch, B.T.Luke, and J.A.Pople, *J. Phys. Chem.*, **87**(1983) 3279.
12. T.R.Dyke and J.S.Muenter, *J. Chem. Phys.*, **60**(1974) 2929. J.A.Odutota and T.R.Dyke, *J. Chem. Phys.*, **72**(1980) 5062. J.A.Odutota, R.Viswanathan and T.R.Dyke, *J. Am. Chem. Soc.*, **101**(1979) 4787.
13. L.A.Curtiss, D.J.Frurip, and M.Blander, *J. Chem. Phys.*, **71**(1979) 2703.

14. J.Reimers, R.Watts, and M.Klein, *Chem. Phys.*, 64(1982) 95.
15. Van Lenthe, J.H.; van Duijneveldt-van de Rijdt, J.G.C.M.; van Duijneveldt, F.B. ab initio Methods in Quantum Chemistry; John Wiley & Sons: New York, 1987; Vol 2, pp 521-566.
16. P.Hobza and R.Zahradnik, *Chem. Rev.*, 88(1988) 871.
17. J.W.Bevan, A.C.Legon, D.J.Millen and S.C.Rogers, *J. Chem. Soc. Chem. Commun.*, (1975) 341.
18. R.K.Thomas, *Proc. Roy. Soc.*, 344A(1975) 579.
19. Z.Kisiel, A.C.Legon, and D.J.Millen, *Proc. Roy. Soc. London*, 381A(1982) 481.
20. A.C.Legon, D.J.Millen and H.M.North, *Chem. Phys. Letters* 135(1987) 303.
21. P.A.Kollman and L.C.Allen, *J. Chem. Phys.*, 52(1969) 5085.
22. W.J.Hehre, R.F.Stewart and J.A.Pople, *J. Chem. Phys.*, 51(1969) 2657.
23. R.Ditchfield, W.J.Hehre and J.A.Pople, *J. Chem. Phys.*, 54(1971) 724.
24. W.A.Lathan, L.A.Curtis, W.J.Hehre, J.B.Lisle, and J.A.Pople, *Prog. Phys. Org. Chem.*, 11(1974) 175.
25. D.G.Lister and P.Palmier, *J. Mol. Struc.*, 39(1977) 295.
26. P.Hobza and J.Sauer, *Theor. Chim. Acta.* 65(1984) 279.
27. M.M.Szczesniak and S.Scheiner, *J. Chem. Phys.*, 81(1984) 5024.
28. K.Somasundram, R.D.Amos and N.C.Handy, *Theor. Chim. Acta.*, 69(1986) 491.
29. G.J.B.Hurst, P.W.Fowler, A.J.Stone and A.D.Buckingham, *Intern. J. Quantum Chem.*, 29(1986) 1223.
30. R.D.Amos, J.F.Gaw, N.C.Handy, E.D.Simandiras and K.Somasundram, *Theor. Chim. Acta.*, 71(1987) 41.
31. Klaus-Peter Schroder, *Chem. Phys.*, 123(1988) 91.

32. E.J.Hamilton,Jr. and C.A.Naleway, *J. Phys. Chem.* 80(1976) 2037.
33. C.N.R.Rao, G.V.Kulkarni, A.Muralikrishna Rao and U.Chandra Singh, *J. Mol. Struct. (Theochem)*, 108(1984) 113.
34. Janet E. Del Bene, *J. Chem. Phys.* 56(1972) 4923.
35. Z.Latajka, H.Ratajczak and W.B.Person, *J. Mol. Struct.* 194(1989) 89.
36. T.M.Hard, R.J.O'Brien, C.Y.Chan, and A.A.Mehrabzadeh, *Environ. Sci. Technol.* 18(1984) 768.
37. T.M.Hard, C.Y.Chan, A.A.Mehrabzadeh, W.H.Pan, and R.J.O'Brien, *Nature* 322(1986) 617.
38. C.Y.Chan, T.M.Hard, A.A.Mehrabzadeh, L.A.George, and R.J.O'Brien, *J. Geophys. Res.* 96(1990) 18569. T.M.Hard, A.A.Mehrabzadeh, C.Y.Chan, and R.J.O'Brien, *Ibid.* In press 1991.
39. W.J.Hehre, L.Radom, P.v.R.Schleyer, and J.A.Pople, *ab initio* Molecular Orbital Theory, Wiley, New York, 1986.
40. M.J.Frisch, J.S.Binkley, H.B.Schlegel, K.Raghavachari, C.F.Melius, R.L.Martin, J.J.P.Stewart, F.W.Bobrowicz, C.M.Rohlfing, L.R.Kahn, D.J.Defrees, R.Seeger, R.A.Whiteside, D.J.Fox, E.M.Fleuder, and J.A.Pople, GAUSSIAN 86, Carnegie-Mellon Quantum Chemistry Publishing Unit, Pittsburgh, PA., 1984.
41. G.Chalasinski and M.Gutowski, *Chem. Rev.*, 88(1988) 943.
42. R.J.Bartlett and G.D.Purvis, *Int. J. Quant. Chem. Symp.*, 14(1978) 561.
43. S.F.Boys and F.Bernardi, *Mol. Phys.*, 10(1979) 553.
44. H.F.Hameka and A.G.Turner, *J. Magn. Reson.*, 64(1985) 66.
45. C.C.J.Rothaan, *Rev. Mod. Phys.*, 179(1960) 32.
46. W.J.Hehre, R.Ditchfield and J.A.Pople, *J. Chem. Phys.*, 56(1972) 2257.
47. P.C.Horihoram and J.A.Pople, *Mol. Phys.*, 27(1974) 209. Also see ref.8.
48. M.J.Frisch, J.A.Pople and J.S.Binkley, *J. Chem. Phys.*, 80(1984) 3265, and references cited therein.

49. T.H.Dunning and P.J.Hay, Modern Theoretical Chemistry (Plenum Press, New York, 1976).
50. R.Krishnan, J.S.Binkley, R.Seeger and J.A.Pople, *J. Chem. Phys.* 72(1980) 650.
51. T.Clark, J.Chandrasekhar, G.W.Spitznagel and P.v.R.Schleyer, *J. Comp. Chem.*, 4(1983) 294.
52. a). C.Moller and M.S.Plesset, *Phys. Rev.* 46(1934) 618.
b). J.A.Pople and Ber. Bunsenges, *Phys. Chem.* 86(1982) 806.
53. J.A.Pople, R.Krishnan, H.B.Schlegel, and J.S.Binkley, *Int. J. Quantum Chem.*, *Quantum Chem. Symp.*, No 13(1979) 225.
54. A.R.Hoy and P.R.Bunker, *J. Mol. Spectrosc.*, 74(1979) 1.
55. S.A.Clough, Y.Beers, G.D.Klein, and L.S.Rothman, *J. Chem. Phys.* 59(1973) 2254.
56. G.Herzberg, Molecular Spectra and Molecular Structure: I.Spectra of Diatomic Molecules (Van Nostrand Reinhold, New York, 1950)
57. W.L.Meerts and A.Dymanus, *Chem. Phys. Lett.*, 23(1973) 45
58. K.P.Huber, G.Herzberg (1979) Constants of Diatomic Molecules. Van Nostrand Reinhold, New York.
59. J.S.Muenter and W.Klemperer, *J. Chem. Phys.*, 52(1970) 6033.
60. a).A.P.L.Rendell, G.B.Bacskay, and N.S.Hush, *Chem. Phys. Lett.*, 117(1985) 400
b).A.D.Buckingham and P.W.Fowler, *Can. J. Chem.*, 63(1985) 2018
c).S-Y.Liu and C.E.Dykstra, *Chem. Phys.*, 107(1986) 343
61. G.Strey, *J. Mol. Spectrosc.*,24(1967) 87.
62. E.J.Hamilton,Jr., *J. Chem. Phys.* 63(1975) 3682
63. E.J.Hamilton,Jr. and R.R.Lii, *Int. J. Chem. Kinet.* 9(1977) 875
64. C.E.Barnes, J.M.Brown, and H.E.Radford, *J. Mol. Spectrosc.* 84(1980) 179
65. S.Saito and C.Matsumura, *J. Mol. Spectrosc.*, 80(1980) 34

66. a). J.W.C.Johns, A.R.W.McKellar, and M.Raggin, *J. Chem. Phys.* 68(1978) 3957
b). C.Yamada, Y.Endo, and E.Hirota, *Ibid.* 78(1983) 4379
c). K.Nagai, Y.Endo, and E.Hirota, *J. Mol. Spectrosc.*, 89(1981) 520
67. C.F.Jackels and D.H.Phillips, *J. Chem. Phys.*, 84(1986) 5013.
68. G.A.Khachkuruzov and I.N.Przhevalskii, *Opt. Spektrosk.*, 36(1974) 299; 44(1978) 194.
69. E.A.Cohen and H.M.Pickett, *J. Mol. Spectrosc.*, 87(1981) 582
70. P.A.Giguere and T.K.K.Srinivasan, *J. Raman Spectrosc.*, 2(1976) 125.
71. T.Tanaka and Y.Morino, *J. Mol. Spectrosc.*, 33(1970) 538.
72. M.Lichtenstein, J.J.Gallagher, and S.A.Clough, *J. Mol. Spectrosc.*, 40(1971) 10.
73. T.J.Lee, *J. Chem. Phys.*, 93(1990) 489.
74. D.H.Magers, W.N.Lipscomb, R.J.Bartlett, and J.F.Stanton, *J. Chem. Phys.*, 91(1989) 1945.
75. K.Raghavachari, G.W.Trucks, J.A.Pople, and E.Replogle, *Chem. Phys. Lett.*, 158(1989) 207.
76. G.E.Scuseria, T.J.Lee, A.C.Scheiner, and H.F.Schaefer, *J. Chem. Phys.*, 90(1989) 5635.
77. A.Barber, C.Secroun, and S.A.Clough, *J. Mol. Spectrosc.*, 49(1974) 171.
78. D.B.Keck and C.D.Hause, *J. Mol. Spectrosc.*, 26(1968) 163.
79. D.E.Terault and L.Andrews, *Spectrochim. Acta*, 30A(1974) 969.
80. C.D.Hause, *J. Mol. Spectrosc.*, 26(1968) 286.
81. G.H.F. Diercksen and A.J. Sadlej, *Mol. Phys.* 58(1986) 889.
82. K.S. Pitzer and W.D. Gwinn, *J. Chem. Phys.* 10(1942) 428.
J.C.M. Li, *J. Am. Chem. Soc.* 78(1956) 1081.

APPENDIX A

CALCULATION OF THERMOCHEMICAL PROPERTIES OF COMPLEXES

The chemical systems are N-body problems. In order to calculate the thermochemical properties of the system, it is necessary to have the set of eigenvalues $\{ E_j(N,V) \}$ of the N-body Schrodinger equation. In general, this is impossible. But the molecules in the gas phase are far away from each other, so the N-body Hamiltonian operator can be written as a sum of independent individual Hamiltonians. Then the total energy of the system can be written as a sum of individual energies.

The molecular systems are antisymmetric under the interchange of identical particles, and they should obey the Fermi-Dirac statistical theory. In the normal conditions they can be treated by the Boltzmann distribution law with indistinguishable particles. So the partition function is

$$Q(N,V,T) = \frac{q^N}{N!} \quad \text{with} \quad q(V,T) = \sum e^{-\epsilon_i / KT}$$

for a system of identical indistinguishable particles satisfying the condition that the number of available molecular states is much greater than the number of particles.

The q is the partition function for each particle. Under the Born-Oppenheimer approximation and the Rigid Rotor-Harmonic Oscillator approximation, the q can be decomposed to

$$q_{\text{nucl}} q_{\text{elect}} q_{\text{trans}} q_{\text{vib}} q_{\text{rot}}$$

then,

$$\begin{aligned}
 E &= K T^2 \left(\frac{\partial \ln Q}{\partial T} \right)_{N,T} \\
 &= E_{\text{nucl}} + E_{\text{elect}} + E_{\text{trans}} + E_{\text{vib}} + E_{\text{rot}} \\
 S &= \frac{E}{T} + K \ln Q \\
 &= S_{\text{nucl}} + S_{\text{elect}} + S_{\text{trans}} + S_{\text{vib}} + S_{\text{rot}} \\
 &\quad + N K \ln(e/N)
 \end{aligned}$$

(Note, the last term is usually included in the S_{trans}).

Now the thermochemical properties will be calculated after each partition function term is evaluated.

$q_{\text{nucl}} = 1$ for any case. This is because the thermochemical properties deal with the electronic level problems, not the nuclear level. So $E_{\text{nucl}} = 0$ and $S_{\text{nucl}} = 0$.

$q_{\text{elect}} = \sum \omega_{e_i} e^{-\epsilon_i/KT}$. Here the ω_{e_i} is the degeneracy and ϵ_i is the energy of the i th electronic level. Usually the ground state energy is set to zero. Then the ϵ_i will be the energies relative to the ϵ_1 . In the ordinary temperature, the ϵ_i ($i > 1$) are typically quite large. So only the first term in the summation is significantly different from zero. So, $q_{\text{elect}} = \omega_{e0}$, $E_{\text{elect}} = 0$ and $S_{\text{elect}} = R \log \omega_{e0}$

$$q_{\text{trans}}$$

$$q_{\text{trans}} = V \left(\frac{2 \pi m k T}{h^2} \right)^{3/2}$$

Here V is the volume of system and $P V = n R T$. $E_{\text{trans}} = (3/2) R T$

$$S_{\text{trans}} = R \ln \left[\left(\frac{2 \pi m k T}{h^2} \right)^{3/2} \frac{V e^{5/2}}{N} \right]$$

The q_{rot} is depended on the symmetry of the molecules. For ideal diatomic gas and polyatomic gas in linear form,

$$q_{\text{rot}} = \frac{T}{\sigma \Theta_r} \quad \text{with } \sigma \text{ is the symmetry number}$$

which is defined as the number of different ways the molecule can be rotated into a configuration indistinguishable from the original, and

$$\Theta_r = \frac{h^2}{8 \pi^2 I k} \quad \text{is the characteristic rotational temperature.}$$

$$E_{\text{rot}} = R T$$

$$S_{\text{rot}} = R \ln \left(\frac{T e}{\sigma \Theta_r} \right)$$

For ideal polyatomic gas in nonlinear form,

$$q_{\text{rot}} = \frac{\pi^{1/2}}{\sigma} \left(\frac{T^3}{\Theta_A \Theta_B \Theta_C} \right)^{1/2}$$

The σ , Θ_A , Θ_B and Θ_C have the same definition as in the polyatomic gas in linear form.

$$E_{\text{rot}} = (3/2) R T$$

$$S_{\text{rot}} = R \ln \left[\left(\frac{T^3}{\Theta_A \Theta_B \Theta_C} \right)^{1/2} \left(\frac{\pi^{1/2} e^{3/2}}{\sigma} \right) \right]$$

The q_{vib} is depended on the symmetry of the molecules.

$$q_{\text{vib}} = \prod \frac{e^{-h\nu/2kT}}{1 - e^{-h\nu/kT}} = \prod \frac{e^{-\Theta_v/2T}}{1 - e^{-\Theta_v/T}}$$

here $\Theta_v = h\nu/k$ is the characteristic vibrational temperature.

The multiplier is from 1 to $3n-5$ for diatomic gas and polyatomic gas in linear forms and from 1 to $3n-6$ for polyatomic gas in nonlinear forms.

$$E_{\text{vib}} = R \sum \left(\frac{\Theta_v}{2} + \frac{\Theta_v}{e^{\Theta_v/T} - 1} \right)$$

$$S_{\text{vib}} = R \sum \left[\left(\frac{\Theta_{\text{vi}}/T}{e^{\Theta_{\text{vi}}/T} - 1} \right) - \ln \left(1 - e^{-\Theta_{\text{vi}}/T} \right) \right]$$

The summation is from 1 to 3n-5 for diatomic gas and polyatomic gas in linear forms and from 1 to 3n-6 for polyatomic gas in nonlinear forms.

After the values of E_{nucl} , E_{elect} , E_{trans} , E_{vib} , E_{rot} , S_{nucl} , S_{elect} , S_{trans} , S_{vib} and S_{rot} have been calculated for the complex and its monomers, the other thermochemical properties can be calculated as outlined in Chapter I.

APPENDIX B

COMPUTER PROGRAM FOR CALCULATION OF THERMOCHEMICAL PROPERTIES OF COMPLEXES

INPUT FILE: THERMOIN

The input data is taken from the output of GAUSSIAN program [40].

```

1
temp=      298.15
Mol. W.    32.99765
polynonlinear
rot. sym. # 1.0
2.73967    51.99069    54.73036
3
1252.8394   1601.9217   4078.1206
2
0.9

```

Line 1 is the number of temperature point: n_{temp} . Then n_{temp} lines are followed to input the temperature.

Line $n_{\text{temp}} + 2$ is the molecule weight.

Line $n_{\text{temp}} + 3$ is the character input: "diatomic", "polylinear" or "polynonlinear".

Line $n_{\text{temp}} + 4$ is the rotational symmetry number.

Line $n_{\text{temp}} + 5$ is the principal moments of inertia of the molecule which are taken from the output of GAUSSIAN program.

Line $n_{\text{temp}} + 6$ is the number of vibration frequencies which include the degeneracy vibrational modes.

Line $n_{\text{temp}} + 7$ is the vibration frequencies in cm^{-1} from the output of GAUSSIAN program.

Line $n_{\text{temp}} + 8$ is the degeneracy of ground electronic states.

Line $n_{\text{temp}} + 9$ is the scaling factor of the vibrational frequencies.

FORTRAN PROGRAM: THERMOCH

```

      real*8 ee, et, er, ev0, ev, se, st, sr, qe, qet, s
      real*8 thev(50), u(50), iabc(3), vib(50), temp
      real*8 rconst, nconst, hconst, cconst, kconst, mass
      real*8 totalvib, totalthev, tempp(50), w(10), e(10),
1      w0, e0, scale
      character*10 word
c      constants r, n, h, c, k
      rconst = 1.98717
      nconst = 6.022045d23
      hconst = 6.626176d-34
      cconst = 2.99792458d10
      kconst = 1.380662d-23
c
c      open (1,file='thermoin', status='old')
c
c      read in the ntemp and the temperature points.
c
      read(1,*) ntemp
      do 20 i=1, ntemp
         read (1,'(10x,f20.10)') tempp(i)
20    continue
c
c      read in all other parameters
c
      read (1,'(10x,f20.10)') mass
      read (1,'(10x,'a10)') word
      read (1,'(10x,f20.10)') s
      read (1,*) iabc(1), iabc(2), iabc(3)
      read (1,*) nvib
      read (1,*) (vib(i), i=1, nvib)
      read (1,*) w0
      read (1,*) scale
50    print*, '
c
c      calculating the scaled vibrational frequencies.
c
      do 60 i=1, nvib
```

```

        vib(i) = scale * vib(i)
60  continue
    itemp = 1
    print*, '      Thermochemical calculation  '
    print*, '      in Dr. O'Brien Modeling Lab'
    print*, '
    print*, ' INPUT: '
    print*, '      Molecular Weight: ', mass
    print*, '      Rotational symmetry Number: ', s
    print*, '      I(a) : ', iabc(1)
    print*, '      I(b) : ', iabc(2)
    print*, '      I(c) : ', iabc(3)
c
c  Print out the vibrational frequencies or scaled
c  vibratioal frequencies.
c
    if ( scale * scale .eq. 1.0) then
        print*, '      Vibrational Frequencies (cm ^-1): '
    else
        write(6,('      Vibrational Frequencies (cm ^-1)",
1      " scaled by ", f4.2, ")") scale
    endif
    do 80 i=1, nvib
        print*, '      ', vib(i)
80  continue
    print*, '
c
c  start point of main routine, first get the temperature
c
    temp = tempp(itemp)
    print*, '      OUTPUT: '
    print*, '
    print*, '      Vibrational Temperature:'
c
c  calculate and print out the vibrational temperature'
c
    totalvib = 0.0
    do 100 i=1, nvib
        thev(i) = hconst * cconst * vib(i) / kconst
        print*, '      ', thev(i)
        totalvib = totalvib + vib(i)
100  continue
    print*, '
c
c  calculate and print out the zero point
c  vibrational energy

```

```

c
    ev0 = 0.5 * nconst * hconst * cconst * totalvib / 4184
    print*, ' Zero point vibrational energy (kcal/mol): ',
1      ev0
120  print*, ''
c
c    print out the temperature
c
    print*, ' -----'
    print*, ' | Temperature: ', temp, ' |'
    print*, ' -----'
    print*, ''
c
c    Calculate the energy of elect., tran., vib. and rot.
c
    ee = 0.0
c
    et = 1.5d-3 * rconst * temp
c
    if (nvib .eq. 1 .or. word .eq. 'polylinear') then
        er = 1.0d-3 * rconst * temp
    else
        er = 1.5d-3 * rconst * temp
    endif
c
    do 140 i=1, nvib
        u(i) = thev(i) / temp
140  continue
    totalthev = 0.0
    do 200 i=1, nvib
        totalthev = totalthev + thev(i) / (dexp(u(i)) - 1)
200  continue
    ev = rconst * 1.0d-3 * totalthev + ev0
c
c    Calculate the entropy of elect., tran., vib. and rot.
c
    se = rconst * dlog(w0)
c
    st = rconst * (2.5*dlog(temp) + 1.5*dlog(mass)
1      - 1.164871)
c
    if (nvib .eq. 1 .or. word .eq. 'polylinear') then
        sr = dlog(iabc(1)) + dlog(0.46497d-40) +
1      dlog(temp) + 89.4077 - dlog(s)
    else
        sr = 1.5* dlog(temp)

```

```

1      + 0.5*dlog(iabc(1)*iabc(2)*iabc(3))
1      + 1.5*dlog(0.46497d-40) - dlog(s) + 134.683828
endif
sr = rconst * sr
c
sv = 0.0
do 300 i=1, nvib
    sv = sv + u(i) / (dexp(u(i)) - 1)
1      - dlog(1-dexp(-u(i)))
300 continue
sv = rconst * sv
c
c print out the results
c
print*, ' E (electrical) : ', ee
print*, ' E (trans)      : ', et
print*, ' E (rotational) : ', er
print*, ' E (vibrational) : ', ev
print*, '
print*, ' E (total:kcal/mol) : ', ee+et+er+ev
c
print*, ' S (electrical) : ', se
print*, ' S (trans)      : ', st
print*, ' S (rotational) : ', sr
print*, ' S (vibrational) : ', sv
print*, '
print*, ' S (total:kcal/mol) : ', se+st+sr+sv
print*, '
if ( itemp .le. ntemp) go to 120
stop
end

```

OUTPUT FILE: THERMOOUT

Thermochemical calculation
in Dr.O'Brien Modeling Lab

INPUT:

Molecular Weight: 32.997650000000000
Rotational Symmetry Number: 1.0000000000000000
I(a) : 2.7396700000000000
I(b) : 51.9906900000000000

I(c) : 54.73036000000000
 Vibrational Frequencies (cm⁻¹, scaled by 0.90):
 1127.5554600000000
 1441.7295300000000
 3670.3085400000000

OUTPUT:

Vibration Temperature:
 1622.311364385915
 2074.340716588579
 5280.789696361966

Zero Point Vib Energy (kcal/mol): 8.919947414134777

Temperature: 298.1500000000000

E (electrical) : 0.0000000000000000
 E (trans) : 0.8887121032500000
 E (rotational) : 0.8887121032500000
 E (vibrational) : 8.9379067755255190

E (total:kcal/mol) : 10.71533098202552

S (electrical) : 1.377401282793307
 S (trans) : 36.41245658105804
 S (rotational) : 16.70634462351519
 S (vibrational) : 7.0759070144989470E-02

S (total:cal/mol.deg) : 54.56696155751152

APPENDIX C

CALCULATION OF THE ENTROPY CONTRIBUTION OF INTERNAL ROTATION IN COMPLEXES

For the water complexes we discussed here, the barrier of internal rotation are quite low. So, the entropy contribution of internal rotation are estimated from the formula of Pitzer and Gwinn [82], using the reduced moment of inertia along the O----O axis. Also the calculation of $\text{CH}_3\text{-Cd-CH}_3$ shown in J.C.M. Li [82] is repeated here with $\text{H}_2\text{O}\cdot\text{H}_2\text{O}$, $\text{H}_2\text{O}\cdot\text{HO}_2$ and $\text{H}_2\text{O}\cdot\text{H}_2\text{O}_2$.

First, the reduced moment of inertia is calculated. Like $\text{CH}_3\text{-Cd-CH}_3$, the length of C-Cd is assumed as 2.15 Å, C-H as 1.10 Å and HCH as tetrahedral angle. For each top,

$$I_1 = m \cdot a^2 = 1.66\text{e-}24 \text{ g} \times (1.8\text{e-}8 \text{ cm})^2$$

$$= 5.38\text{e-}40 \text{ g.cm}^2$$

$$I_r = 0.5 \cdot I_1 = 2.7\text{e-}40 \text{ g.cm}^2$$

Same calculation is for $\text{H}_2\text{O}\cdot\text{H}_2\text{O}$, $\text{H}_2\text{O}\cdot\text{HO}_2$ and $\text{H}_2\text{O}\cdot\text{H}_2\text{O}_2$.

$$\text{H}_2\text{O}\cdot\text{H}_2\text{O} \quad : \quad I_r = 0.7925\text{e-}40 \text{ g.cm}^2$$

$$\text{H}_2\text{O}\cdot\text{HO}_2 \quad : \quad I_r = 1.832\text{e-}40 \text{ g.cm}^2$$

$$\text{H}_2\text{O}\cdot\text{H}_2\text{O}_2 \quad : \quad I_r = 1.8\text{e-}40 \text{ g.cm}^2$$

Then, the partition function Q_f is calculated. Like $\text{CH}_3\text{-Cd-CH}_3$, n is 3, which is symmetric number.

$$Q_f = \left(\frac{8 \pi^3 I_r k T}{n^2 h^2} \right)^{1/2}$$

$$= 2.64$$

$$\text{For } \text{H}_2\text{O}\cdot\text{H}_2\text{O} \quad : \quad n=2 \quad \text{and} \quad Q_f = 2.146$$

For $\text{H}_2\text{O} \cdot \text{HO}_2$: $n=2$ and $Q_f = 3.264$

For $\text{H}_2\text{O} \cdot \text{H}_2\text{O}_2$: $n=2$ and $Q_f = 3.23$

Third, the entropy is calculated from partition function Q_f . Like

$\text{CH}_3\text{-Cd-CH}_3$, $S_f = (0.5 + \ln Q_f) = 2.9 \text{ cal/mol.deg}$

For $\text{H}_2\text{O} \cdot \text{H}_2\text{O}$ $S_f = 2.5 \text{ cal/mol.deg}$

For $\text{H}_2\text{O} \cdot \text{HO}_2$ $S_f = 3.3 \text{ cal/mol.deg}$

For $\text{H}_2\text{O} \cdot \text{H}_2\text{O}_2$ $S_f = 3.3 \text{ cal/mol.deg}$

Fourth, the correction of rotational barrier from the table in reference 82 is taken into account.

For $\text{H}_2\text{O} \cdot \text{H}_2\text{O}$ $S = 0.65 \text{ cal/mol.deg}$

For $\text{H}_2\text{O} \cdot \text{HO}_2$ $S = 1.3 \text{ cal/mol.deg}$

For $\text{H}_2\text{O} \cdot \text{H}_2\text{O}_2$ $S = 2.4 \text{ cal/mol.deg}$

Last, the entropy increases because of internal rotation are derived as following.

For $\text{H}_2\text{O} \cdot \text{H}_2\text{O}$ $S_f - s = 1.85 \text{ cal/mol.deg}$

For $\text{H}_2\text{O} \cdot \text{HO}_2$ $S_f - s = 2.0 \text{ cal/mol.deg}$

For $\text{H}_2\text{O} \cdot \text{H}_2\text{O}_2$ $S_f - s = 0.9 \text{ cal/mol.deg}$